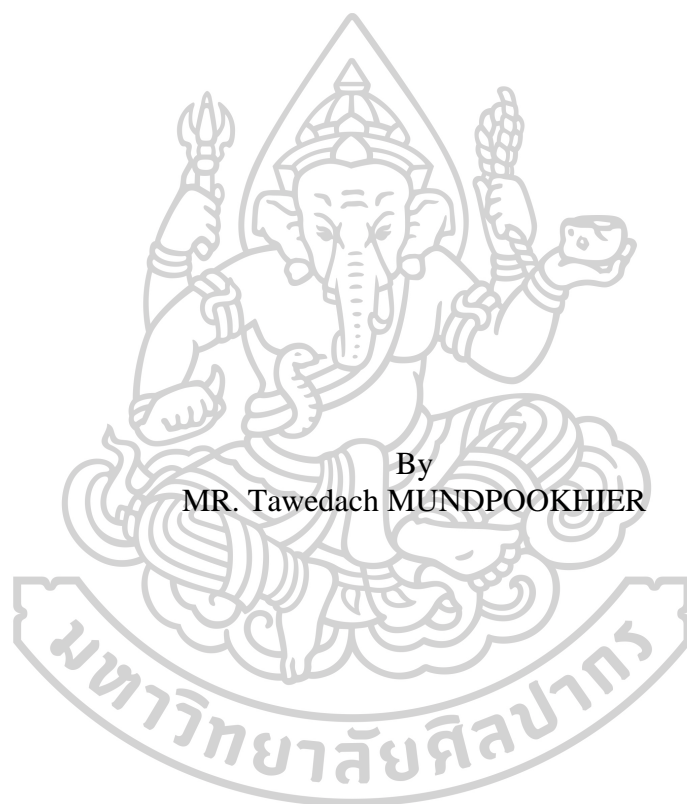




DRYING OF BANANA: EXPERIMENTS AND MODELLING



A Thesis Submitted in Partial Fulfillment of the Requirements
for Doctor of Philosophy (PHYSICS)
Department of PHYSICS
Graduate School, Silpakorn University
Academic Year 2018
Copyright of Graduate School, Silpakorn University

การอบแห้งกล้วย: การทดลองและการจำลองแบบ



โดย
นายทวีเดช หมั่นภูเขียว

วิทยานิพนธ์นี้เป็นส่วนหนึ่งของการศึกษาตามหลักสูตรปรัชญาดุษฎีบัณฑิต

สาขาวิชาฟิสิกส์ แบบ 1.1 ปรัชญาดุษฎีบัณฑิต

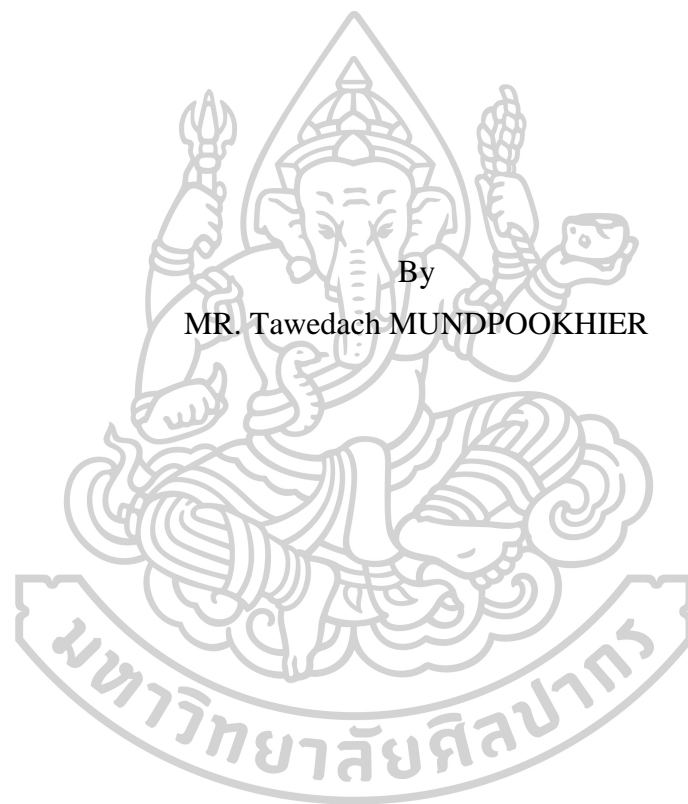
ภาควิชาฟิสิกส์

บัณฑิตวิทยาลัย มหาวิทยาลัยศิลปากร

ปีการศึกษา 2561

ลิขสิทธิ์ของบัณฑิตวิทยาลัย มหาวิทยาลัยศิลปากร

DRYING OF BANANA: EXPERIMENTS AND MODELLING



By
MR. Tawedach MUNDPOOKHIER

A Thesis Submitted in Partial Fulfillment of the Requirements
for Doctor of Philosophy (PHYSICS)
Department of PHYSICS
Graduate School, Silpakorn University
Academic Year 2018
Copyright of Graduate School, Silpakorn University

Title	Drying of banana: Experiments and modelling
By	Tawedach MUNDPOOKHIER
Field of Study	(PHYSICS)
Advisor	Serm Janjai

Graduate School Silpakorn University in Partial Fulfillment of the
Requirements for the Doctor of Philosophy

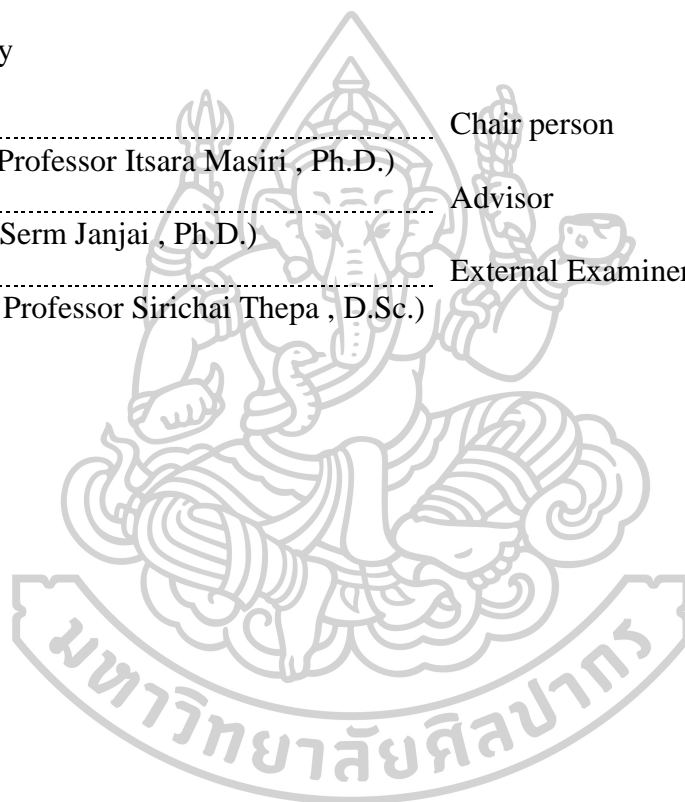
..... Dean of graduate school
(Associate Professor Jurairat Nunthanid, Ph.D.)

Approved by

..... Chair person
(Assistant Professor Itsara Masiri , Ph.D.)

..... Advisor
(Professor Serm Janjai , Ph.D.)

..... External Examiner
(Associate Professor Sirichai Thepa , D.Sc.)

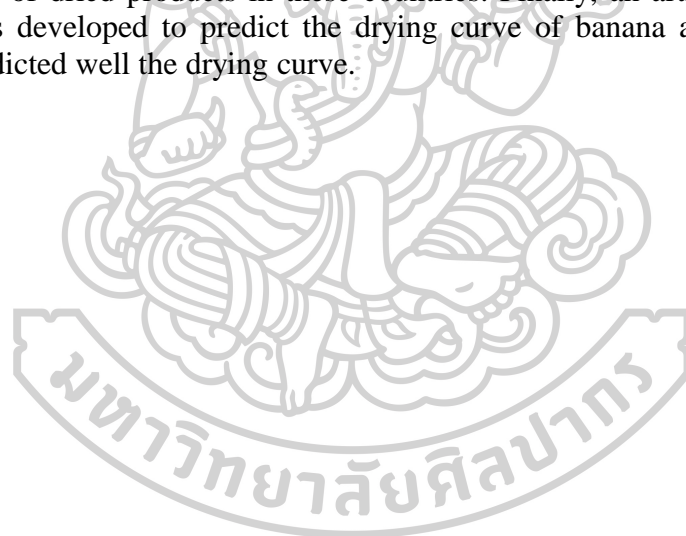


59306801 : Major (PHYSICS)

Keyword : BANANA, FINITE ELEMENT MODELING, PARABOLIC GREENHOUSE SOLAR DRYER

MR. TAWEDACH MUNDPOOKHIER : DRYING OF BANANA: EXPERIMENTS AND MODELLING THESIS ADVISOR : PROFESSOR SERM JANJAI, Ph.D.

In this work, drying characteristics of banana, performance of the parabolic greenhouse solar dryer for banana drying and modelling of this type of dryer have been carried out. The results of the work are as follows. For the thin layer drying, it was found that temperature and relative humidity of drying air had strong influence on the drying curves of thin layer drying of banana, and the “Logarithmic model” predicts best the drying curve of banana. In addition, a two-dimensional finite element model has been developed to predict the moisture distribution inside banana, and it was found that this model predicted reasonably the drying curve of banana. For the dryer, the performance of the parabolic greenhouse solar dryer for banana drying in Thailand and for various agricultural products in other Asian countries was experimentally evaluated and the results revealed that this type of dryer could be used effectively to dry banana and various agricultural products for commercial-scale production of dried products in these countries. Finally, an artificial neural network model was developed to predict the drying curve of banana and it was found this model predicted well the drying curve.



ACKNOWLEDGEMENTS

This thesis is submitted in partial fulfillment of the requirements for the degree of Doctor of Philosophy (Physics), Graduate School, Silpakorn University.

I would like to thank all the people who contributed in some ways to the work described in this thesis. First and foremost, I thank my academic advisor, Professor Serm Janjai, Ph.D., for his helpful guidance and support throughout this study.

I would like to acknowledge the Department of Physics, Faculty of Science, Silpakorn University. Additionally, I would also like to thank Assistant Professor Itsara Masiri, Ph.D. and Associate Professor Sirichai Thepa, D.Sc. for examining this thesis.

Finally, I would like to acknowledge friends and family who supported me during my study at Silpakorn University.

Tawedach MUNDPOOKHIER

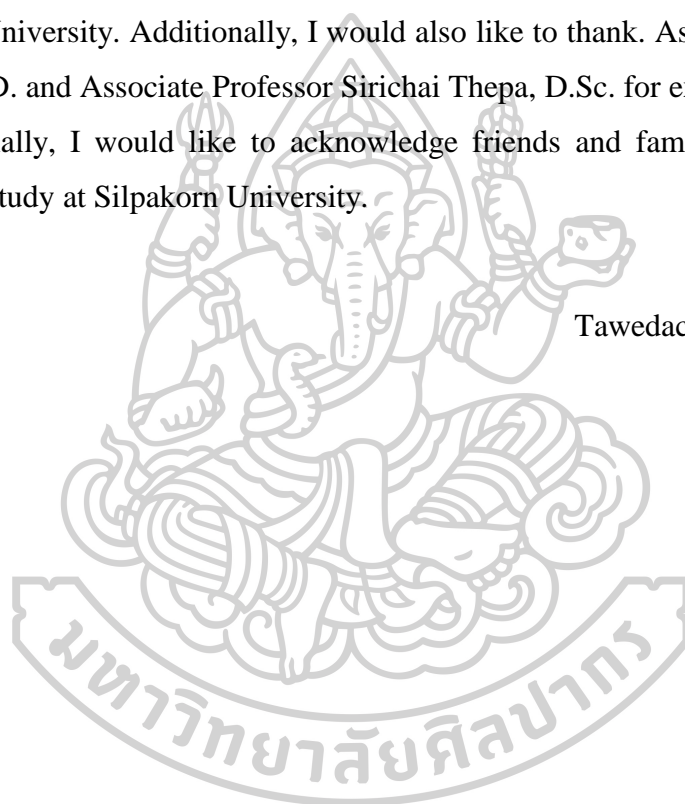


TABLE OF CONTENTS

	Page
ABSTRACT.....	D
ACKNOWLEDGEMENTS.....	E
TABLE OF CONTENTS.....	F
List of Tables	I
List of Figures	J
Chapter 1 Introduction	1
1.1 Rationale.....	1
1.2 Objectives	1
1.3 Organization of the thesis	2
Chapter 2 Thin Layer Drying of Banana	3
2.1 Introduction.....	3
2.2 Materials and methods	3
2.2.1 Drying experiments.....	3
2.2.2 Mathematical modeling	4
2.3 Results and discussions.....	6
2.3.1 Drying characteristics of banana	6
2.3.2 Mathematical modeling of thin-layer drying.....	10
2.4 Conclusions.....	10
Chapter 3 Modeling of Banana Drying Using Finite Element Method	11
3.1 Introduction.....	11
3.2 Materials and methods	11
3.2.1 Experimental study.....	11
3.2.2 Uncertainty analysis	12
3.2.3 Finite element modeling of banana	12
3.3 Thermo-physical properties of banana	15

3.3.1 Moisture diffusivity of banana	15
3.3.2 Equilibrium moisture content of banana	15
3.3.3 Shrinkage.....	15
3.3.4 Surface mass transfer coefficient	16
3.3.5 Method of solution	16
3.4 Results and discussions.....	17
3.5 Conclusions.....	19
Chapter 4 Drying of Banana in a Parabolic Greenhouse Solar Drying	20
4.1 Introduction.....	20
4.2 Materials and methods.....	20
4.3 Results and discussions.....	22
4.4 Conclusions.....	25
Chapter 5 Performance of parabolic greenhouse solar dryer equipped with rice husk burning system for banana drying*.....	26
5.1 Introduction.....	26
5.2 Materials and methods	27
5.2.1 Parabolic greenhouse solar dryer equipped with rice husk burning system	27
5.2.2 Performance of the burning system.....	29
5.2.3 Experimental procedure	29
5.2.4 Uncertainty analysis	30
5.2.5 Drying efficiency.....	30
5.3 Results and discussions.....	31
5.3.1 Performance of the rice husk burning system	31
5.3.2 Performance of greenhouse solar dryer equipped with rice husk burning system.....	31
5.3.3 Economic evaluation	34
5.4 Conclusions.....	38
Chapter 6 Performance Investigation of a Parabolic Greenhouse Solar Dryer Equipped with Phase-Change-Thermal Energy Storages*	39

6.1 Introduction.....	39
6.2 Materials and methods	39
6.2.1 Latent heat storage.....	39
6.2.2 Experimental study.....	40
6.3 Results and discussion	43
6.4 Conclusions.....	45
Chapter 7 Performance of the Parabolic Greenhouse Solar Dryer in Southeast Asian and Modelling of this Type of Dryer Using the Artificial Neural Network*	46
7.1 Introduction.....	46
7.2 Materials and methods.....	47
7.2.1 Drying experiments	47
7.2.2 Modeling of the parabolic greenhouse solar dryer by using the artificial neural network (ANN).....	49
7.3 Results and discussions.....	50
7.3.1 Experimental performance of the greenhouse solar dryer.....	50
7.3.2 Performance of the ANN model.....	53
7.4 Conclusions.....	53
Chapter 8 Conclusions	54
Appendix	55
Appendix 1 Testing of ANN for Litchi Drying*	56
Appendix 2 Publications	70
Appendix 3 Nomenclature	71
REFERENCES	74
VITA.....	77

List of Tables

	Page
Table 1 The 7 selected thin-layer drying models.....	6
Table 2 Parameter value, coefficient of determination (R^2) and root mean square error (RMSE) value of the different models for banana.....	9
Tables 3 Economic and production data used for the economic evaluation.	35

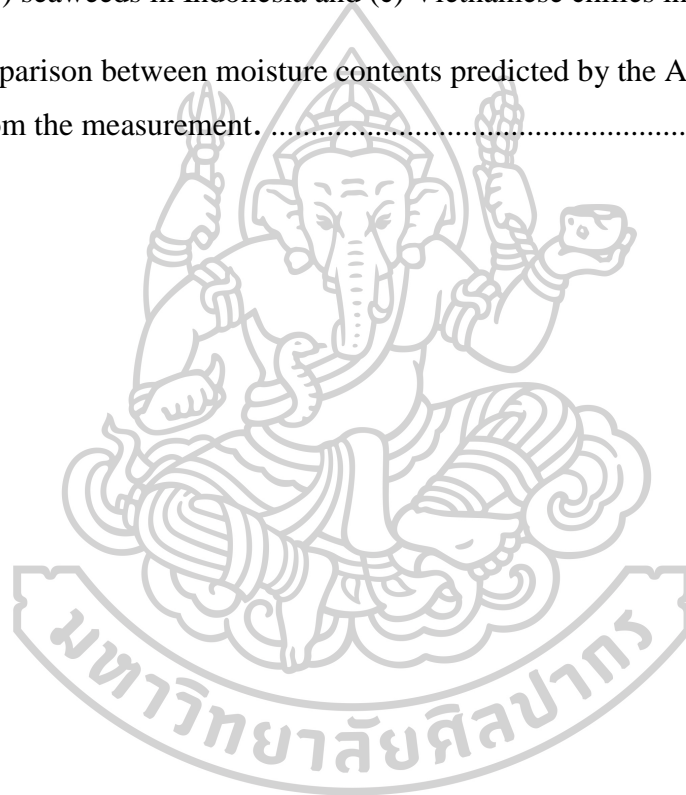


List of Figures

	Page
Fig 1 Schematic diagram of the laboratory dryer	4
Fig 2 Thin layer drying of banana at different temperatures (40°C, 50°C and 60°C) and relative humidity (10%) from the experiments.....	6
Fig 3 Thin layer drying of banana at different temperatures (40°C, 50°C and 60°C) and relative humidity (20%) from the experiments.....	7
Fig 4 Thin layer drying of banana at different temperatures (40°C, 50°C and 60°C) and relative humidity (30%) from the experiments.....	7
Fig 5 Predicted and observed moisture content of banana using Logarithmic model at the temperatures of 40°C, 50°C and 60°C and relative humidity of 10%.	7
Fig 6 Predicted and observed moisture content of banana using Logarithmic model at the temperatures of 40°C, 50°C and 60°C and relative humidity of 20%.	8
Fig 7 Predicted and observed moisture content of banana using Logarithmic model at the temperatures of 40°C, 50°C and 60°C and relative humidity of 30%.	8
Fig 8 Mesh distribution and geometry considered in the finite element model of banana	14
Fig 9 Example of comparison of the finite element predicted moisture contents with the experimental data of banana at $T_a=50^\circ\text{C}$ and $rh=20\%$	17
Fig 10 Contours of moisture contents inside the banana for different drying times....	18
Fig 11 Pictorial view of the parabolic greenhouse dryer	20
Fig 12 The structure of the dryer and positions of the measurements (M_i , Rh_i , T_i are weight of the sample, relative humidity and air temperature at location i , $i=1, 2, \dots, n$)	22
Fig 13 Variation of solar radiation during a drying run for banana.....	22
Fig 14 Comparison of the ambient temperature and the temperature inside the dryer for drying for banana.	23
Fig 15 Drying air temperatures at the different levels of the shelves versus solar radiation	23
Fig 16 Relative humidity at various points inside the dryer and ambient relative humidity for drying the banana.....	24

Fig 17 Comparison of the moisture contents for drying the banana inside the dryer and that from natural sun drying.....	24
Fig 18 Parabolic greenhouse solar dryer equipped with a rice husk burning system a) pictorial view, b) schematic diagram.....	27
Fig 19 Rice husk burning system a) pictorial view b) schematic diagram.....	28
Fig 20 Variations of solar radiation during drying period.....	31
Fig 21 Variation of energy input with time inside the greenhouse solar dryer.....	32
Fig 22 Comparison of temperature variations inside the greenhouse dryer with the burning system and the ambient air temperature.....	33
Fig 23 Comparison of relative humidity inside the dryer and ambient air.....	33
Fig 24 Moisture contents of banana drying in greenhouse dryer with the burning system in comparison with the natural sun drying.....	34
Fig 25 Dried banana a) banana inside the dryer b) banana dried by natural sun.....	34
Fig 26 The components of thermal energy storage system: a) steel box containing paraffin b) cart for placing the paraffin box.....	41
Fig 27 Thermal energy storage system.....	41
Fig 28 Parabolic greenhouse solar dryer equipped with thermal energy storage system.....	41
Fig 29 Parabolic greenhouse solar dryer equipped with thermal energy storage system and without thermal energy storage.....	42
Fig 30 Variation of solar radiation with time of the day during drying of banana.....	43
Fig 31 Variation of ambient temperature and drying air temperature at the middle of parabolic greenhouse solar dryer.....	44
Fig 32 Variation of moisture content of banana.....	44
Fig 33 Dried banana: a) natural sun drying b) inside the parabolic greenhouse solar dryer.....	44
Fig 34 Pictorial view of the greenhouse solar dryer installed in (a) Thailand (b) Myanmar (c) Indonesia and (d) Vietnam.....	48
Fig 35 The structure of the artificial neural network of parabolic greenhouse solar dryer. t is time, I_t is solar radiation, T is drying air temperature at the middle of the dryer, RH is relative humidity and MC is moisture content.....	49
Fig 36 Variation of solar radiation during a drying run for red chilies in Myanmar.....	50

Fig 37 Comparison of the ambient temperature and the temperature inside the dryer for drying red chilies in Myanmar	50
Fig 38 Relative humidity at various points inside the dryer and ambient relative humidity for drying the red chilies in Myanmar	51
Fig 39 Comparison of the moisture contents for drying the red chilies inside the dryer and that from natural sun drying in Myanmar	51
Fig 40 Comparison of the moisture contents of the products inside the greenhouse solar dryer and with those obtained by the natural sun drying for drying (a) bananas in Thailand, (b) seaweeds in Indonesia and (c) Vietnamese chilies in Vietnam.....	52
Fig 41 Comparison between moisture contents predicted by the ANN model and those obtained from the measurement.....	53



Chapter 1

Introduction

1.1 Rationale

Banana (*Musa x paradisiaca* L) is an economically important fruit in Thailand. There are a number of varieties of banana in this country and the variety called “Namwa” is very popular. Namwa banana is available year round, with the annual production of 6,000 tons. Namwa banana is consumed both as fresh and dried fruits, and dried banana is very popular snack in Thailand. To dry efficiently namwa banana, it is necessary to know the drying characteristics and the knowledge on these characteristics is relatively limited.

In Thailand namwa banana is usually dried using the traditional sun drying method both for commercial and personal consumption purposes. According to this method, banana is peeled and spread on bamboo trays then it is exposed to solar radiation until the final moisture content of about 15-20% is reached. Although this method is cheap, banana being dried is usually subjected to considerable losses due to rain, insects and animals. Recently, parabolic greenhouse solar dryers have been introduced to banana producers to overcome such problem. However, the knowledge on the performance of this type of dryer and the modelling of the dryer is very limited. Therefore, the investigation of the drying characteristics of banana and the examination of the performance of the parabolic greenhouse solar dryer for banana drying are still required.

1.2 Objectives

The specific objectives of this work are as follows.

- 1) To study thin layer drying of banana
- 2) To investigate a drying characteristics of banana using a finite element approach
- 3) To investigate the performance of a parabolic greenhouse dryers equipped with a rice-husk burning system for banana drying
- 4) To examine the performance of a parabolic greenhouse solar dryer equipped with phase-change heat storage.
- 5) To perform a modelling of the parabolic greenhouse dryer for banana drying using an artificial neural network

1.3 Organization of the thesis

The thesis consists of 8 chapters. Chapter 1 presents the introduction of the work. Chapter 2 describes the thin layer drying of banana. Chapter 3 presents the finite element modelling of banana. Chapter 4 describes solar drying of banana in a parabolic greenhouse solar dryer. Chapter 5 presents the performance of the greenhouse solar dryer equipped with rice husk burning system for banana drying. Chapter 6 reports the performance of the parabolic greenhouse solar dryer equipped with phase change thermal energy storage. Chapter 7 presents the modelling of the parabolic greenhouse solar dryer for banana drying using an artificial neural network. Finally, chapter 8 presents the conclusion of the work.



Chapter 2

Thin Layer Drying of Banana

2.1 Introduction

Thin layer drying of products is a drying of products which are spread in thin layer on drying tray and are dried by drying media surrounding the products. Knowledge on thin layer drying is required for planning efficient drying strategy. In addition, it is also needed for a simulation of a drying process of the products. As the knowledge on thin layer drying of banana is still relatively limited, we propose to carry out thin layer drying experiments of banana under controlled drying condition of temperature and relative humidity. Then thin layer drying model of banana was also proposed.

2.2 Materials and methods

2.2.1 Drying experiments

The banana used in this experiment was obtained from a market in Nakhon Pathom, Thailand. It had initial moisture content about 70% (wb.). The banana was placed on a tray in a thin layer in a laboratory dryer and dried under controlled conditions of temperature and relative humidity. The banana was dried at the temperature of 40°C, 50°C and 60°C the relative humidity of 10%, 20% and 30% with the air speed of 1 ms⁻¹.

A schematic diagram of this laboratory dryer is shown in Fig 1. The laboratory dryer comprises a ceramic packed bed for producing saturated air at a given temperature, an electrical heater, a blower, a drying section, measurement sensors data recording device and a controlling system. In this laboratory dryer, the blower forces ambient air through a humid ceramic packed bed. The air absorbs moisture while it passes through the packed bed. At the top of the packed bed, this air leaves in a humidified condition. Then, this saturated air is heated by the air heater and passes across the product placed in the tray. The relative humidity (rh) and temperature of the drying air are controlled by adjusting the power supply to the air heater and the water heater using a psychrometric chart as a guideline.

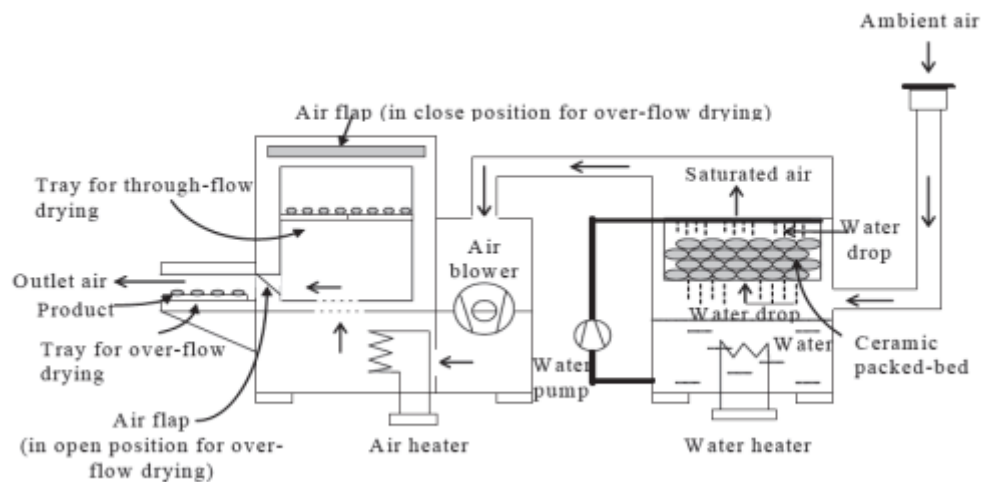


Fig 1 Schematic diagram of the laboratory dryer

Prior to an experiment, the laboratory dryer was allowed to run for 1 hour to obtain a steady temperature. For each experiment banana about 230 g were placed in the drying tray. The drying air temperatures were monitored using thermocouples (K type, accuracy $\pm 2\%$). These thermocouples were connected to a digital data logger (Yokogawa, Model DC100). Voltage from the thermocouples was converted into temperature by internal software of the data logger. The weights of banana were monitored by a digital balance.

The thin layer drying experiments were conducted at the temperature of 40°C, 50°C and 60°C and the relative humidity of the drying air of 10%, 20% and 30%. Nine sets of experiments were conducted for the banana.

2.2.2 Mathematical modeling

There are three approaches to the modeling of thin layer drying of agricultural products (Bala, 1998). These are: (a) theoretical approach, (b) semi-theoretical approach and (c) empirical approach. A theoretical equation gives a better understanding of the transport processes but an empirical equation gives a better fit to the experimental data without any understanding of the transport processes involved. The semi-theoretical equation gives some understanding of the transport processes.

Thin layer drying models of experimental data of the banana are expressed in the form of moisture content ratio of samples during drying, and it is expressed as:

$$MR = \frac{M - M_e}{M_0 - M_e} \quad (2.1)$$

where MR is the dimensionless moisture content or moisture ratio; and M, M_0 and M_e are the moisture content at any given time, the initial moisture content and the equilibrium moisture content, respectively.

In general, an agricultural moist product is composed of water and dried solid mass. The moisture content (M) of the product in dry basis (% , db.) can be calculated from the following equation:

$$M = \frac{m - m_{\text{solid}}}{m_{\text{solid}}} \times 100\% \quad (2.2)$$

where m is mass of the product and m_{solid} is mass of dried solid mass of the product. m can be obtained by using a balance or load cell. In order to obtain dried solid mass (m_{solid}), the water in the product must be totally removed by drying the product in an oven at the temperature of 103°C for 24 hours Bala (1998).

To select a suitable model for describing the drying process of banana, seven different thin-layer drying models were selected to fit the thin-layer experimental data of banana. The selected thin-layer drying models are presented in table 1.

The models were fitted to the experimental data by direct least square. The coefficient of determination (R^2) was one of the main criteria for selecting the best equation. In addition to R^2 , the goodness of fit was determined by root mean square error (RMSE). For the best fit, the R^2 value should be high and RMSE values should be low RMSE and R^2 are defined as:

$$\text{RMSE} = \sqrt{\frac{\sum_{i=1}^n (\text{MR}_{\text{model},i} - \text{MR}_{\text{exp},i})^2}{N}} \times 100\% \quad (2.3)$$

$$R^2 = \frac{1 - \text{Residual sum of squares}}{\text{Corrected total of squares}} \quad (2.4)$$

where $\text{MR}_{\text{exp},i}$ and $\text{MR}_{\text{model},i}$ are the moisture ratio derived from the experiments and the moisture ratio derived from the model. $\overline{\text{MR}}_{\text{exp}}$ is mean moisture ratio obtained from experiments, N is the number of observations.

Table 1 The 7 selected thin-layer drying models.

No.	Model equation	Name of the model
1	$MR=\exp(-kt)$	Newton (Mujumdar, 1987)
2	$MR=\exp(-kt^n)$	Page (Diamante, 1993)
3	$MR=\exp(kt^n)$	Modified Page (Whith et al., 1978)
4	$MR=a \exp(-kt)$	Handerson and Pabis (Zhan et al., 1991)
5	$MR=a \exp(-kt)+c$	Logarithmic (Yangcioglu et al., 1999)
6	$MR=a \exp(-kt)+b\exp(-gt)$	Two term (Handerson ,1974)
7	$MR=a\exp(-kt)+b\exp(-gt)+c \exp(-pt)$	Modifile Handerson and Pabis (Karathanos et al., 1999)

2.3 Results and discussions

2.3.1 Drying characteristics of banana

The changes in moisture contents with time for different drying air temperatures are shown in Fig 2, 3 and 4 for banana. The final moisture content of samples dried under different conditions ranged from 20% to 50% (db.) for banana. The drying rate is higher for higher air temperature. As a result, the time taken to reach the final moisture content is less, as shown in Fig 2, 3 and 4 for banana. Therefore, the drying air temperature has an important effect on the drying of banana. The variations of moisture contents with time for different levels of relative humidity in the range of 10%, 20% and 30% can also be seen in Fig 2, 3 and 4 for banana, respectively.

Fig 5, 6 and 7 show the comparisons of the predicted and experimental data of thin layer drying of banana for Logarithmic model, respectively.

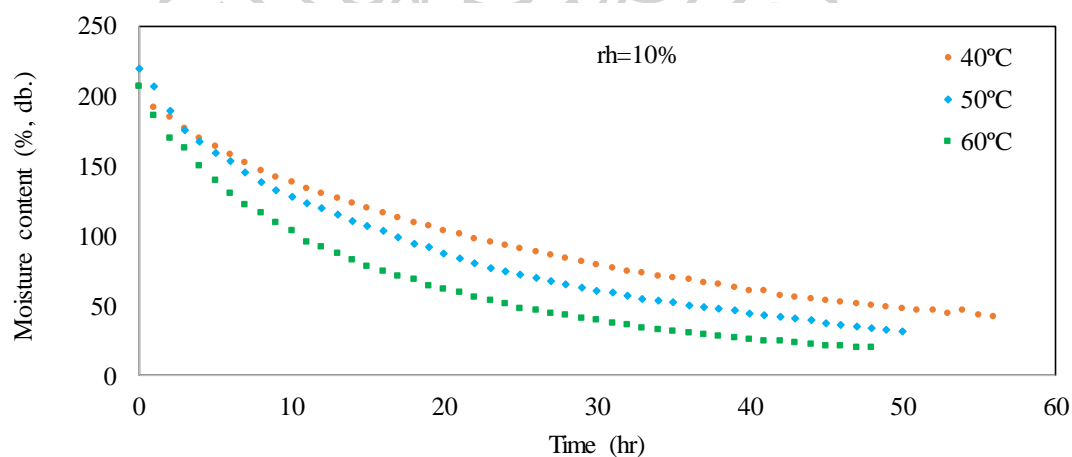


Fig 2 Thin layer drying of banana at different temperatures (40°C, 50°C and 60°C) and relative humidity (10%) from the experiments.

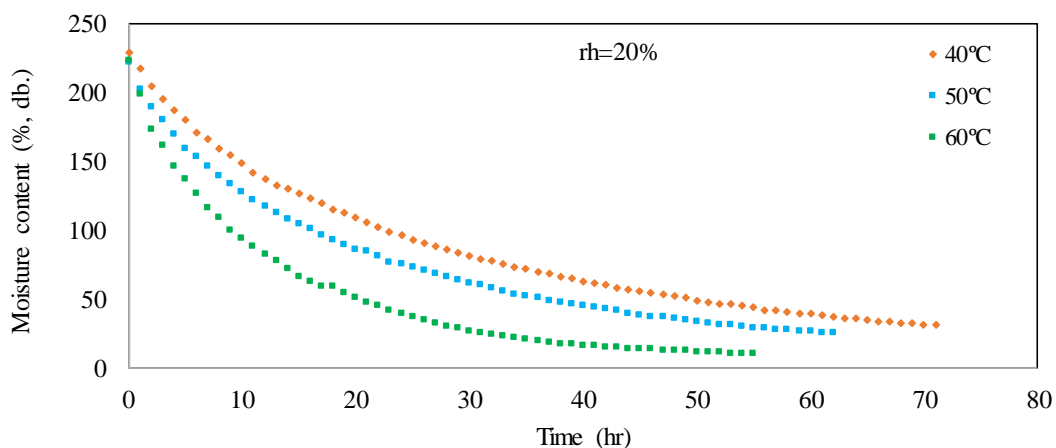


Fig 3 Thin layer drying of banana at different temperatures (40°C, 50°C and 60°C) and relative humidity (20%) from the experiments.

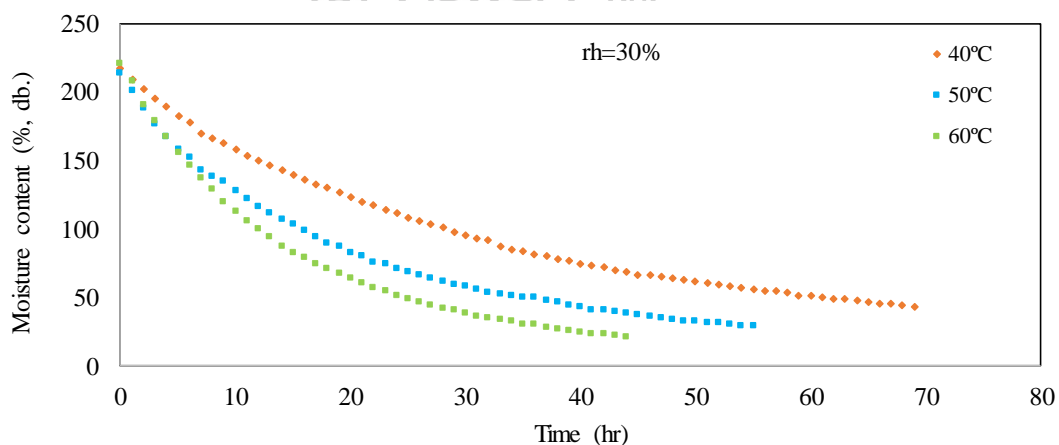


Fig 4 Thin layer drying of banana at different temperatures (40°C, 50°C and 60°C) and relative humidity (30%) from the experiments.

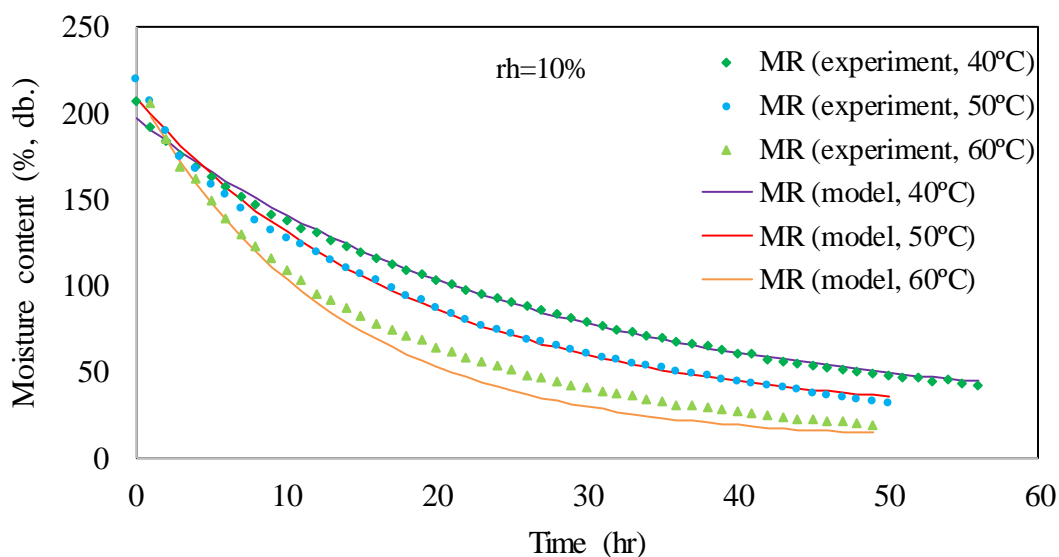


Fig 5 Predicted and observed moisture content of banana using Logarithmic model at the temperatures of 40°C, 50°C and 60°C and relative humidity of 10%.

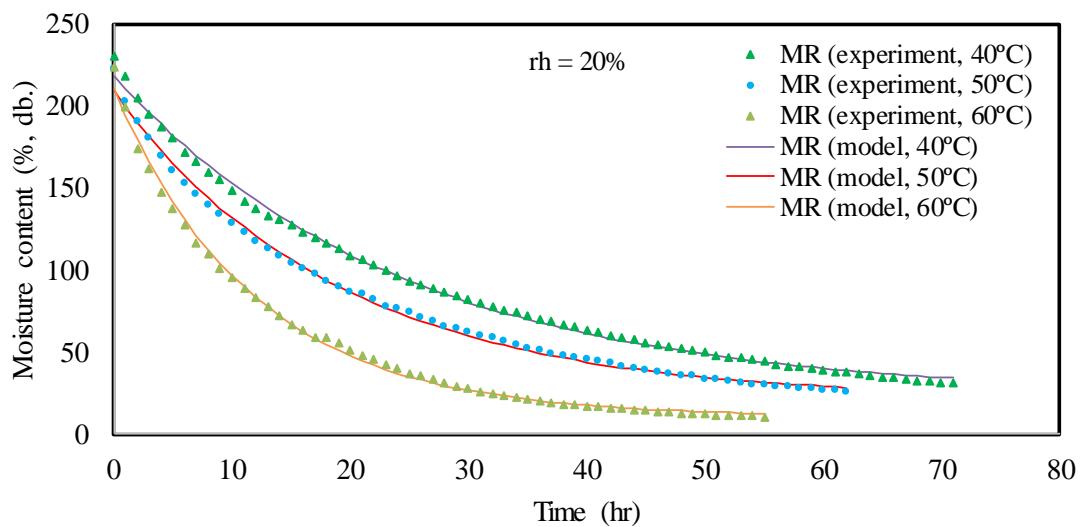


Fig 6 Predicted and observed moisture content of banana using Logarithmic model at the temperatures of 40°C, 50°C and 60°C and relative humidity of 20%.

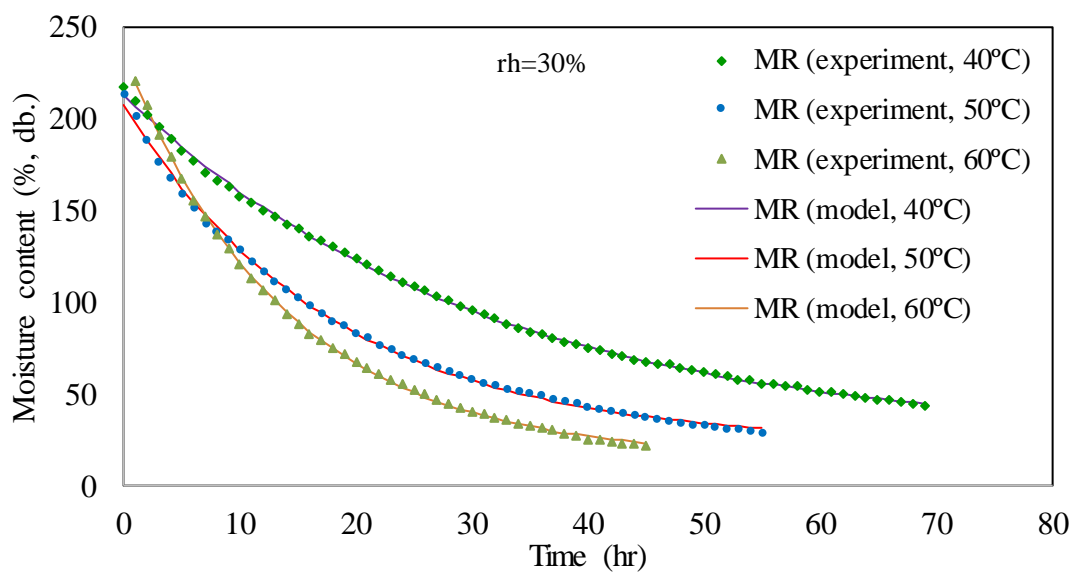


Fig 7 Predicted and observed moisture content of banana using Logarithmic model at the temperatures of 40°C, 50°C and 60°C and relative humidity of 30%.

Table 2 Parameter value, coefficient of determination (R^2) and root mean square error (RMSE) value of the different models for banana.

Models	T°C	rh(%)	k	a	b	c	n	g	p	R^2	RMSE (%)
Newton	40	10	0.0526							0.9913	7.9925
	50	10	0.0648							0.9933	7.7130
	60	10	0.0944							0.9870	18.060
	40	20	0.0479							0.9948	7.1324
	50	20	0.0603							0.9949	8.4647
	60	20	0.0898							0.9959	10.219
	40	30	0.0421							0.9943	7.4637
	50	30	0.0630							0.9971	5.2679
	60	30	0.0791							0.9986	4.6858
Page	40	10	0.0533				0.9954			0.9913	4.6516
	50	10	0.0756				0.9476			0.9937	4.3591
	60	10	0.1161				0.8901			0.9933	12.747
	40	20	0.0566				0.9489			0.9953	6.6605
	50	20	0.0835				0.8903			0.9964	6.5819
	60	20	0.1394				0.8234			0.9991	8.2404
	40	30	0.0383				1.0195			0.9957	7.3850
	50	30	0.0653				0.9877			0.9972	5.2209
	60	30	0.0703				1.0427			0.9985	4.0316
Modified Page	40	10	-0.0536				0.9601			0.9997	7.4278
	50	10	-0.0540				1.0366			0.9997	6.3902
	60	10	-0.0542				1.1721			0.9964	11.558
	40	20	-0.0440				1.0084			0.996	8.9029
	50	20	-0.0589				0.9885			0.9965	9.8233
	60	20	-0.0844				0.9913			0.9967	13.447
	40	30	-0.0245				1.1465			0.9963	7.8640
	50	30	-0.0474				1.0731			0.9973	9.2430
	60	30	-0.0500				1.1332			0.9976	10.399
Henderson and Pabis	40	10	0.0510	0.9717						0.9927	4.7398
	50	10	0.0622	0.9611						0.9946	4.0766
	60	10	0.0939	0.9942						0.9874	9.6870
	40	20	0.0460	0.9617						0.996	6.0109
	50	20	0.0567	0.9427						0.9963	5.9558
	60	20	0.0839	0.9366						0.9966	6.9222
	40	30	0.0426	1.0137						0.9937	7.3515
	50	30	0.0619	0.9823						0.9976	4.9551
	60	30	0.0800	1.0116						0.9984	4.2465
Logarithmic	40	10	0.0368	1.0368		-0.1012				0.9977	2.2824
	50	10	0.0545	0.9859		-0.0456				0.9962	3.2961
	60	10	0.0775	1.0114		-0.0547				0.9968	3.6084
	40	20	0.0411	0.9801		-0.0376				0.9973	4.7532
	50	20	0.0530	0.9516		-0.0208				0.9969	5.3865
	60	20	0.0842	0.9364		-0.0009				0.9966	6.9191
	40	30	0.0329	1.0806		-0.1060				0.9994	2.1521
	50	30	0.0559	0.9987		-0.0339				0.9988	3.3375
	60	30	0.0720	1.0291		-0.0359				0.9996	1.9182
Two-term	40	10	0.0484	0.5413	0.4130			0.0484	0.0510	0.9946	4.7984
	50	10	0.0748	4.7822	-3.8317			0.0788	0.0622	0.9947	3.9603
	60	10	0.0900	0.5483	0.4305			0.0900	0.0856	0.9904	9.8899
	40	20	0.0457	0.4749	0.0839			0.0456	0.0454	0.9961	6.0323
	50	20	0.0567	0.4713	0.4713			0.0567	0.0566	0.9963	5.9558
	60	20	0.6910	0.1298	0.8739			0.0788	0.0566	0.9993	3.4973
	40	30	0.0424	0.5062	0.5058			0.0424	0.0408	0.9939	7.3578
	50	30	0.0619	0.4859	0.4964			0.0619	0.0616	0.9979	4.9551
	60	30	0.0796	0.4995	0.5101			0.0796	0.0789	0.9984	4.2998
Modified Henderson and Pabis	40	10	0.0510	0.3261	0.3184	0.3271		0.0510	0.0510	0.9927	4.3798
	50	10	0.0622	0.3048	0.3149	0.3412		0.0622	0.0622	0.9946	4.0766
	60	10	0.5093	0.0452	0.1591	0.7828		0.0833	0.0856	0.9923	10.516
	40	20	0.0454	0.3114	0.3143	0.3309		0.0454	0.0454	0.9963	6.0794
	50	20	0.0566	0.3679	0.2684	0.3054		0.0566	0.0566	0.9964	5.9580
	60	20	0.0784	0.4871	0.3804	0.1345		0.0780	0.6187	0.9993	3.5191
	40	30	0.0480	0.3492	0.3279	0.3209		0.0408	0.0408	0.9956	7.9041
	50	30	0.0616	0.3291	0.3303	0.3112		0.0616	0.0616	0.9977	4.9651
	60	30	0.0789	0.3495	0.3029	0.3539		0.0789	0.0789	0.9986	4.6375

2.3.2 Mathematical modeling of thin-layer drying

Seven thin layer drying model (Table 1) is fitted to the experimental data of moisture ratio of banana dried at different temperatures and relative humidity. The parameter values, R^2 and RMSE, are also shown in Table 2 of banana. The Logarithmic model was found to be the best, followed by the modified Handerson and Pabis model. The value of R^2 of the Logarithmic model was 0.9962-0.9966 and 0.9904-0.0993 of banana respectively, indicating good fit and RMSE was 1.91%-6.91% and 3.51%-10.51% of banana respectively. Empirical expressions were developed for the drying parameters of the Logarithmic model and the drying parameters were found to be a function of drying air temperature (T in °C) and relative humidity (rh in %).

$$k = 34609.76 - 1369.52T + 1897.71rh - 32Trh + 7.20T^2 + 24.80rh^2 \quad (2.5)$$

$$c = -20472.9 + 10.70T - 815.6rh - 18Trh + 22.4T^2 - 4.4rh^2 \quad (2.6)$$

2.4 Conclusions

Thin layer drying of banana was investigated in this study and the drying rate increases with the increase of air temperatures. The entire drying process occurred in the falling rate period. Seven thin layer drying models were fitted to the experimental data of banana to describe the drying characteristics of banana. Drying parameter of Logarithmic model was found to be a function of drying air temperature and relative humidity. The Logarithmic model was the best, followed by the modified Handerson and Pabis model. The Logarithmic model can be used both to assess the drying behavior of banana and for simulation and optimization of the dryer for efficient operation.



Chapter 3

Modeling of Banana Drying Using Finite Element Method

3.1 Introduction

Several numerical methods available in simulation study, the finite element method have been widely applied to model heat and mass transfer. The finite element method assumes that any continuous quantity such as moisture content can be approximated by a discrete model composed of a set of piecewise continuous functions defined over a finite number of sub-domains or element (Janjai et al., 2008; Segerlind, 1984). Element are connected at nodal points along the boundaries and their equations are obtained by minimizing a function of the physical problem. The finite element method has been extensively used to solve problems having irregular geometrical configurations and material properties depending on the temperature and moisture.

The finite element method is one of the most appropriate techniques to model the moisture transport inside the banana for an accurate prediction of moisture movement and moisture content profiles inside the banana. Optimum design and operation of banana dryer can also be accomplished by using drying model of the banana. In order to conserve energy during banana drying and for proper understanding of transfer processes during drying for production of quality dried products, knowledge of drying characteristics of the products is essential.

Reported finite element simulation of heat and mass transfer of banana slices considering a rectangular boundary (Ranjan, Irudayaraj, Reddy, & Mujumdar, 2004). As a result, it does not provide accurate moisture distribution profiles inside the banana for better understanding of the transport process during drying. Thus, there is a research gap in the finite element modeling of drying of banana for providing accurate moisture distribution profiles inside the banana for better understanding of the transport process during drying. Also no systematic finite element simulation study on drying of banana has been reported so far. Therefore, the objective of this work was to develop a finite element simulation model of banana considering the irregular boundary of the banana for accurate prediction of the moisture movement and moisture distribution profiles inside the banana during drying.

3.2 Materials and methods

3.2.1 Experimental study

Thin layer drying of banana (Namwa variety) was conducted to compare the finite element model predictions with the experimental values and to determine the moisture diffusivity of banana. It was collected from a market in Nakhon Pathom, Thailand and stored at room temperature. Thin layer drying of banana was conducted under controlled conditions of temperature of 40°C, 50°C and 60°C and relative humidity of 20-40% in a laboratory dryer. Banana was dried as a whole fruit. The laboratory dryer used is the same as that described in chapter 2.

3.2.2 Uncertainty analysis

Uncertainty analysis refers to the uncertainty or error in experimental data. In general, it can be categorized as systematic error and random error. The systematic error can be removed by a calibration. The random error cannot be removed but it can be statistically quantified.

The variable x_i that has an uncertainty Δx_i is expressed as (Doiebelin, 1976; Holman, 1978; van Nydeck Schenck & Hawks, 1979);

$$x_i = x_{\text{mean}} (\text{measures}) \pm \Delta x_i \quad (3.1)$$

where x_i is actual value, x_{mean} is measured value (mean value of the measurements) and Δx_i is uncertainty in the measurement. There is an uncertainty in x_i that may be as large as Δx_i . The value of Δx_i is the precision index that is usually taken as 2 times the standard deviation and it encloses approximately 95% of the population for a single sample analysis. In this study, statistical analysis was carried out to estimate root mean square error (RMSE) (Iqbal, 1983) between the finite elements predicted moisture content and experimentally determined values, and correlation coefficient (R^2) (Iqbal, 1983).

3.2.3 Finite element modeling of banana

Moisture transport within banana during drying process can be figured as the following equation (Bala, 2017) :

$$\frac{\partial M}{\partial t} = \nabla \cdot (D \nabla M) \quad (3.2)$$

where M is moisture content on dry basis, D is moisture diffusivity, and t is time.

The hypotheses for solving Eq. (3.2) for banana by finite elements simulation are as follows:

- 1) Drying process is isothermal.
- 2) Flesh of banana is dried and it is relatively homogeneous.
- 3) Initial moisture content is uniform for the banana.
- 4) Moisture transport within banana is two directional.

The equation for diffusion in two dimensions is as follows:

$$\frac{\partial M}{\partial t} = D \left(\frac{\partial^2 M}{\partial x^2} + \frac{\partial^2 M}{\partial y^2} \right) \quad (3.3)$$

with initial and boundary conditions as:

$$\text{at } t = 0, M = M_0 \quad (3.4)$$

$$\text{and } t > 0; -D \frac{\partial M}{\partial n} = h_m (M_s - M_e) \quad (3.5)$$

where h_m is the mass transfer coefficient, M_s is surface moisture content on dry basis, M_e is the equilibrium moisture content on dry basis and n is the magnitude of a normal vector to the surface.

Finite element equations are derived from an incorporation of Galerkin's formulation of the weighted residual method, and using Galerkin's method it can be expressed as:

$$\int_{\Omega} [N]^T \left[D \left[\frac{\partial^2 M}{\partial x^2} + \frac{\partial^2 M}{\partial y^2} \right] - \frac{\partial M}{\partial t} \right] d\Omega = 0 \quad (3.6)$$

where $[N]$ a matrix of interpolating is function and Ω is the banana domain

An equation system is developed by evaluating the weighted residual integral and using Green's theorem. This results in a first order differential equation as follows:

$$[c] \frac{d\{M\}}{dt} + [k]\{M\} = \{f\} \quad (3.7)$$

where

$$[c]: \text{element capacitance matrix} = \int_{\Omega} [N]^T [N] d\Omega \quad (3.8)$$

$$[k]: \text{element stiffness matrix} = \int_{\Omega} D \left(\frac{\partial [N]}{\partial x} \frac{\partial N}{\partial x} + \frac{\partial [N]}{\partial y} \frac{\partial N}{\partial y} \right) d\Omega \quad (3.9)$$

$\{M\}$: vectors of unknown, which can be defined as

$$M = [N]\{M\} \quad (3.10)$$

$\{f\}$: element force vector

when the element matrices $[c]$ are summed up with the element matrices $[k]$ by using the direct stiffness procedure, the final outcome of the system can be obtained in terms of first order differential equations as follows (Segerlind, 1984):

$$[C] \left\{ \frac{\partial M}{\partial t} \right\} + [K]\{M\} = \{F\} \quad (3.11)$$

where $[C]$: global capacitance matrix

$[K]$: global stiffness matrix

$[F]$: load force vector

Eq. (3.11) can be written as in the finite difference form as follows:

$$([C] + \Delta t[K])\{M\}_{t+\Delta t} = [C]\{M\}_t + \Delta t\{F\}_{t+\Delta t} \tag{3.12}$$

where Δt is the time step.

The final system of Eq. (3.11) has the following form:

$$[A]\{M\}_{t+\Delta t} = [P]\{M\}_t + \{F_*\} \tag{3.13}$$

where

$$[A] = ([C] + \Delta t[K])$$

$$[P] = [C]$$

and

$$\{F_*\} = \Delta t\{M_e\}_{t+\Delta t} \tag{3.14}$$

Moisture moves from inside of the banana to the outer surface and passes through uniform diffusivity. To analyze the problem, a two-dimensional finite element triangular grid is used to model the banana and the domain of the whole banana in two dimensions is solely taken into account because of the irregular geometry of the banana. The domain consists of banana flesh. The finite element discretization of the banana in two dimensional sections is shown in Fig 8. The average moisture content of banana was calculated using the method proposed by Haghghi and Segerlind (Haghghi, 1988). Fig 8 shows finite element discretization for two dimensional sections of the banana consisting of 664 grids and 1230 triangular elements.

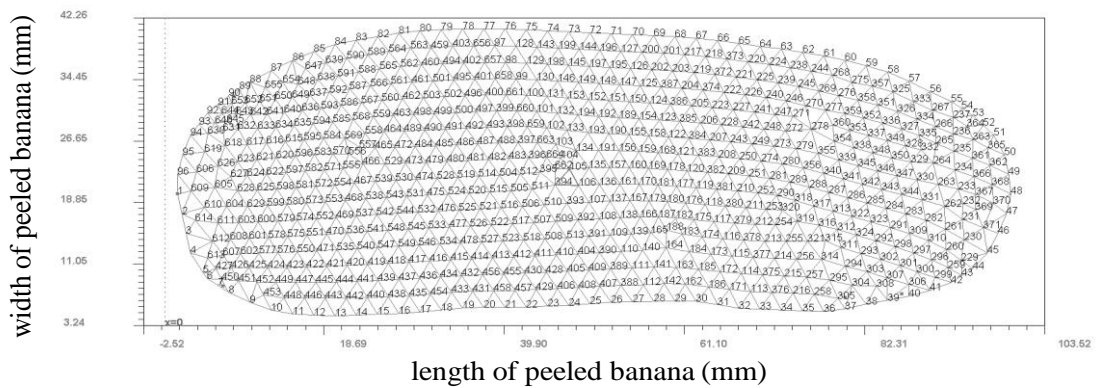


Fig 8 Mesh distribution and geometry considered in the finite element model of banana

3.3 Thermo-physical properties of banana

3.3.1 Moisture diffusivity of banana

In this study, Fick's law of diffusion incorporated with drying experiments was used to determine moisture diffusivity of banana. Banana was assumed to have a cylindrical shape and the analytical solution of the Fick's law for banana was fitted to the drying experiments to obtain the diffusivity. As a result, the diffusivity (D) of banana can be expressed as a function of the absolute temperature (T_{ab}) using the Arrhenius type equation as follows:

$$D = 9.869 \times 10^{-6} \exp(-2527.53/T_{ab}) \quad (3.15)$$

This equation was used to compute the moisture diffusion within banana.

3.3.2 Equilibrium moisture content of banana

Equilibrium moisture contents of banana were determined experimentally using the method and equipment similar to that of longan (*Dimocarpus longan* Lour) (Janjai et al., 2006). The desorption isotherm curves of banana were constructed from the experimental results. Five models of the isotherm, namely Day and Nelson (Day & Nelson, 1965), modified Halsey (Champion & Halsey Jr, 1953; Pankaew, 2016), modified Chung-Pfost (Chung & Pfost, 1967; Pankaew, 2016) modified Oswin (Oswin, 1946; Pankaew, 2016) and Kaleemullah (Kaleemullah & Kailappan, 2004) were fitted to the experimental data of the isotherm. It was found that the modified Oswin model fitted the best to the isotherm of banana and the model with the coefficient for banana can be written as:

$$a_w = \frac{1}{1 + \left[\frac{389.6555 + (-1.0562)T}{M_e} \right]^{2.8370}} \quad (3.16)$$

where T is temperature ($^{\circ}\text{C}$), a_w is water activity (decimal) and M_e is equilibrium moisture content (% db.).

3.3.3 Shrinkage

In general, volumetric shrinkage of biological materials is a function moisture content (Souraki & Mowla, 2008). In this study, drying experiments were conducted in the laboratory dryer described in section 2.1. Dimensions of banana were measured to determine its volume and weight of the banana was monitored for moisture content determination. From the experimental data, the volumetric shrinkage of banana can be expressed as:

$$\frac{V}{V_i} = 0.351 + 0.648 \frac{M}{M_i} \quad (3.17)$$

where V_i is initial volume of banana with the moisture is content M_i and V is volume of banana having moisture content M . This shrinkage model was used in the process of obtaining numerical solution of the finite element model.

3.3.4 Surface mass transfer coefficient

The surface mass transfer coefficient of banana (h_m) is computed by using the relation developed by Patil and Subbaraj (1988):

$$h_m = \frac{D_{air}}{d} (2.0 + 0.522 Re^{0.5} Sc^{0.33}) \quad (3.18)$$

where D_{air} is diffusivity of air (m^2/s), d is equivalent diameter of banana (m), Re is Reynolds number and Sc is Schmidt number. Air diffusivity values used for the simulation are $2.346 \times 10^{-5} m^2/s$ and $2.632 \times 10^{-5} m^2/s$ for the temperature of $40^\circ C$ and $60^\circ C$, respectively (Cengel, 2008).

Reynolds number (Re) and Schmidt number (Sc) can be defined as follows:

$$Re = \frac{ud\rho_{air}}{\mu} \quad (3.19)$$

$$Sc = \frac{\mu}{\rho_{air} D_{air}} \quad (3.20)$$

where u is air velocity (m/s), d is equivalent diameter (m), ρ_{air} is air density (kg/m^3), D_{air} is diffusivity of air (m^2/s) and μ is air viscosity (m^2/m)

3.3.5 Method of solution

The solution is started with computation of equilibrium moisture content (M_e) using Eq. (3.16) and surface mass transfer coefficient (h_m) of banana is computed by using Eq. (3.18) and then these are substituted in the element equations at the surface of banana. Next, the element Eq. (3.7) is assembled in form of the global Eq. (3.11) which has triangular zed element which is solved by the method of back substitution and then the average moisture content is computed. The process is repeated until reaching the time limit or final average moisture content is achieved.

3.4 Results and discussions

Finite element model for banana drying was simulated to predict the moisture content changes and moisture content profiles inside the banana during drying and it was programmed in Compaq Visual FORTRAN version 6.5. The simulated moisture contents averaged over the whole fruit of banana were compared with the experimental values for the temperature of 40-60°C and relative humidity of 20-40% in order to validate the model. The discrepancy in term of root mean square error (RMSE) was in the range of 2.2-14.6% and the coefficient of determination (R^2) is in the range of 0.97-0.99. These results reveal that the moisture content obtained from the model and that from the experiment is in reasonable agreement. Fig 9 shows the example of the comparison for the temperature (T_a) of 50°C and relative humidity (rh) of 20%.

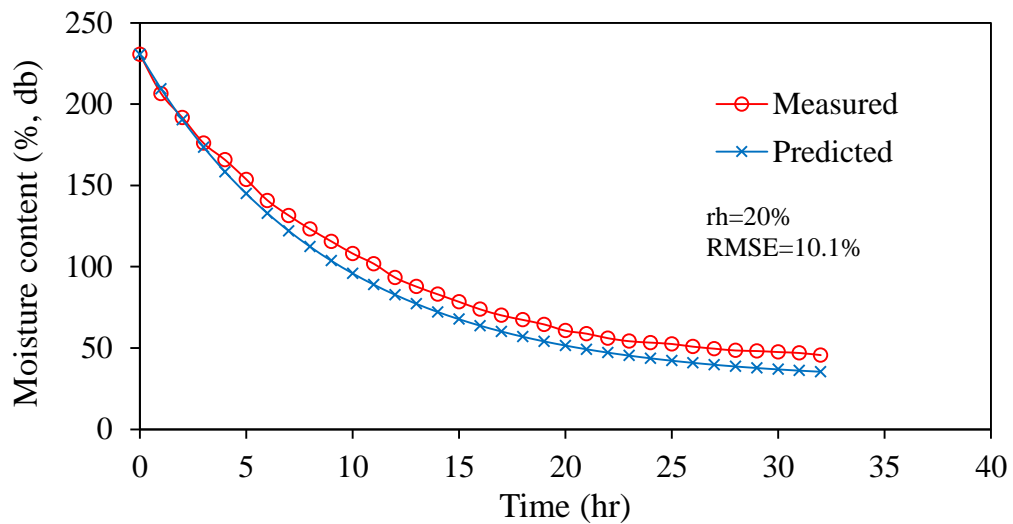


Fig 9 Example of comparison of the finite element predicted moisture contents with the experimental data of banana at $T_a=50^\circ\text{C}$ and $\text{rh}=20\%$.

Fig 10 shows the contour plots of the predicted moisture contents at various times of drying of the banana and these profiles provide pictures of how moisture moves from inside of the banana to the outer surface of the banana smoothly. As drying continues, the dried zone and drying front move further inside the banana with passage of time until the banana is fully dried to equilibrium moisture content in equilibrium with drying air (Janjai et al., 2008) also reported patterns of moisture movement in finite element simulated drying of mango slices.

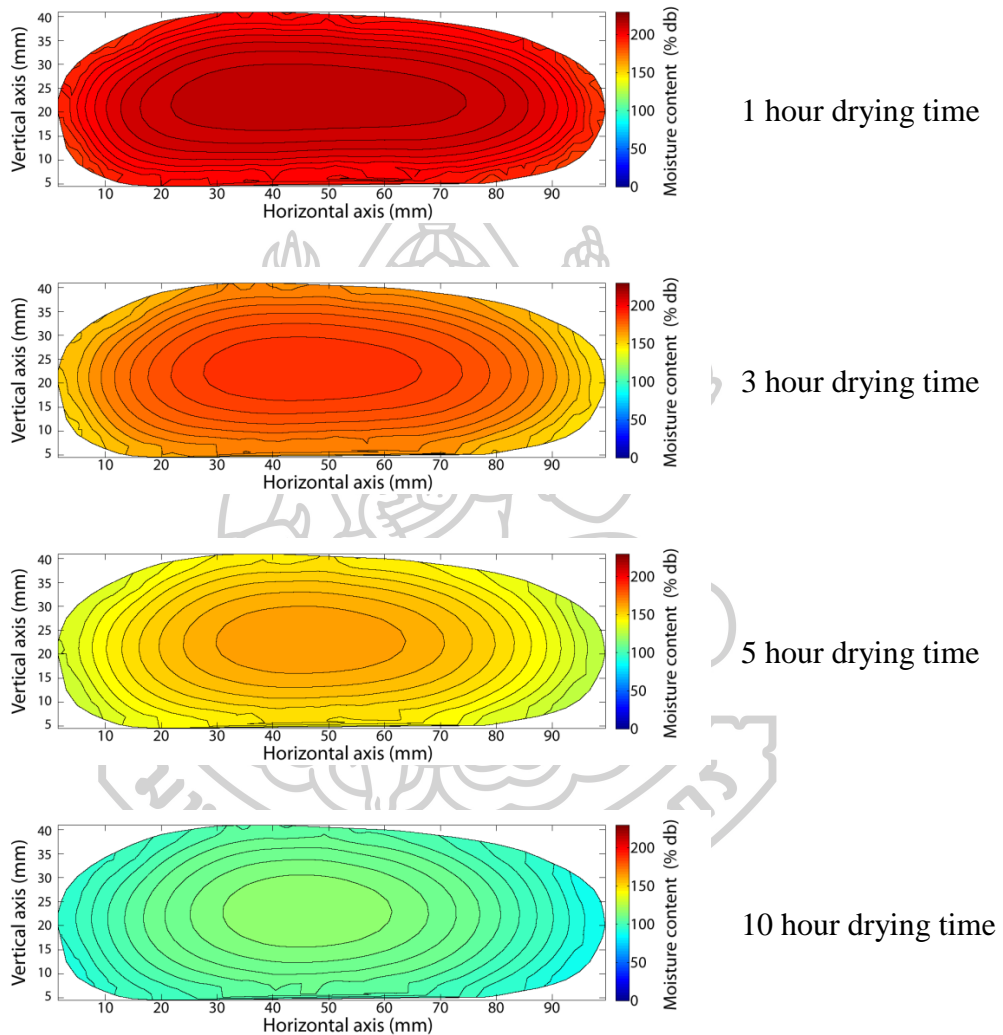


Fig 10 Contours of moisture contents inside the banana for different drying times.

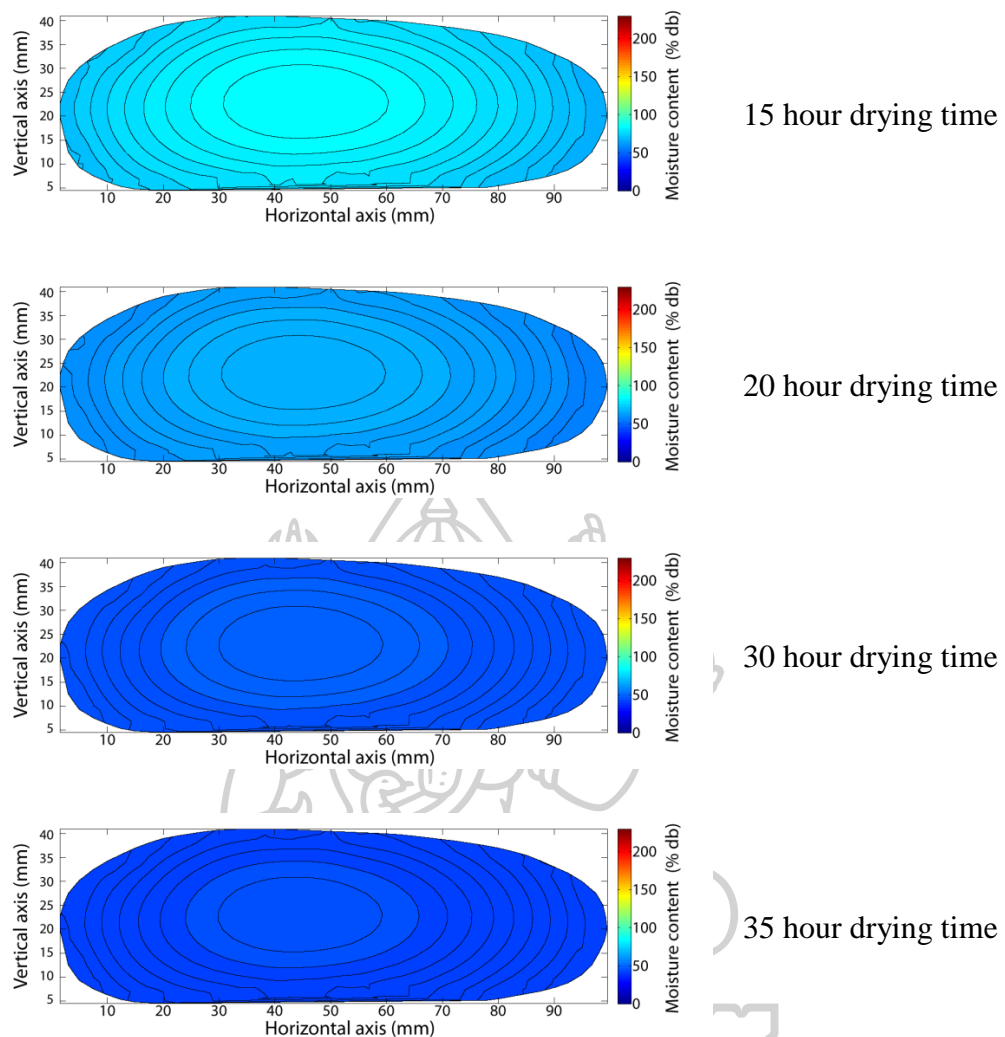


Fig 10 Contours of moisture contents inside the banana for different drying times.
(continue)

3.5 Conclusions

A two-dimensional finite element model has been developed for drying of banana. The models for moisture diffusivity, sorption isotherm and volumetric shrinkage have been also experimentally determined and then used in the finite element model. The model provides the moisture content distribution inside banana and the average moisture contents obtained from this distribution reasonably agree with the moisture contents of whole fruit of banana obtained from the experiments. The information on the dynamics of moisture movement and progression of moisture content profiles during drying of banana has been revealed by the model. This model has high potential to be used for optimal design of banana dryers.

Chapter 4

Drying of Banana in a Parabolic Greenhouse Solar Drying

4.1 Introduction

Thailand is located in a tropical zone which receives relatively high solar radiation Janjai et al., (2005a) , making solar drying technologies to be a promising solution of the drying problems. Consequently, several types of solar dryer have been proposed to dry agricultural products in Thailand (Boonlong et al., 1984 ; Exell & Kornsakoo, 1976 ; Soponronnarit, Assayo, & Rakwichian, 1991 ; Wibulsawas & Thaina, 1980). However, prior to this work very few solar dryers were used in the field. This is mainly due to the fact that these dryers could not meet the demand of users. Realizing this problem, a parabolic greenhouse type solar dryer was developed. The objective of this paper is to present the field performance of this type of dryer to dry banana.

4.2 Materials and methods

The parabolic greenhouse solar dryer consists of a parabolic roof structure made from polycarbonate sheets on a concrete floor. The dryer has a width of 8.0 m, length of 12.0 m and height of 3.5 m with a loading capacity of about 300 kg of bananas. Nine DC fans powered by three 50-Watt solar cell modules were installed in the wall opposite to the air inlet to suck humid air from the dryer to surrounding environment. A pictorial view of the dryer is shown in Fig 11.



Fig 11 Pictorial view of the parabolic greenhouse dryer

For each drying experiment, about 300 kg of these products was placed on the trays in thin layer. To monitor the moisture content, product samples were also placed on the trays and were weighted periodically at 1-hour interval using a digital balance (Kern, model 474-42). Also, about 160 g of product sample was dried outside the dryer (natural sun drying) in order to compare the drying behavior of the product with those dried in the dryer. At the end of the experiment the dry solid mass of the samples was determined by the oven method (103°C for 24 hours). Solar radiation, drying air temperature and relative humidity were monitored. Solar radiation was measured by a pyranometer (Kipp&Zonen, model CM 11) placed on the roof of the dryer. Thermocouples (type K) were used to measure air temperature in the dryer and ambient air. The relative humidity of drying air and ambient air were periodically measured by hygrometers (Elektronik, model EE23). Voltage signals from the pyranometer, hygrometers and thermocouples were recorded every 10 minutes by a multi-channel data logger (Yokogawa, model DC100). Before the installations, the pyranometer was calibrated against a pyranometer recently calibrated by the manufacturer. The hygrometers were calibrated using standard saturated salt solutions. All drying experiments were carried out during the period January 2019. The experiments were started at about 8:00 am and continued till 6:00 pm. For all banana drying experiments, banana in the dryer was collected at 6:00 pm and put in plastic bags for fermentation process and redistribution of the moisture in banana fruits during the night. Then it was again placed in the dryer in the next morning about 8:00 am. The drying was continued on subsequent days until the desired moisture content (21%, wb.) was reached.

In addition, samples of banana from different positions in the dryer and one sample dried outside the dryer with natural sun drying were weighted every 1 hour and then the weight data were used to determine moisture content of banana. The position of the measurements is shown in Fig 12. A typical result from the drying experiments is shown in Fig 13-17.

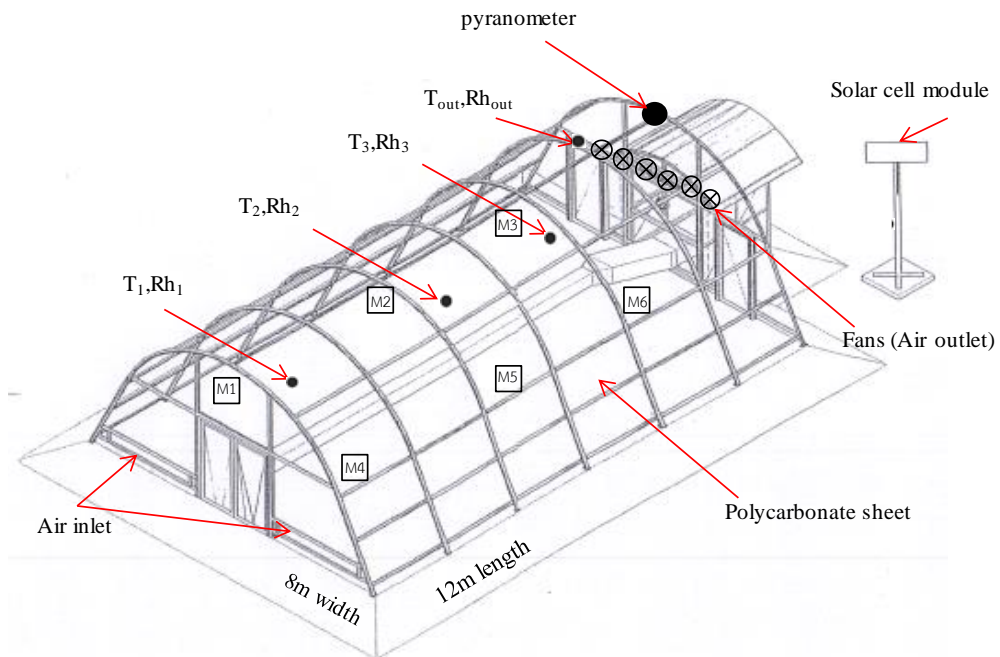


Fig 12 The structure of the dryer and positions of the measurements (M_i , Rh_i , T_i are weight of the sample, relative humidity and air temperature at location i , $i=1, 2, \dots, n$)

4.3 Results and discussions

The experimental tests of the parabolic greenhouse dryer for drying banana products were carried out during January, 2019. The typical result for drying banana during 24 to 27 January, 2019 are shown in Fig 13-17. Fig 13 during the drying of banana, solar radiation increased sharply from 8.00 am to noon but it considerably decreased in the afternoon. The overall cyclic patterns of the solar radiation were similar for every day because the experiment was carried out in January corresponding to the dry season with the majority of clear days.

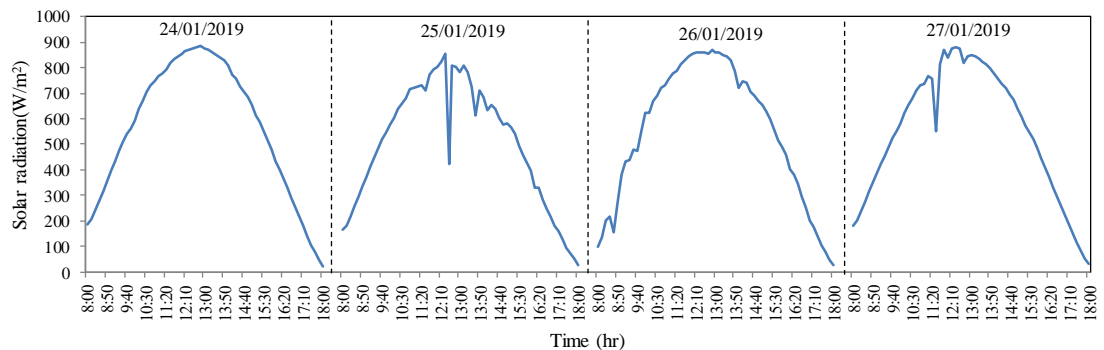


Fig 13 Variation of solar radiation during a drying run for banana.

Fig 14 shows the comparison of air temperatures at three different locations inside the dryer and the ambient air temperature for typical experimental runs of the solar drying of banana. The patterns of temperature changes in different positions were comparable for all locations. Temperatures in different positions at these three locations vary within a narrow band. In addition, temperatures at each location differed significantly from the ambient air temperature.

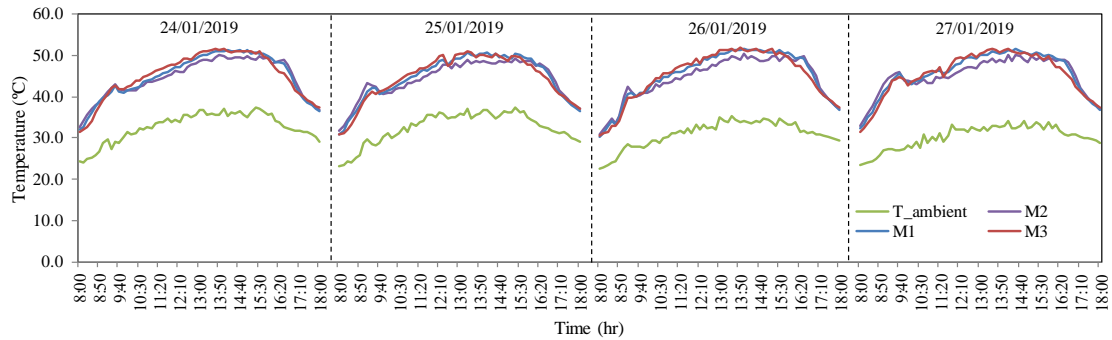


Fig 14 Comparison of the ambient temperature and the temperature inside the dryer for drying for banana.

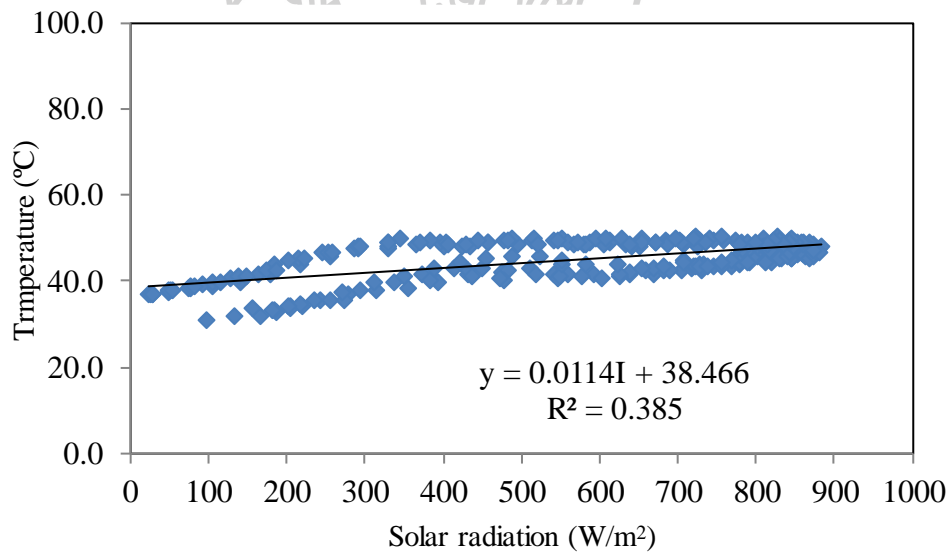


Fig 15 Drying air temperatures at the different levels of the shelves versus solar radiation

Fig 15 shows the plot of drying air temperature at the middle of the dryer versus solar radiation during drying of banana in the greenhouse solar dryer. The relation between the temperature and solar radiation can be expressed as:

$$T=38.466+0.0114I \quad R^2=0.385 \quad (4.1)$$

where T is temperature in °C, I is solar radiation in W/m².

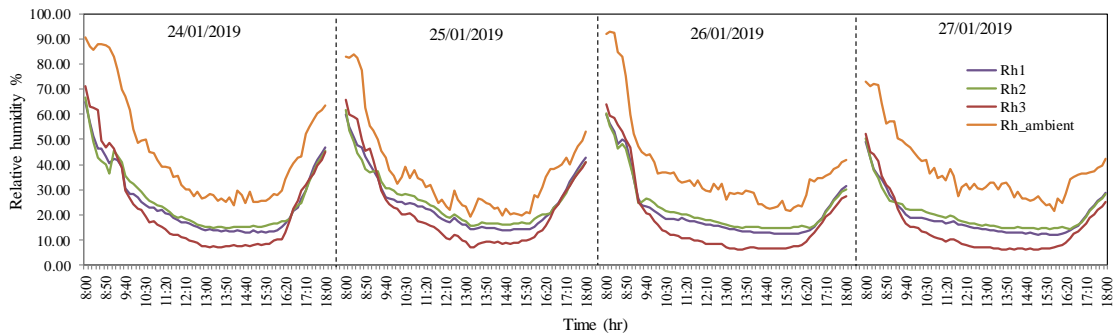


Fig 16 Relative humidity at various points inside the dryer and ambient relative humidity for drying the banana

Fig 16 shows relative humidity inside the dryer for typical experimental runs during solar drying of bananas. Relative humidity decreases with time inside the dryer during the first half of the day. This caused by the decrease of relative humidity of the ambient air and increase of air temperature, whereas the opposite is true for the latter half of the day. The relative humidity of the air inside the dryers is always lower than that of the ambient air and the lowest relative humidity occurs at 2:00-4:00 pm. Thus, the time of day with the most potential for solar drying is between 8:00 am and 6:00 pm. Furthermore, the air leaving the dryer has lower relative humidity than that of the ambient air, which indicates that the exhaust air from the dryer still has drying potential.

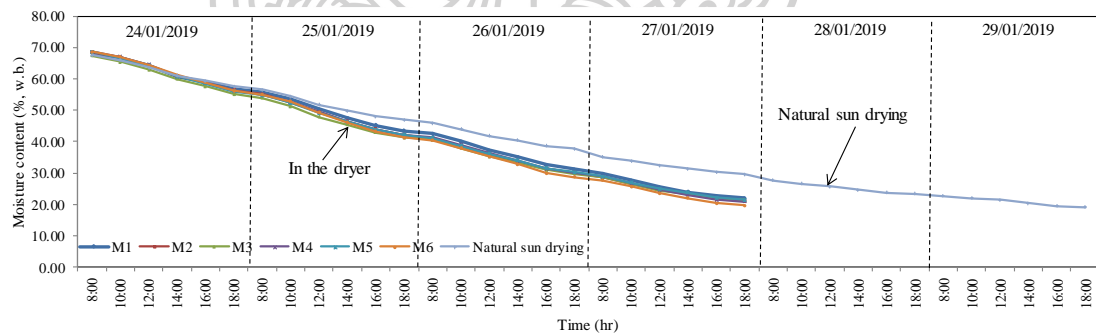


Fig 17 Comparison of the moisture contents for drying the banana inside the dryer and that from natural sun drying

Fig 17 shows the variations in moisture content of banana samples at different positions in the dryer for typical experimental runs compared to the control samples dried in the open-air sun drying. Moisture contents in different positions at these six locations vary within a narrow band. Additionally, moisture content at each location differed significantly from the natural sun drying. The moisture content of bananas in the greenhouse solar dryer was reduced from an initial value of 70% (wb.) to a final value of 19-21% (wb.) within 4 days whereas the moisture content of the sun-dried samples was reduced to 20% (wb.) within the same period. Thus, drying in the solar greenhouse dryer results in a reduced drying time. In addition, the bananas being

dried in this dryer were completely protected from rain, insects and dust, and the dried bananas were of high quality.

4.4 Conclusions

A parabolic greenhouse solar dryer was installed at Silpakorn University in Thailand and a field performance of this dryer was experimentally evaluated. It was found that the dryer helps to shorten the drying time as compared to that of the natural sun drying. In addition, the dryer also helps to protect bananas being dried from rain, insects and birds and good quality of dried bananas was obtained. This type of dryer was installed in many locations in Thailand for small-scale industrial production of dried banana.



Chapter 5

Performance of parabolic greenhouse solar dryer equipped with rice husk burning system for banana drying*

5.1 Introduction

Drying of banana is sensitive to the drying air temperature. If the first day of banana drying in the parabolic greenhouse dryer is cloudy or rainy, banana will be spoiled. Therefore, auxiliary heater as a backup protection is needed for drying of the banana in the parabolic greenhouse solar dryer to provide heat during cloudy or rainy days to avoid this spoilage. Biomass burning system is one of efficient auxiliary units (Fudholi et al., 2010) among other traditional types of auxiliary heaters such as electric heating (Pratoto et al., 1998), LPG gas burner (Smitabhindu et al., 2008) and diesel engine (Eissen et al., 1985). Solar and biomass are two main renewable energy sources suitable for drying applications. The use of biomass burning system would be more appropriate from the costs and reliability points of view to provide clean air with uniform temperature for better quality dried product.

Over the past few decades, several researches on using biomass burner for auxiliary heating of the solar dryers have been reported. Bena and Fuller (Bena & Fuller, 2002) combined a direct-type natural convection solar dryer with a simple biomass burner to demonstrate solar drying technology for drying of small-quantity (20-22kg) of fruits and vegetables in non-electrified area in Australia. Sonthikun (Sonthikun et al., 2016) designed and constructed a solar-biomass hybrid dryer for household scale production (320 kg) for drying of natural rubber sheet in Thailand. There is a research and literature gap in auxiliary heater integrated greenhouse solar dryer. Therefore, the objectives of this study are to develop the parabolic greenhouse solar dryer equipped with rice husk burning system and to assess the performance of this dryer.

*Part of this work was has been accepted to publish in the Journal of Renewable Energy and Smart Grid Technology, 2019, Vol. 14 No. 1

5.2 Materials and methods

5.2.1 Parabolic greenhouse solar dryer equipped with rice husk burning system

The parabolic greenhouse solar dryer equipped with rice husk burning system is shown in Fig 18. The parabolic greenhouse solar dryer, previously called PV-ventilated solar greenhouse dryer, comprises mainly a parabolic roof structure covered by polycarbonate sheets, arrays of trays for placing products to be dried, ventilating fans and a concrete floor (Janjai et al., 2009).

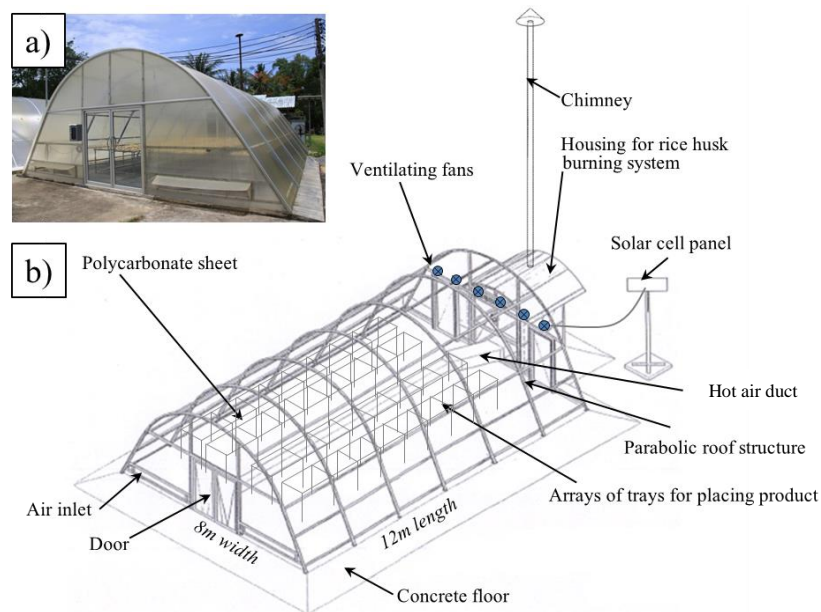


Fig 18 Parabolic greenhouse solar dryer equipped with a rice husk burning system a) pictorial view, b) schematic diagram

In this study, we designed this rice-husk burning system to use it as an auxiliary heater for drying banana in the parabolic greenhouse dryer. The burning system consists of a burning chamber, air-to-air heat exchanger, screw feeder of rice husk and controller (Fig 19).

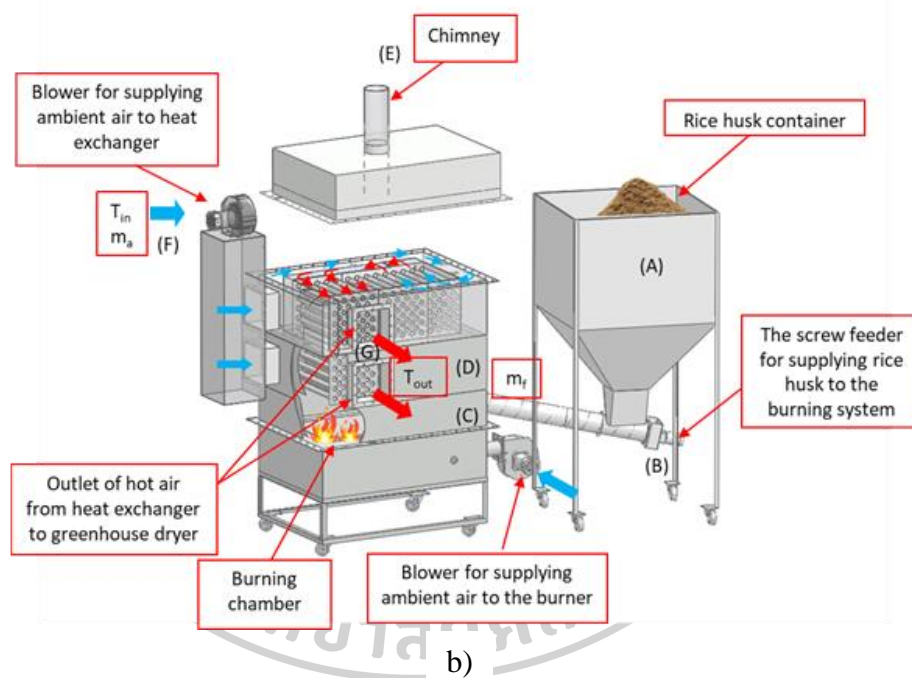


Fig 19 Rice husk burning system a) pictorial view b) schematic diagram

The function of the rice husk burning system can be described as follows. Rice husk from the container (A) is supplied to the burning chamber (C) by a screw feeder (B). Ambient air is blown to the chamber to supply air for rice husk burning and to blow flue gas through air-to-air heat exchanger (D) situated above the burning chamber. Then flue gas leaves the heat exchanger to ambient environment through a chimney (E). For the transfer of thermal energy, a blower (F) sucks ambient air and blows it to the heat exchanger. Hot air from the outlet of the heat exchanger (G) is supplied to the dryer. The controller regulates the rice husk feeder and the ignition of rice husk in the burning chamber according to the setup temperature of the outlet air of the heat exchanger.

5.2.2 Performance of the burning system

The performance of the burning system was measured in terms of the effectiveness (ε) which is defined as:

$$\begin{aligned}\varepsilon &= \frac{\text{actual heat transfer rate}}{\text{maximum heat transfer rate}} \\ &= \frac{m_a C_{pa} (T_{out} - T_{in})}{m_f h_f}\end{aligned}\quad (5.1)$$

where m_a is mass flow rate of ambient air to the heat exchanger ($\text{kg}\cdot\text{s}^{-1}$), m_f is flow rate of rice husk to the burning system ($\text{kg}\cdot\text{s}^{-1}$), h_f is heating value of rice husk, (J kg^{-1}), C_{pa} is specific heat of air, ($\text{J}\cdot\text{kg}^{-1}\cdot\text{°C}^{-1}$), T_{out} is outlet temperature of hot air from the heat exchanger (°C) and T_{in} is ambient air temperature (°C).

5.2.3 Experimental procedure

Four drying experiments were conducted during 12-30 July 2017. For each experiment, 300 kg of ripe banana collected from local market was dried in the parabolic greenhouse solar dryer equipped with the rice husk burning system installed at Silpakorn University, Nakhon Pathom, Thailand. The solar energy was employed for direct heating of inside air during sunny days while the rice husk burning system was used to supply hot air to the dryer during cloudy and rainy days. The drying was started at 8:00 am and continued till 6:00 pm. To compare the performance of the parabolic greenhouse solar dryer equipped with rice husk burning system with that of natural sun drying, three control samples were placed on trays and dried at the same weather condition outside the dryer. Weights of the representative samples at various positions inside dryer and control samples outside the dryer were periodically recorded at 3-hour interval using a digital balance (Kern, model 474-42, accuracy ± 0.1 g). There was some rainfall in every day of the experiment. The rice husk burning system was operated when rain started and the temperature inside the dryer was maintained above 50°C by controlling supply of rice husk.

Important parameters affecting the dryer performances including solar radiation, air temperature, relative humidity and air velocity were measured. Solar radiation was measured by a pyranometer (Kipp&Zonen model CM 11, accuracy $\pm 0.5\%$) and it was placed on the roof of the dryer. Temperature was measured by K-type thermocouples. Hot wire anemometer (Airflow, model TA5, accuracy $\pm 2\%$) was used to measure the air velocity at the air inlet, air outlet of the dryer. The relative humidity of ambient air and drying air was periodically measured by hygrometers (Elektronik, model EE23, accuracy $\pm 2\%$). Voltage signals from the pyranometer, hygrometers and thermocouples were recorded every 10 minutes by a multi-channel data logger (Yokogawa, model DC100). The moisture content of the samples was determined by the oven method (103°C for 24 hours).

5.2.4 Uncertainty analysis

Uncertainty analysis refers to the uncertainty or error in experimental data. In general, there are two types of error: namely, systematic error and random error. The systematic error in the experimental data is a repeated error of constant value and the random error is due to imprecision. Systematic error can be removed by calibration but random error cannot be removed. The imprecision due to random error can be defined statistically from a number of measurements.

In this study, the pyranometer, thermocouples and hygrometers were calibrated prior to the use in the experiments. The mean value of the measurements and standard deviation of the data on solar radiation, ambient air temperature, drying air temperature and relative humidity were determined. The variable x_i that has an uncertainty δx_i is expressed as (Doiebelin, 1976; Holman, 1978; JP., 1978; van Nydeck Schenck & Hawks, 1979):

$$x_i = x_{\text{mean(measured)}} \pm \delta x_i \quad (5.2)$$

where x_i is actual value, x_{mean} is measured value (mean value of the measurements) and δx_i is uncertainty in the measurement. There is an uncertainty in x_i that may be as large as δx_i . The value of δx_i is the precision index that is usually taken as 2 times the standard deviation and it encloses approximately 95% of the population for a single sample analysis.

5.2.5 Drying efficiency

The drying efficiency is defined as the ratio of energy output of the drying system to energy input to the drying system (Bala, 1998). Solar radiation input (E_{solar}) on the parabolic greenhouse dryer is computed as:

$$E_{\text{solar}} = A_{\text{dryer}} \int S_r(t) dt \quad (5.3)$$

where A_{dryer} is dryer area (m^2) and $S_r(t)$ is solar radiation at time t (W/m^2)

The output of the dryer in terms of energy (E_{dryer}) is

$$E_{\text{dryer}} = m_r L_g \quad (5.4)$$

where m_r is moisture removed (kg), L_g is latent heat of vaporization of moisture (J/kg)

Thus, the efficiency of the dryer (ϵ_{eff}) is

$$\epsilon_{\text{eff}} = \frac{E_{\text{dryer}}}{E_{\text{solar}} + E_{\text{PV}} + E_{\text{rice husk}}} \times 100\% \quad (5.5)$$

where E_{PV} is energy output from solar cell panel (J) and $E_{rice\ husk}$ is energy output from rice husk burner (J). Note that this dryer uses a solar cell panel to power the ventilation system.

5.3 Results and discussions

Typical results were presented as follows.

5.3.1 Performance of the rice husk burning system

The average consumption rate of dry rice husk was 12 kg/hour and the heating value of the rice husk sample used in this study is 14.51 MJ/kg. Maximum power input from the rice husk burning system was 132.49 kW and the average power needed from the husk burning system was 39.75 kW for drying of banana during cloudy or rainy days. The overall effectiveness of the rice husk burning system was 87.7%. The burning system has the capacity to support the greenhouse dryer properly in rainy and cloudy days to maintain the set temperature of the drying air as a backup protection for production of high quality banana.

5.3.2 Performance of greenhouse solar dryer equipped with rice husk burning system

The variations of the solar radiation during the drying period are shown in Fig 20. The fluctuations of the solar radiation during the period of drying were very high especially during first, second and third days of the drying. For all of the days of drying, the sky was cloudy. The solar radiation increased sharply in the in second day up to 1200 W/m² and fourth day up to 1000 W/m². There was little rainfall in the morning and afternoon of first day and in the afternoon of third day. The second day and fourth day were cloudy.

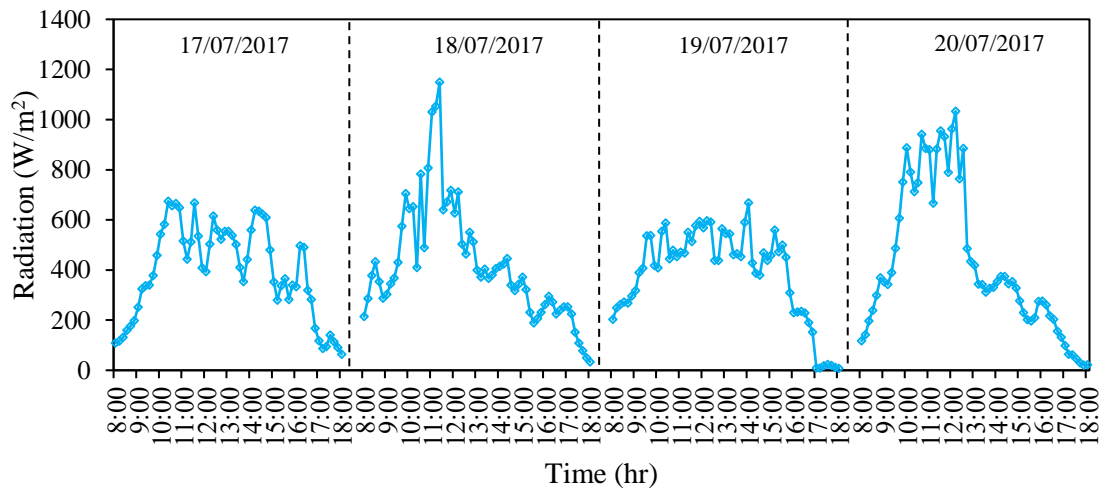


Fig 20 Variations of solar radiation during drying period

Fig 21 shows energy inputs from solar radiation and biomass burning system to the greenhouse solar dryer. Energy input to the greenhouse solar dryer from solar radiation follows the pattern of the solar radiation, but the energy input from the biomass burning system provides heat to raise the desired drying air temperature during cloudy and rainy days. Fig 21 shows that most of the energy input from biomass burning system was needed in the first and third day and the least in the second and fourth day.

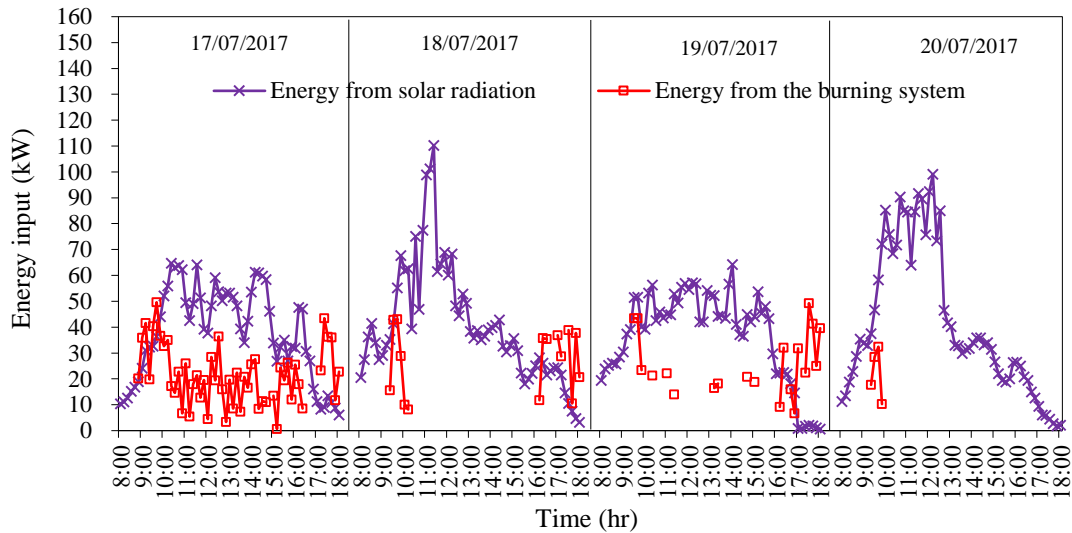


Fig 21 Variation of energy input with time inside the greenhouse solar dryer

The temperatures at different points inside the greenhouse dryer are shown in Fig 22 and these temperatures are significantly different from the ambient temperature outside the dryer. The temperature inside the dryer was maintained fairly constant to the set temperature of 50°C , but the fluctuations of the temperatures of the air supplied from the burning system during auxiliary heating from biomass are produced in such fashion that the set temperature for drying of banana is maintained. Fig 22 shows that the air temperature inside the dryer supported by the burning system was approximately 20°C higher than the ambient air temperature and it was maintained at 50°C for most of the drying time.

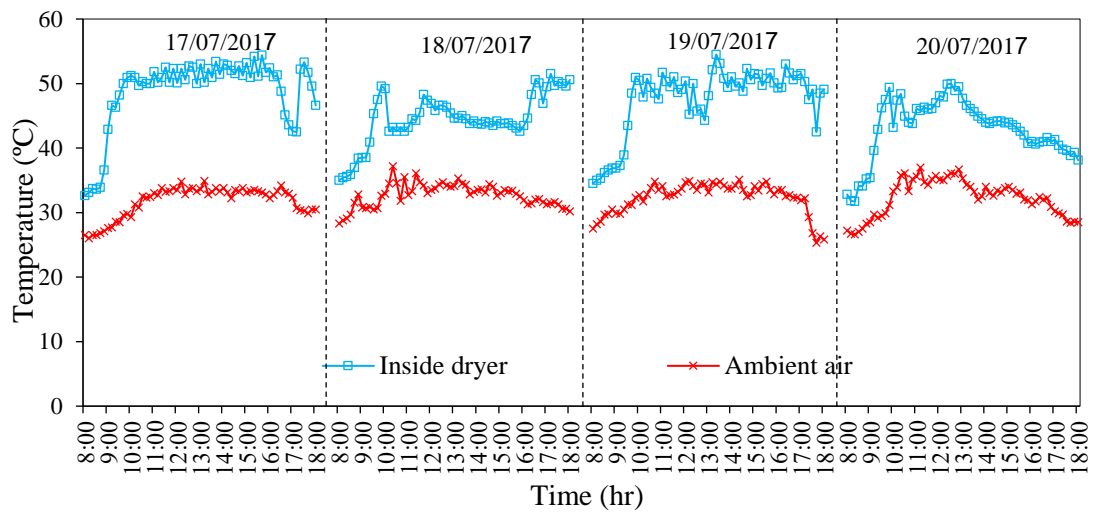


Fig 22 Comparison of temperature variations inside the greenhouse dryer with the burning system and the ambient air temperature

The variations of the relative humidity of the air inside the greenhouse solar dryer equipped rice husk burning system and the ambient air outside the dryer are shown in Fig 23. The relative humidity (%) of the air inside the dryer decreased when the temperature increased. The relative humidity outside the dryer was always 40% higher than the humidity inside the dryer. The relative humidity of the air at the noon was always less than those of the morning and afternoon.

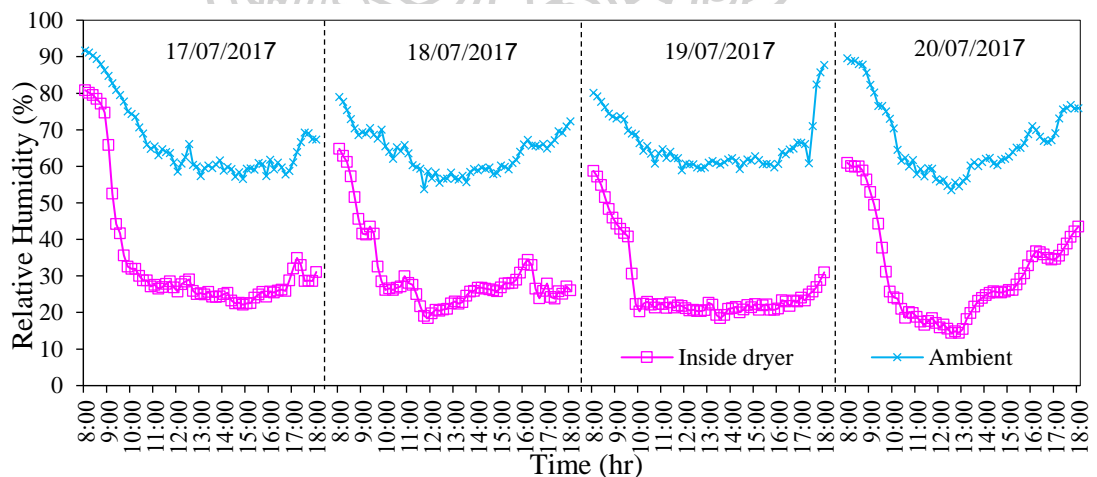


Fig 23 Comparison of relative humidity inside the dryer and ambient air

Fig 24 shows the comparison of moisture content changes of banana inside the greenhouse dryer with the burning system and natural sun drying. Banana inside the greenhouse dryer coupled with the biomass burning system was dried to a final moisture content of 15% (wb.) within 4 days from an initial moisture content of 68% (wb.) while the drying in natural sun drying took 6 days to achieve the final moisture of about 15%. The banana dried in the greenhouse dryer supported by the rice husk

burning system was a better quality dried banana compared to the sun dried banana (Fig 25). Commercially, the dried banana has a moisture content less than 20% (wb.) (Bowrey et al., 1980; Nguyen & Price, 2007) while the dried banana in this study was 15% (wb.), which has a better shelf life. The overall efficiency of the solar greenhouse dryer was 12.95%. Fudholi (De Neufville, 1990) also reported the overall efficiency of the solar greenhouse dryer to be 12.7%.

More than half of the dried banana from natural sun drying was deteriorated due to fungus attack. But banana dried inside the greenhouse dryer was very good quality both in color and pungency.

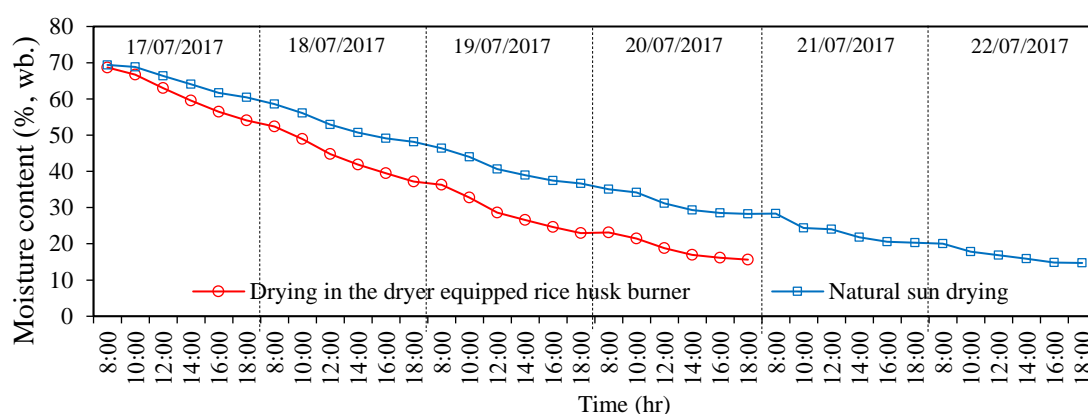


Fig 24 Moisture contents of banana drying in greenhouse dryer with the burning system in comparison with the natural sun drying



Fig 25 Dried banana a) banana inside the dryer b) banana dried by natural sun

5.3.3 Economic evaluation

The economic evaluation of the parabolic greenhouse solar dryer equipped with the rice husk burning system was carried out based on economic data in Thailand during the past 5 years (2012-2017) and experimental data undertaken in this study. These data are shown in Table 3.

Tables 3 Economic and production data used for the economic evaluation.

Item	Value
1) Cost of the parabolic greenhouse dryer (C_{dryer})	500,000 Baht
2) Cost of rice husk burning system (C_{burner})	120,000 Baht
3) Labor cost per batch for operating the dryer equipped with the burning system (C_{labor})	1,200 Baht
4) Number of drying batches per year	90 batches
5) Drying time per batch	4 days
6) Quantity of fresh banana per batch (M_f)	300 kg
7) Quantity of dried banana obtained from the dryer per batch (M_d)	100 kg
8) Average number of cloudy or rainy days per year, when auxiliary heat from the rice husk burning system are needed*	57 days
9) Quantity of rice husk required per day (during cloudy or rainy days)**	61 kg
10) Unit cost of rice husk	1.7 Baht/kg
11) Electricity required per batch (for operating various blowers and feeders during cloudy or rainy days)	45 kWh
12) Unit cost of electricity (Unit electricity)	2.76 Baht/kWh
13) Price of fresh banana (P_f)	15 Baht/kg
14) Price of dried banana (P_d)	100 Baht/kg
15) Interest rate (I_{in})***	7.83%
16) Inflation rate (I_f)***	2.1%
17) Life span of the dryer equipped with the burning system (N)	10 years

* It is estimated from the level of solar radiation and sky condition recorded at a nearby solar radiation monitoring station.

** It is estimated from experimental data during the study period.

***Average values (2012-2017) from the National Bank of Thailand

(1 USD=31.72 Baht)

Three economic parameters were calculated as follows.

1) Drying cost

The following steps were carried out to estimate the drying cost. Firstly, the capital cost (C_T) of the parabolic greenhouse dryer equipped with the rice husk burning system was computed from

$$C_T = C_{\text{dryer}} + C_{\text{burner}} \quad (5.6)$$

where C_{dryer} is the cost of the parabolic greenhouse dryer and C_{burner} is the cost of the rice husk burning system.

Then, the annual cost (C_{annual}) of the dryer equipped with the burning system for banana drying was estimated using the formula proposed by Audsley (Audsley & Wheeler, 1978) as follows:

$$C_{\text{annual}} = \left[C_T + \sum_{i=1}^N (C_{\text{main},i} + C_{\text{op},i}) \omega^i \right] \left[\frac{\omega - 1}{\omega(\omega^N - 1)} \right] \quad (5.7)$$

$$\omega = \frac{(100 + i_{\text{in}})}{(100 + i_{\text{f}})} \quad (5.8)$$

and

where $C_{\text{main},i}$ and $C_{\text{op},i}$ are the maintenance cost and operating cost at year i , respectively. i_{in} is interest rate and i_{f} is inflation rate. The maintenance cost was assumed to be 1% of the capital cost.

The operating cost comprises the rice husk consumption cost (C_{husk}), electricity consumption cost ($C_{\text{electricity}}$) and labor cost (C_{labor}) for operating the dryer equipped with the burning system. Therefore, the operating cost can be written as follows:

$$C_{\text{op}} = C_{\text{husk}} + C_{\text{electricity}} + C_{\text{labor}} \quad (5.9)$$

The cost of rice husk (C_{husk}) was calculated from

$$C_{\text{husk}} = C_{\text{unit_husk}} \cdot M_{\text{husk}} \quad (5.10)$$

where $C_{\text{unit_husk}}$ is the unit cost of the rice husk, M_{husk} is the amount of rice husk used per year and it is estimated from solar radiation level and sky condition recorded at Nakhon Pathom solar monitoring station during 2012-2017. The amount of rice husk required by the burning system during cloudy and rainy days was estimated from the drying experiments.

The cost of electricity consumption ($C_{\text{electricity}}$) can be computed from

$$C_{\text{electricity}} = C_{\text{unit_electricity}} \cdot M_{\text{electricity}} \quad (5.11)$$

where $C_{\text{unit_electricity}}$ is the unit cost of the electricity and $M_{\text{electricity}}$ is the amount of electricity consumed per year.

Finally, the drying cost (Z) was calculated from

$$Z = \frac{C_{\text{annual}}}{M_d} \quad (5.12)$$

where M_d is the amount of dried product per year. From the above-mentioned equations and the data in Table 3, the drying cost was calculated to be 20.5 Baht/kg.

2) Payback period

The payback period (PB) was estimated using the following equation adopted from (Dhanushkodi et al., 2015; Fudholi et al., 2016)

$$PB = \frac{C_T}{M_d P_d + M_f P_f + M_d Z} \quad (5.13)$$

where M_f is the amount of fresh banana used per year and P_f is the price of fresh banana. Based on the data in Table 3 and Eq. 5.13, the payback period of the parabolic greenhouse dryer equipped with the rice husk burning system was estimated to be 2.2 years.

3) Internal rate of return

The internal rate of return (IRR) was estimated using a formula adopted from Park (2013) as follows:

$$\sum_{i=1}^N \frac{C_i}{(1 + IRR)^i} = 0 \quad (5.14)$$

where C_i is the cash flow at year i due to the investment on the dryer equipped with the burning system. By using the iteration method and the related data in Table 3, IRR was found to be 45%.

5.4 Conclusions

Rice husk burner with a heat exchange was designed to provide flue gas free clean heated air for the solar greenhouse dryer and the maximum effectiveness of the rice husk burner and heat exchanger was 87.7%. Field-level drying experiments of banana was carried out using solar greenhouse dryer equipped with rice husk burning system for drying of banana. Banana was dried this dryer to 15% (wb.) of moisture content from an initial moisture content of about 68% (wb.) during 4 days of drying while the moisture content of similar samples in the open sun drying method took 2 more days. Thus, there is a considerable reduction in drying time in the solar greenhouse dryer equipped with a rice husk burning system in comparison to natural sun drying. The overall energy efficiency of the greenhouse solar dryer was 12.9%. Finally, this study demonstrates that the dryer equipped with the burning system is fully capable of providing clean heat to maintain the desired temperature during cloudy and rainy days and also thereby it can produce high quality dried bananas.



Chapter 6

Performance Investigation of a Parabolic Greenhouse Solar Dryer Equipped with Phase-Change-Thermal Energy Storages*

6.1 Introduction

Thailand has a large population of agricultural occupations and produces a lot of agricultural products. Some products are processed into dried products. The business of small and medium sized industries spread throughout the country. Most of the production of dried products are dried using natural sun drying method and the dried product producers usually face the problem of contamination by dust, disturbance of animals and insects, and problem of rewetting by rain. As a result of this problem, parabolic greenhouse solar dryer type has been developed at Silpakorn University in collaboration with the Department of Alternative Energy Development and Efficiency. Such type of dryers has high potential for commercial use (Janjai et al., 2007; Janjai et al., 2009; Janjai et al., 2011). Although this type of dryer helps to solve the problem of contamination by dust, insect infestation and the problem of rain, there are still drying problems for products with high moisture such as banana. When the solar radiation is not enough, the banana is spoiled. The objective of this study is to evaluate the performance of the parabolic greenhouse solar dryer equipped with phase change heat energy storage to solve such problems.

6.2 Materials and methods

6.2.1 Latent heat storage

A phase change material (PCM) is a substance with a high heat of fusion which, melting and solidifying at a certain temperature, is capable of storing and releasing large amounts of energy. Heat is absorbed when the material changes from solid to liquid and heat is released when the material changes from liquid to solid. Initially, solid-liquid PCMs behave like sensible heat storage (SHS) materials; their temperature rises as they absorb heat. Unlike conventional SHS materials, however, when PCMs reach the temperature at which they change phase (their melting temperature) they absorb large amounts of heat at an almost constant temperature. The PCM continues to absorb heat without a significant rise in temperature until all the material is transformed to the liquid phase. When the ambient temperature around a liquid material falls, the PCM solidifies, releasing its stored latent heat. Thus, PCMs are classified as latent heat storage (LHS) units. Latent heat storage (LHS) is the heat

*This work was presented at 14th Conference on Energy Network of Thailand, 13-15 June 2018.

absorption or release when a storage material undergoes a change of phase from solid to liquid or liquid to gas or vice versa at more or less constant temperature (Doiebelin, 1976). The storage capacity of the LHS system with a phase change material (PCM) medium (El-Sebaai, Aboul-Enein, Ramadan, & El-Gohary, 2002) is given by

$$Q = \int_{T_i}^{T_m} mC_{sp}dT + ma_m\Delta h_m + \int_{T_m}^{T_r} mC_{lp}dT \quad (6.1)$$

where a_m is the proportion of molten mass compared to the total mass of phase change material (-)

Δh_m is latent heat of PCM (J/kg)

T_m is the melting temperature of PCM (°C)

C_{sp} is the heat capacity of PCM in solid state (J/kg.°C)

C_{lp} is the heat capacity of PCM in liquid state (J/kg.°C)

6.2.2 Experimental study

We developed a thermal energy storage system that uses phase change as a thermal storage. The system consists of 3 parts: 1) steel box size 43 x 111 x 5.2 cm³ 2) phase change material (PCM), which is paraffin, because the paraffin has a melting point of about 50-51°C and has a latent heat of 200 kJ/kg. This melting temperature is within the temperature range of the parabolic greenhouse solar dryer 3) Cart has a size of 45x112x70 cm³ for placing the box of phase change material (Fig 26 and 27). We have created 15 units of thermal energy storage system; each unit contain 18 kg of paraffin.

Heat energy collected for 1 unit of thermal energy storage system can be calculated by Eq. 6.1. It was found that the amount of heat accumulated in 1 unit of thermal energy storage system is 5,947.2 kJ. Therefore, the total heat energy accumulated in the thermal energy storage system is equal to 89.2 MJ.

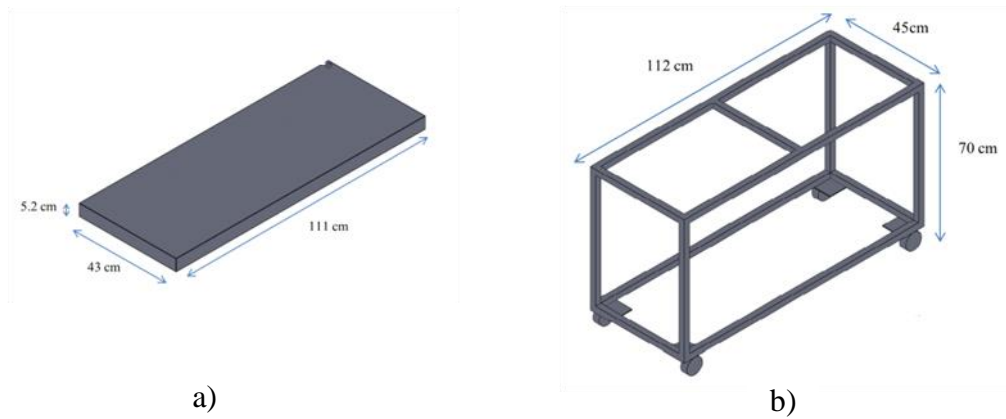


Fig 26 The components of thermal energy storage system: a) steel box containing paraffin b) cart for placing the paraffin box



Fig 27 Thermal energy storage system

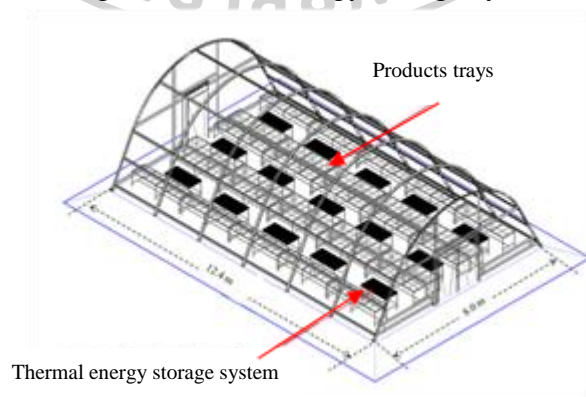


Fig 28 Parabolic greenhouse solar dryer equipped with thermal energy storage system

The parabolic greenhouse solar dryer consists of a parabolic roof structure made from polycarbonate sheet (80% of transmittance) on a concrete floor coated in black with carbon powder for improving the absorption of solar radiation (Janjai et al., 2009; Janjai et al., 2007; Janjai et al., 2011). The dryer has a width of 8.0 m, length of 12.4 m and height of 3.5 m with a loading capacity of about 600 kg of fresh fruits or vegetables. Nine DC fans operated by three 50 W solar cell modules were installed in the wall opposite to the air inlet to ventilate the dryer (Fig 28).

In this study, two parabolic greenhouse solar dryers were built in the same area: one dryer was equipped with PCM storage system and the other was without PCM storage system (Fig 29)

For each dryer, 300 kg of ripped banana (initial moisture about 70% wb.) was used. The banana was placed on the product trays in a thin layer. The experiments were started at 8:00 am and continued till 10:00 pm. The drying was continued on subsequent days until the desired moisture content (about 13% wb.). Product samples were placed in the dryer at various positions and were weighted periodically at 2-hour intervals using a digital balance (ZEPPER model ES-500HA). At the end of the experiments, the exact dry solid mass of the product samples was determined by the oven method (103°C for 24 hours).

Solar radiation was measured by a pyranometer (Kipp&Zonen CMP11) placed on the roof of the parabolic greenhouse solar dryer. Inside air temperatures were measured in various positions in the dryer by thermocouple (type k). A hot wire anemometer (AIRFLOW model TA5) was used to monitor the air velocity at the air-outlet of the dryer. The relative humidity of ambient air and drying air were periodically measured by hygrometers (Electronic, model EE23). All data were recorded every 10 minute by a multi-channel data logger (Yokogawa, model DC100).



Fig 29 Parabolic greenhouse solar dryer equipped with thermal energy storage system and without thermal energy storage

6.3 Results and discussion

Three full scale tests of the parabolic greenhouse solar dryer for drying of banana were carried out in September 2017. Typical results for drying of banana are shown in Fig 30-32. Solar radiation varied from 12.76 W/m² to 981.16 W/m² during this experimental period.

Fig 30 shows variations of solar radiation during a typical experimental run of solar drying of banana. In 3 days of this experimental run, solar radiation increased sharply in the morning but was decreased in the afternoon with fluctuations due of clouds. This radiation causes the moisture of banana in the dryer without PCM storage system and that of natural sun drying can be removed slowly.

The comparison of air temperatures in the dryer with PCM storage system and ambient temperature in the drying period shows in Fig 31. It was found that inside air temperature was in range of 40-60°C which is higher than ambient temperature about 20°C. It can be noted from the results that the inside air temperature gradually reduced when the solar radiation was less intense. In the absence of solar radiation period, the air temperature was also higher than 40°C (the lowest temperature suitable for drying), thus the banana can continue to dry for an additional 3 hours.

Fig 32 shows the comparison of moisture content changes of banana inside the parabolic greenhouse solar dryer: with PCM storage system, without PCM storage system and natural sun drying. It can be observed that banana inside the dryer coupled with PCM storage system was dried to a final moisture content of 13.2% (wb.) within 52 hours from an initial moisture content of 68.9% (wb.) while the drying inside the dryer without PCM storage system took 66 hours and the natural sun drying took 80 hours to achieve the moisture content of 20%. The results show that the heat transferred from the thermal energy storage system can reduced the drying time of banana comparing to the two others drying. It was also found that more than half of dried banana from natural sun drying were deteriorated due to insects and fungus effect, but dried banana inside the parabolic greenhouse solar dryer was in good quality (Fig 33).

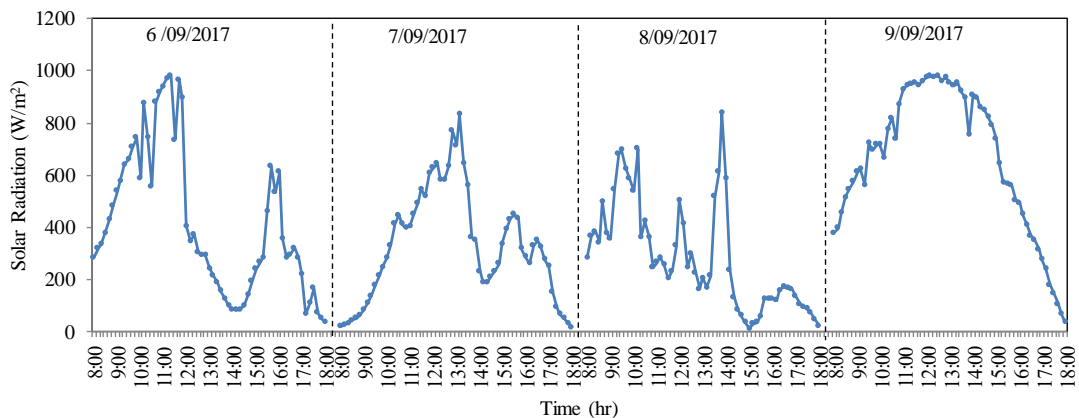


Fig 30 Variation of solar radiation with time of the day during drying of banana.

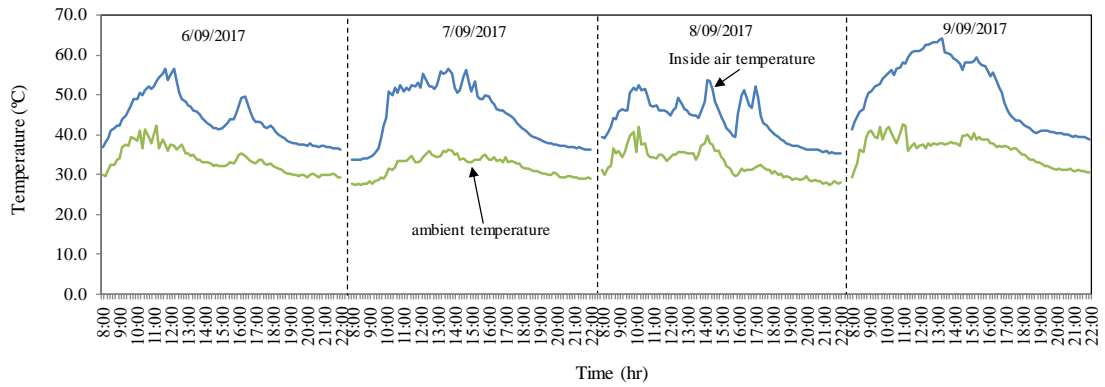


Fig 31 Variation of ambient temperature and drying air temperature at the middle of parabolic greenhouse solar dryer.

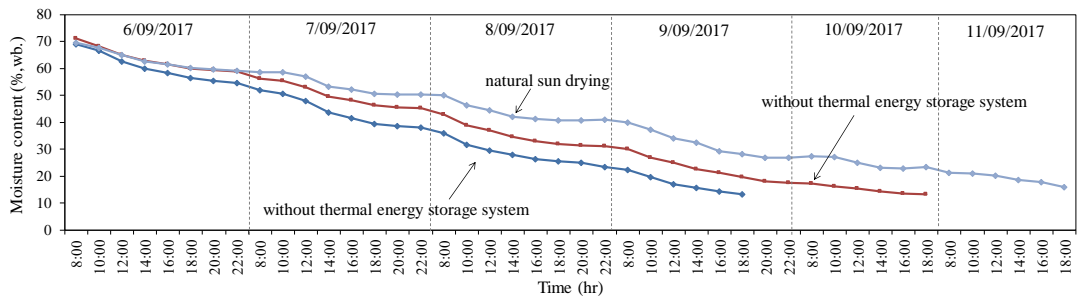


Fig 32 Variation of moisture content of banana.



Fig 33 Dried banana: a) natural sun drying b) inside the parabolic greenhouse solar dryer.

6.4 Conclusions

In this work, the performance of the parabolic greenhouse solar dryer equipped with PCM storage system was investigated. Paraffin was used as a material for heat storage. The dryer was equipped with 15 units of PCM storage system (18 kg/unit) which have the total heat accumulated equal to 82 MJ.

The results show that the PCM storage system can reduce the drying time due to the released heat transferred from the PCM to the air inside the dryer. Therefore, the drying time of banana inside the dryer equipped with PCM storage system was 52 hours which is shorter than the drying inside the dryer without PCM storage system and natural sun drying.



Chapter 7

Performance of the Parabolic Greenhouse Solar Dryer in Southeast Asian and Modelling of this Type of Dryer Using the Artificial Neural Network*

7.1 Introduction

Southeast Asian countries produce a number of tropical agricultural products. They are consumed both as fresh and dried products. To produce dried products, the natural sun drying method is usually used in these countries. Although, it is a cheap method, products being dried are usually subjected to losses and damages due to insects, animals and rain. Situated in equatorial zone, Southeast Asian countries receive relatively high solar radiation (Janjai et al., 2005a; Janjai et al., 2011; Janjai et al., 2013). As a result, a number of researches have proposed various types of solar dryers for drying agricultural products in these countries (Abdullahet et al., 2001; Boonlong et al., 1984; Exell & Kornsakoo, 1976; Fudholi et al., 2015; Soponronnarit et al., 1991; Wibulsawas & Thaina, 1980). However, only a few dryers have been used in the fields in these countries. This is due to several factors such as impractical aspect and limited loading capacity of the dryers. Having realized these problems, a parabolic greenhouse type solar dryer was developed at Silpakorn University in Thailand (Janjai et al., 2005b; Janjai et al., 2007). The dryer was previously called “PV-ventilated greenhouse dryer” and now commonly named “parabolic greenhouse solar dryer” or “parabola dome”. The dryer has advantages that it has high loading capacity and is easy to use. The objectives of this work are to present the experimental performance of this type of dryer in Asian countries and to perform the neural network modeling of the dryer.

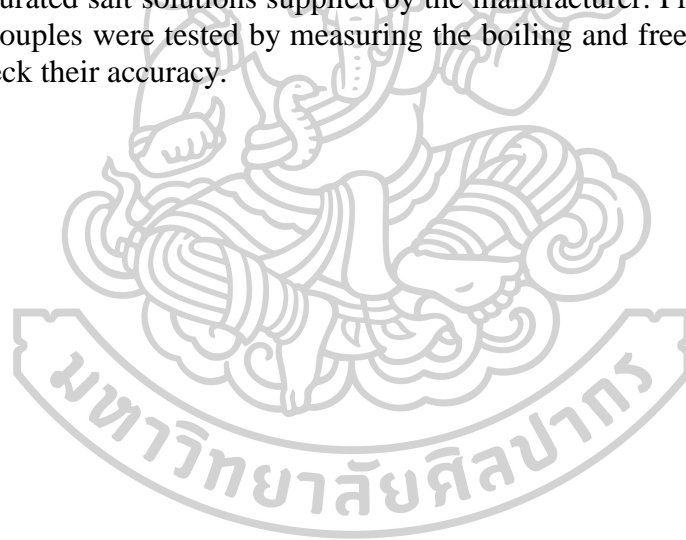


*Part of this work was presented at the 2nd Nordic Baltic Drying Conference, Hamburg, Germany, 7 - 9 June, 2017

7.2 Materials and methods

7.2.1 Drying experiments

To investigate the performance of this type of dryer in Southeast Asia, the dryers were built in Thailand, Myanmar, Indonesia and Vietnam (Fig 34) and drying experiments were conducted. To monitor the performance of each dryer, various sensors were installed at the dryer. A pyranometer (Kipp&Zonen, model CMP11) was installed on the roof of the dryer to measure solar radiation. Thermocouples (type K) were used to measure air temperature at different points in the dryer. Hot wire anemometers (Airflow, model TA 5) were used to monitor the air speed at the air inlet and air outlet of the dryer. Another anemometer was also used to monitor the ambient wind speed. The relative humidity of ambient air and drying air was measured by hygrometers (Elektronik, model EE23). Voltage signals from the pyranometer, hygrometers and thermocouples were recorded every 10 min by a multi-channel data logger (Yokogawa, model DC100). The air speeds were manually recorded during experiments. Before the installations, the pyranometer was calibrated at the Calibration Laboratory for Solar Radiation Instrument of Silpakorn University, which had been accredited by ISO/IEC 17025. The hygrometers were calibrated using standard saturated salt solutions supplied by the manufacturer. Prior to the utilization, the thermocouples were tested by measuring the boiling and freezing temperatures of water to check their accuracy.



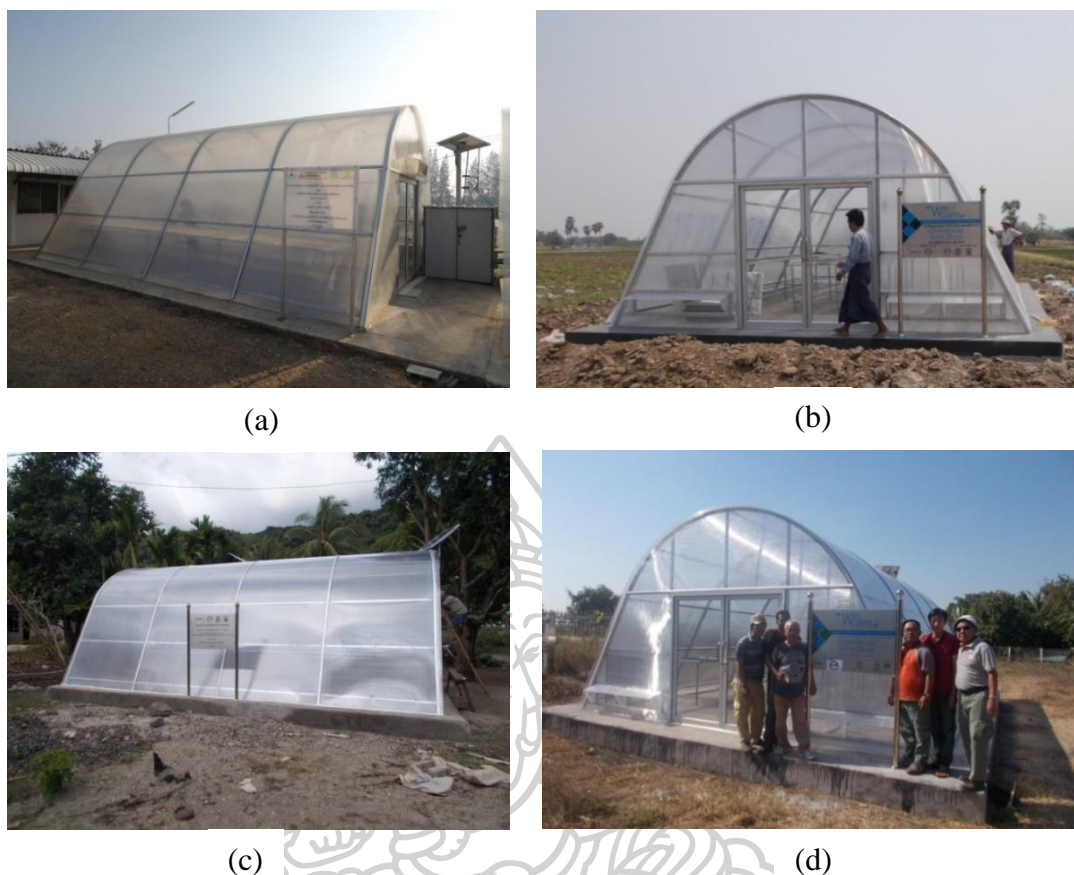


Fig 34 Pictorial view of the greenhouse solar dryer installed in (a) Thailand (b) Myanmar (c) Indonesia and (d) Vietnam

The agricultural products used in the drying experiments in the dryers installed in Thailand, Myanmar, Indonesia and Vietnam are bananas, red chilies, seaweeds and Vietnamese chilies, respectively. For each drying experiment, about 100 kg of these products was placed on the trays in thin layer. To monitor the moisture content, product samples were also placed on the trays and were weighted periodically at 1-hour interval using a digital balance (Kern, model 474-42). Also, about 100 g of product sample was dried outside the dryer (natural sun drying) in order to compare the drying behavior of the product with those dried in the dryer. At the end of the experiment the dry solid mass of the samples was determined by the oven method (103°C for 24 hours). All drying experiments were carried out during the period: July 2016-February 2017. The experiments were started at about 8:00 am and continued till 5:00 pm. For banana drying experiments, bananas in the dryer were collected at 5:00 pm and put in plastic bags for fermentation process and redistribution of the moisture in banana fruits during the night. Then they were again placed in the dryer in the next morning about 8:00 am. The drying was continued on subsequent days until the desired moisture content (24%, wb.) was reached. For the other products, they were kept in the dryer during night time. The typical results of the experiments are shown in the next section.

7.2.2 Modeling of the parabolic greenhouse solar dryer by using the artificial neural network (ANN)

A model of greenhouse solar dryer is an important tool for predicting the performance of the dryer for different operating parameters under various environmental conditions. It can also be used for the optimization of the dryer. In general, there are several approaches to model the dryer. In this work, the artificial neural network (ANN) approach was selected for modeling the parabolic greenhouse solar dryer. The advantage of this approach is that ANN does not require thermal properties of the products dried in this dryer and less assumptions are needed, as compared to the classical analytic modeling approach. It required only drying experiment data. The ANN approach is shaped after biological neural function and structures. The function of ANN is developed not by programming it, but by exposing it to carefully selected data on which it can learn how to perform the required processing test. In this work, an independent multilayer ANN of the parabolic greenhouse solar greenhouse dryer was developed to represent the performance of the dryer for drying bananas. The model has a four-layer network, which has a number of processing elements called neurons (Fig 35).

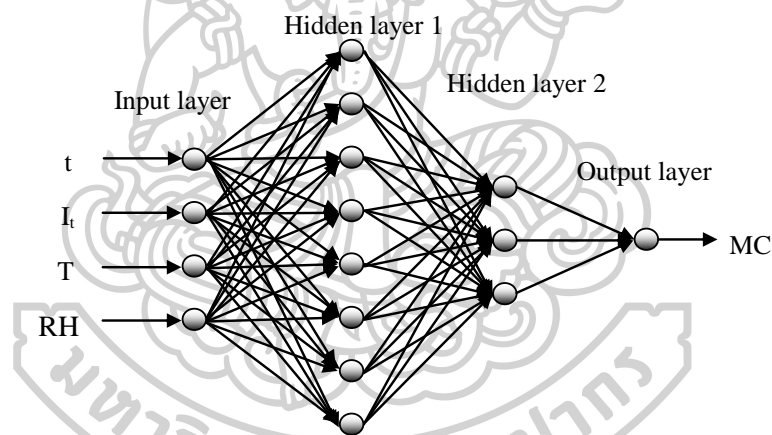


Fig 35 The structure of the artificial neural network of parabolic greenhouse solar dryer. t is time, I_t is solar radiation, T is drying air temperature at the middle of the dryer, RH is relative humidity and MC is moisture content

The input layer of the model comprises four neurons corresponding to (1) drying time (t), (2) solar radiation (I_t), (3) drying air temperature at the middle of the dryer (T) and (4) relative humidity (RH). The output layer has one neuron that represents the moisture content (MC) in the model. This ANN has two hidden layers. All inputs were normalized to obtain their values between 0.00 and 1.00. The ANN model was trained by the back-propagation approach (Wasserman, 1989) using data from the drying experiments of bananas in Thailand. All ANN calculations were programmed in C++. To examine the performance of the ANN model, it was used to predict the drying curve of banana obtained from the experiment and the result is shown in the next section. In order to survey the possibility of using ANN, the ANN model for drying litchi in the parabolic greenhouse dryer was done and the result is presented in Appendix 1.

7.3 Results and discussions

7.3.1 Experimental performance of the greenhouse solar dryer

The experimental tests of the parabolic greenhouse dryer for drying various products were carried out during January, 2016 to February, 2017 in Thailand, Myanmar, Indonesia and Vietnam. Typical results for drying red chilies in Myanmar during 18 July, 2016 to 21 July, 2016 are shown in Fig 36-39. Fig 36 shows the variation of solar radiation during the experimental drying of red chilies in Myanmar. At that time period, it rained most of the time. Solar radiation varied from 100 W/m² to 1,100 W/m².

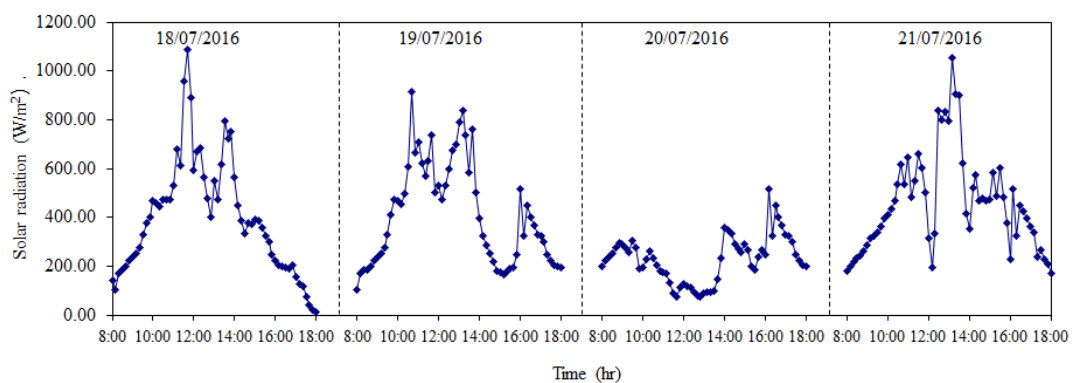


Fig 36 Variation of solar radiation during a drying run for red chilies in Myanmar.

Fig 37 shows the comparison of the ambient temperature and the temperature inside the dryer for a typical experiment of greenhouse solar dryer of red chilies. There is significant different between the air temperature inside and outside the dryer. The ambient temperature was quite stable, around 30°C for the whole period, while the temperature inside the dryer reached the maximum of 55°C.

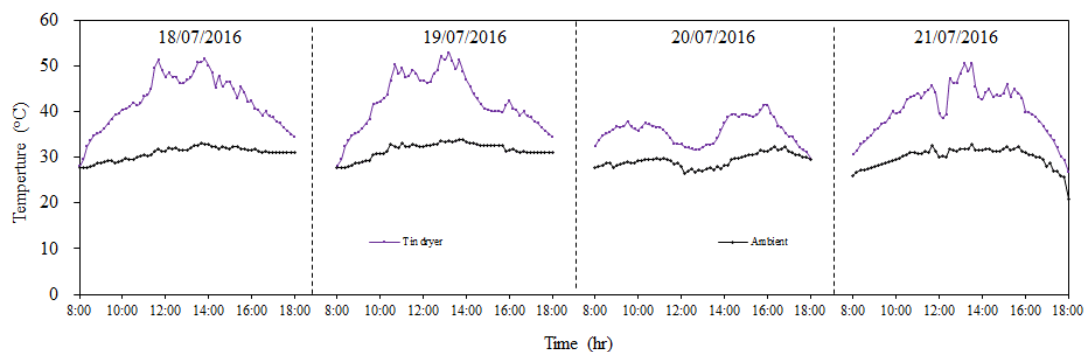


Fig 37 Comparison of the ambient temperature and the temperature inside the dryer for drying red chilies in Myanmar

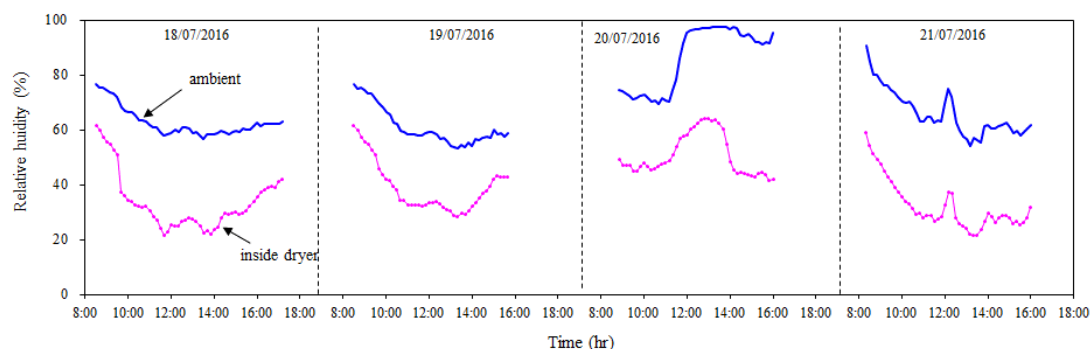


Fig 38 Relative humidity at various points inside the dryer and ambient relative humidity for drying the red chilies in Myanmar

Fig 38 shows the relative humidity inside the dryer and outside the dryer during the typical experimental run of the red chilies. The relative humidity frequently decreased over time excepted the rainy hour. The relative humidity of the air inside the dryer is usually lower than the ambient relative humidity.

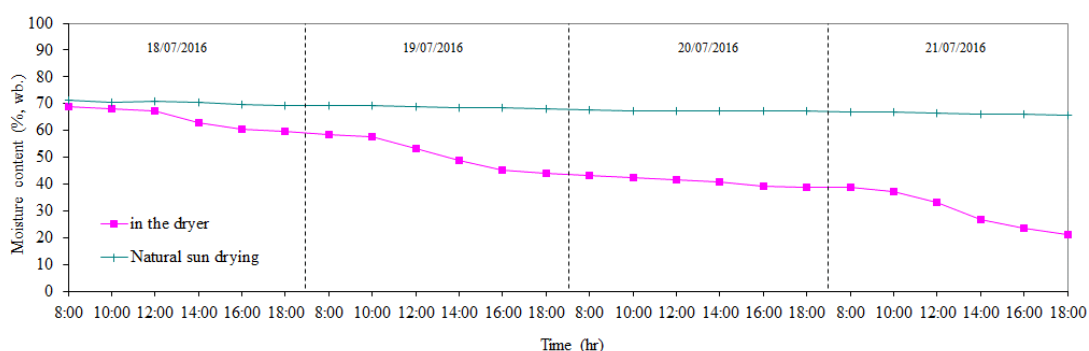


Fig 39 Comparison of the moisture contents for drying the red chilies inside the dryer and that from natural sun drying in Myanmar

Fig 39 shows the variation of moisture content of red chilies in the dryer compared to the control sample dried by natural sun drying. It was observed that the moisture content of red chilies in the dryer was reduced from an initial value of 70% (wb.) to a final value of 21% (wb.) within 4 days even it rained most of the time, whereas the moisture content of the open-air sun drying was not reduced because of the rain.

Fig 40 shows the variation of the moisture content of bananas, seaweed and Vietnamese chilies from typical experiments in Thailand, Indonesia and Vietnam, respectively. The moisture content of bananas in the dryer decreased from 67% (wb.) to 15% (wb.) within 4 days, whereas the moisture content of the open-air sun drying reduced to 25% (wb.) for the same period. The moisture content of seaweeds in the dryer was reduced from 91% (wb.) to 8% (wb.) within 4 days, whereas the moisture content of the open-air sun drying reduced to 27% (wb.) within 4 days. For the case of Vietnamese chilies, the moisture content of Vietnamese chilies in the dryer decreased

from 75% (wb.) to 20% (wb.) within 6 days, whereas the moisture content of chilies dried in open-air sun drying reduced to 58% (wb.) for the same period. These results revealed that the drying time of products in dryers was significantly shorter than that of the product dried naturally outside the dryers. It was also observed that the products being dried in the dryers were completely protected from insects, animals and rains and good quality of the final dried products were obtained. As the loading capacity of the dryers is relatively high and they are convenient to use, these dryers are now employed for producing commercially dried products in the communities where the dryers are located.

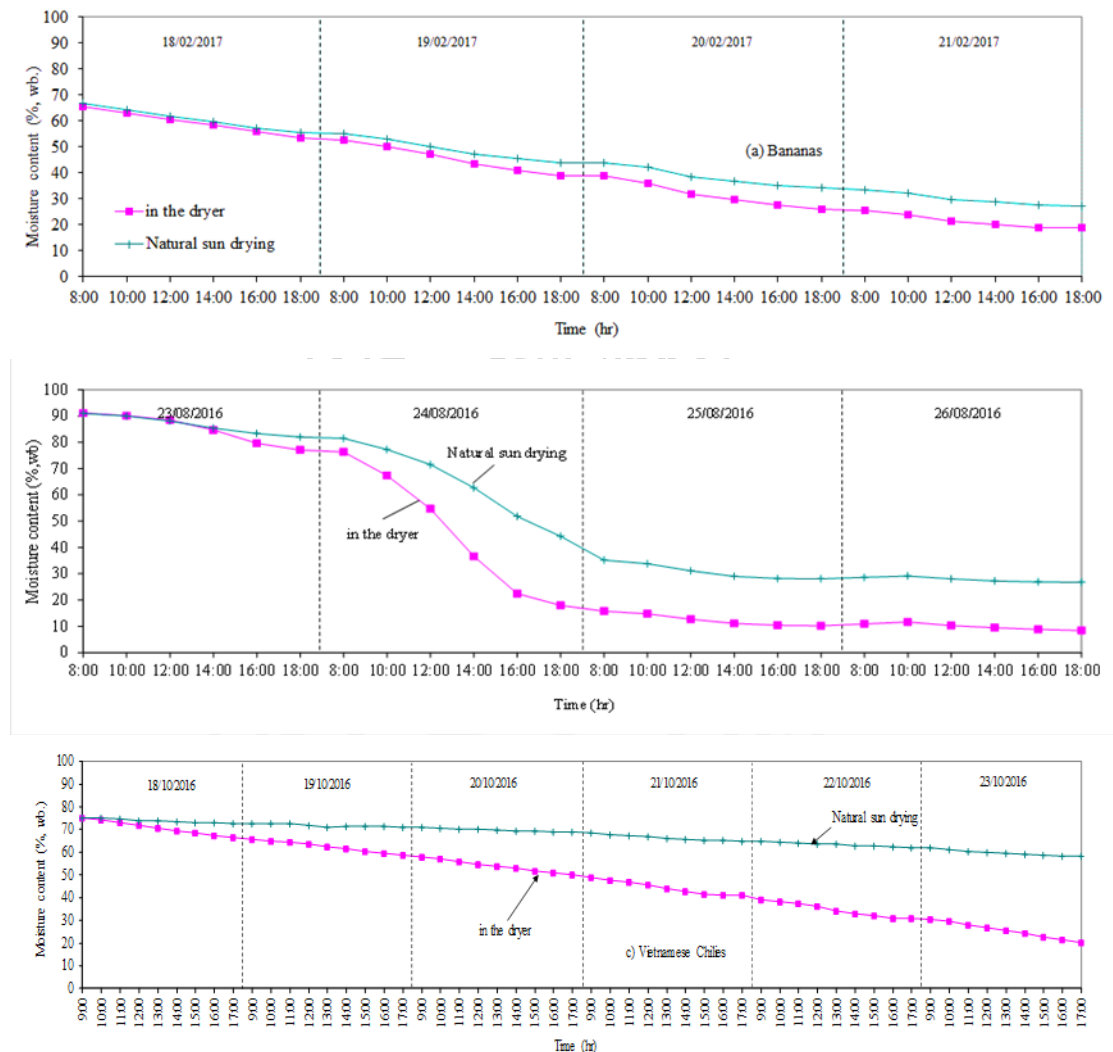


Fig 40 Comparison of the moisture contents of the products inside the greenhouse solar dryer and with those obtained by the natural sun drying for drying (a) bananas in Thailand, (b) seaweeds in Indonesia and (c) Vietnamese chilies in Vietnam.

7.3.2 Performance of the ANN model

After having sufficiently trained, the ANN model was employed to predict the moisture contents of bananas and the results was compare to the moisture contents obtained from the experiments as shown in Fig 41.

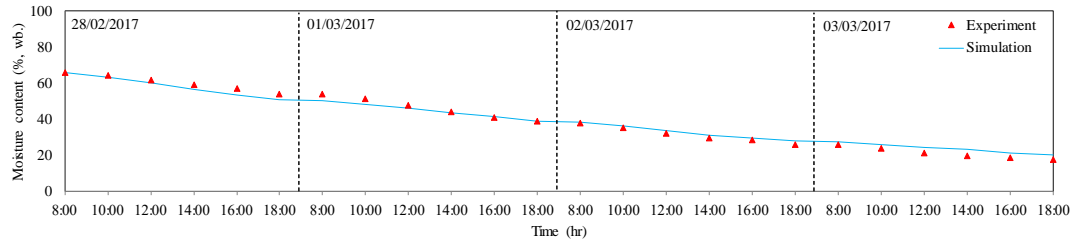


Fig 41 Comparison between moisture contents predicted by the ANN model and those obtained from the measurement.

Fig 41, it is observed that the patterns of both drying curves of bananas are similar and the discrepancy in terms of root mean square difference (RMSD) and mean bias difference (MBD) are 5.3% and -0.1%, respectively.

7.4 Conclusions

The parabolic greenhouse type greenhouse solar dryers were constructed in Thailand, Myanmar, Indonesia and Vietnam. Drying experiments were conducted. The results revealed that all dryers under this investigation performed well. All products being dried in the dryer were completely protected from insects, animals and rain and good quality of dried products were obtained. All of these dryers are now in use for producing commercially dried products. Finally, the ANN model of the dryer for drying bananas was performed. The model predicted well the performance of the dryer.

Chapter 8

Conclusions

In this work, various aspects of banana drying were investigated. These includes; thin layer drying, finite element modeling, drying of banana in a parabolic greenhouse solar dryer without auxiliary heat storage and in a parabolic greenhouse with rice-husk burning system. The performance of the parabolic greenhouse solar dryer equipped with a phase change thermal storage for banana drying was also undertaken. Finally, modelling of the parabolic greenhouse solar dryer for banana drying using an artificial neural network was also carried out. The results of the works can be summarized as follows.

- 1) The drying curves of thin layer drying of banana showed that the drying air temperature and the relative humidity have been important effect on the drying. An increase of drying air temperature and reduction of the relative humidity can reduce the moisture content of banana and the Logarithmic model is best fitted to the drying curves of banana.
- 2) The finite element method can be used to predict the distribution of the moisture inside banana. The average moisture contents obtained from this distribution reasonably agree with the moisture contents of whole fruit of banana obtained from the experiments, with and the root mean square error (RMSE) was in the range of 2.2-14.6%, and the coefficient of determination (R^2) was in the range of 0.97-0.99.
- 3) The parabolic greenhouse solar dryer equipped with rice husk burning system helps to solve the problem of banana spoilage during cloudy or rainy days. It can be also controlled the stable temperature as 50°C.
- 4) Drying of banana in the parabolic greenhouse solar dryer reduced significantly the drying time comparing to natural sun drying. The moisture content of banana in the parabolic greenhouse solar dryer was reduced from an initial value of 70 % (wb.) to a final value of 19-21% (wb.) within 4 days while the natural sun drying takes 6 days. In addition, the dryer also helps to protect banana form rain, insects and birds.
- 5) The parabolic greenhouse solar dryer equipped with phase change material can reduce the drying time, as compared to the same type of drying without the net storage unit. It shows that the drying time of the dryer with phase change material is shorter than that of without phase change material.



Appendix

Appendix 1

Testing of ANN for Litchi Drying*

Before using ANN for banana drying, Ann for litchi drying was tested and the details have been published in Journal of Renewable Energy and Smart Grid Technology, Volume 13. 2018. The paper is shown as follows.



*Part of this work was has been accepted to publish in the Journal of Renewable Energy and Smart Grid Technology, 2018, Vol. 13 No. 1

Experimental performance and artificial neural network modeling of solar drying of litchi in the parabolic greenhouse dryer

K. Tohsing^a, S. Janjai^{a*}, N. Lamlert^b, T. Mundpookhier^a, W. Chanalert^a, B. K. Bala^c

^aSolar Energy Research Laboratory, Department of Physics, Faculty of Science, Silpakorn University, Nakhon Pathom 73000, Thailand
Tel. +66-34-270761, Fax. +66-34-271189 E-mail: serm.janjai@gmail.com

^bPhysics and General Science Program, Faculty of Science and Technology Phetchaburi Rajabhat University, Phetchaburi 76000, Thailand

^cDepartment of Agro Product Processing Technology, Jessore University of Science and Technology, Bangladesh

*Corresponding author: serm.janjai@gmail.com

Abstract

This paper presents experimental performance and artificial neural network modeling of drying of litchi flesh in a parabolic greenhouse solar dryer. The dryer consists of a parabolic roof structure covered with polycarbonate sheets on a concrete floor. This dryer has the base area of 5.5×8.2 m² and the height of 3.25 m. To investigate the experimental performance of the dryer for the drying of litchi flesh, 10 experiments were conducted. One hundred kilograms of litchi flesh were used for each experiment. The drying time of litchi flesh in the dryer was 3 days, whereas 5-6 days were required for natural sun drying under similar weather conditions. An artificial neural network (ANN) approach was used to model the performance of the dryer for the drying of litchi flesh. Using solar drying data of litchi flesh, the ANN model has been trained using the back-propagation algorithm. Seven sets of data were used for training and three sets were used for testing the ANN model. The performance of the dryer predicted by model was found to be very good.

Keywords: *Artificial neural network, parabolic greenhouse dryer, litchi, drying*

1. Introduction

Litchi (*Litchi Chinensis* Sonn.) is one of the major fruits in Southeast Asia, grown mainly in northern Thailand and northern Vietnam. The mature litchi is almost spherical shape and has a dark red colour. The flesh of this fruit is consumed both as fresh and dried products. It is a seasonal fruit. The drying of this fruit during harvesting season ensures year round availability and preserves the taste of litchi. Furthermore, dried fruits are becoming popular as an alternative to fresh fruits because of the special flavor of the dried fruits which cause the demand for dried fruits to increase consistently in international markets.

A drying model for litchi is useful for optimum design and operation of the litchi dryer. For proper understanding of the transfer processes during drying for production of quality dried products and in order to conserve energy during litchi drying, it is essential to know its drying characteristics.

Considerable studies have been conducted to describe the drying of food and non-food materials [1-23]. Kaminski et al. [24] reported the application of an artificial neural network (ANN) to the modeling of drying kinetics and degradation kinetics and a theoretical foundation of the drying process description by means of ANN was presented. Several studies have been reported on ANN modeling of drying of food materials [25-35]. Trelea et al. [26] presented a methodology for building a fast nonlinear dynamic model of drying and wet-milling degradation using ANN, and the model was based on experimental data. Farkas et al. [27] applied ANN to an agricultural fixed bed dryer and concluded that the ANN could be effective for modeling of the grain-drying process. Bala et al. [29] reported on ANN modeling of the drying of jackfruit bulbs and leather using a solar tunnel dryer and Erenturk and Erenturk [30] concluded that ANN prediction of drying characteristics is better than genetic algorithms. More recently Khazaei et al. [35] developed a ANN model for grape drying and it had better performance than multiple regression models and might be useful for automatic control systems for hot air dryers.

Classical mathematical modeling is still the basic tool for performance prediction of agricultural and industrial dryers. Although a mathematical model is available for simulation of solar greenhouse dryers [33], the model is relatively complicated and it is not for litchi flesh. Recently, an alternative and a qualitatively new tool for solving ill-posed, complex processing problems has been developed –artificial neural network (ANN) technique– and this enables the conduction of very fast and simple simulations. The technique does not require the formulation of an analytical description. Instead, a black-box model is constructed and exposed to carefully selected data to train the model for prediction of the performance. No study has been reported on ANN modeling of litchi and the previous work [29] on solar drying of jackfruit bulbs and leather in a solar tunnel dryer is not applicable to litchi due to the fact that the ANN is based on data and input-output analysis.

In terms of the performance of a parabolic greenhouse solar dryer, the performance of this type of dryer for drying banana, longan and chili has been investigated [36, 37]. However, the experimental performance of drying litchi flesh has not been reported. Therefore, the objectives of this work are to investigate the performance of the parabolic greenhouse solar dryer for drying litchi flesh and to perform ANN modeling of this dryer for drying litchi flesh.

2. Methodology

2.1 Experimental performance of solar drying of litchi flesh in the parabolic greenhouse dryer

2.1.1 Description and working principle of the dryer

The parabolic greenhouse solar dryer in this investigation consists of a parabolic roof structure made from polycarbonate sheets on a concrete floor. The structure of the dryer is made of galvanized iron bars. The products to be dried are placed as a thin layer on four arrays of trays. Polycarbonate sheet was selected to be the transparent cover of the dryer, because it has high transmittance (0.8) in shortwave solar radiation and low infrared transmittance (about 0.2), thus creating the greenhouse effect in the dryer. Three DC fans operated by a 50-W solar cell module were installed in the wall opposite to the air inlet to ventilate the dryer. With this solar cell module, the dryer can be used in rural areas without access to electricity grids. The parabolic cross-sectional shape helps to reduce wind load and a pictorial view of the dryer used in this study is shown in Fig. 1. The structure and dimension of the dryer are depicted in Fig. 2.

Solar radiation passing through the polycarbonate roof heats the products being dried on the trays, the concrete floor and all solid parts inside the dryer. Ambient air is drawn in through a small opening at the bottom of the rear side of the dryer and is heated by the floor and all parts inside the dryer. Heated air, while passing through and over the product, transfers its thermal energy to the product by convection, causing water evaporation and moisture transfer from the product to the air. This moist air is sucked from the dryer by three 14-Watt PV fans located at the top of the front side of the dryer.



Figure 1 Pictorial view of the parabolic greenhouse solar dryer

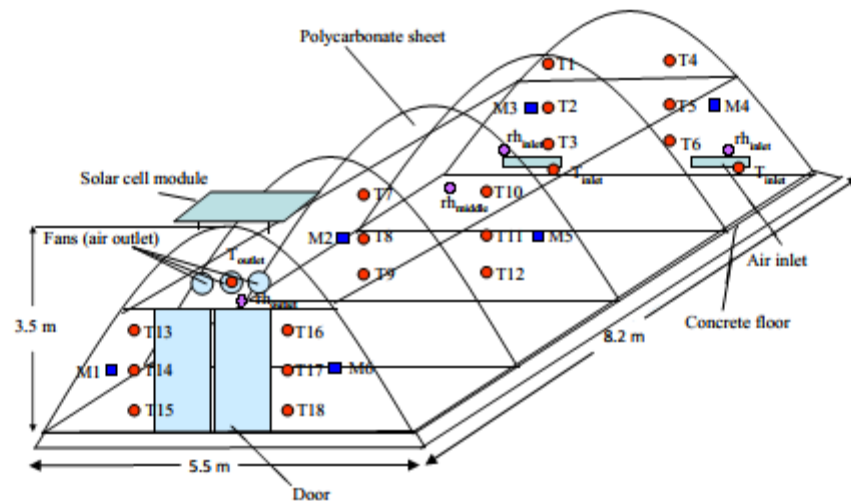


Figure 2 The structure and dimensions of the dryer and the positions of the thermocouples (T), hygrometers (rh), and product samples for moisture content determining (M)

2.1.2 Experimental procedure

Litchi was dried in the parabolic greenhouse solar dryer installed at Silpakorn University (13.82° N, 100.04°), Nakhon Pathom, Thailand. A total of ten experiments were conducted during three harvest seasons of litchi in 2008, 2009 and 2015. It is to be noted that normal litchi harvest season lasts about 3 months (April-June). To monitor the performance of the dryer, various sensors were installed in the dryer. Solar radiation was measured by a pyranometer (Kipp & Zonen, model CM 11, accuracy $\pm 0.5\%$) placed on the roof of the dryer. Temperature was measured by using K-type thermocouples. Hot wire anemometers (Airflow, model TA5, accuracy $\pm 2\%$) were used to monitor the air speed at the air outlet of the dryer. Another anemometer was also used to monitor the ambient wind speed. The relative humidity of ambient air and drying air was periodically measured by hygrometers (Elektronik, model EE23, accuracy $\pm 2\%$). The positions of these measurements are shown in Fig. 2. Voltage signals from the pyranometer, hygrometers and thermocouples were recorded every 10 minutes by a multi-channel data logger (Yokogawa, model DC100). For each drying test, 100 kg of litchi flesh was used. The experiments were started at 8.00 am and continued till 6.00 pm. Litchi flesh was kept in the dryer during night time and the drying was continued until the desired moisture content of 12% (wet basis) was reached. The final moisture content corresponds to the moisture content of high quality dried products in local markets. Product samples were placed in the dryer at various positions (Fig. 2) and were periodically weighed at 1-hour intervals using a digital balance (Kern, model 474-42, accuracy ± 0.1 g). Also, samples of about 100 g of the fresh product were placed outside the dryer and the mass was monitored at 1-hour intervals. The moisture contents of the products inside the dryer were compared against the control samples (open-air natural sun dried) dried outside the dryer. The moisture content during drying was estimated from the weight of the product samples and the dried solid mass of the samples. At the end of the experimental drying run, the exact dry solid mass of the product samples was determined by the oven method (103°C for 24 hours).

2.1.3 Measurement of the colour of dried product

The colour of solar dried litchi was measured by chromometer (Hunter Lab, Miniscan XE plus) which provides the colour according to Commission Internationale l'Eclairage (CIE) chromaticity coordinates. The parameter L^* is a measure of lightness ($L^*=0$ for black, $L^*=100$ for white), a^* is an indicator of redness ($a^*>0$ for red, $a^*<0$ for green) and b^* is an indicator of yellowness ($b^*>0$ for yellow, $b^*<0$ for blue). The $L^*a^*b^*$ [38-39] and L^*C^*h [40] colour systems were selected for this work because these are the most-used systems for evaluation of the colour of dried food materials. The instrument was standardized each time with a white ceramic plate. Three readings were taken at each place on the surface of samples and then the mean values of L^* , a^* and b^* were averaged. The different colour parameters were calculated using the following equations [40]:

Hue angle (h) indicating colour combination is defined as:

$$h = \begin{cases} \tan^{-1}(b^*/a^*) & (\text{when } a^* > 0) \\ 180^\circ + \tan^{-1}(b^*/a^*) & (\text{when } a^* < 0) \end{cases} \quad (1)$$

and chroma (C^*) indicating colour intensity or saturation is defined as:

$$C^* = (a^{*2} + b^{*2})^{1/2} \quad (2)$$

2.2. Artificial neural network (ANN) modeling

The methods of system modeling and identification are fundamental both for explanation of naturally occurring phenomena and for designing man-made engineering processes [24]. For the drying process, classical mathematical modeling such as using a partial differential equation model is still the basic tool used for process description. In spite of unquestionable advantages in using the mathematical process modeling approaches i.e. the equation for drying rate, there are also disadvantages that are often difficult to overcome. These include, among others, the necessity to determine many process state parameters like kinetic coefficients and physicochemical characteristics of a material and the drying agent. The costs involved in the experimental determination of these coefficients frequently diminish the advantages that can be gained from development of a mathematical model of the process. ANN techniques, by their nature, can overcome these problems, and thereby open new pathways in approaching a model design problem of this sort. However, in the literature, there are a few studies concerning mathematical modeling of the drying process by means of ANN. In addition, there is a hybrid modeling approach that combines an ANN model with a mathematical model. These types of models, however, are limited.

The neuro-computing techniques are shaped after biological neural functions and structures. Thus, they are popularly known as ANN. Similarly, as for their biological counterparts, the functions of ANN are being developed not by programming them, but by exposing them to carefully selected data on which they can learn how to perform the required processing task. In such a modeling approach, there is no need to formulate an analytical description of the process. Instead, a black-box process model is constructed by interacting the network with representative samples of measurable quantities that characterize the process.

2.2.1 Structure of ANN model of the parabolic greenhouse solar dryer

Artificial neural networks are biologically inspired; they are composed of elements that perform in a manner that is analogous to the most elementary functions of the biological neuron. The artificial neuron is designed to mimic the first order characteristics of the biological neuron. In essence, a set of inputs are applied, each representing the output of another neuron. Each input is multiplied by corresponding weight and all of the weighted inputs are summed to determine the activation level of neurons. The summed body corresponds to the biological cell body producing an

output. The simplest network is a group of neurons arranged in a layer and multilayer networks are formed by simply cascading a group of single layers, the output of one layer provides the input to subsequent layers.

An independent multilayer ANN model of the parabolic greenhouse solar dryer was developed to represent the drying system of litchi flesh. Although the equation for predicting the drying rate of litchi flesh is available [41], the ANN does not require such equation. The ANN model developed for litchi flesh has a four-layered network, which has a large number of simple processing elements called neurons (Fig. 3). The input layer of the model consists of four neurons that correspond to the four input variables, while the output layer has one neuron that represents the moisture content (MC) in the model. The input variables are: (1) time (t); (2) solar radiation (I_s); (3) temperature at the middle of the dryer (T) and (4) airflow rate (\dot{m}). I_s , T and (\dot{m}) were obtained from measurements. These three variables varied with time and their values from the measurements were used as input data of the ANN.

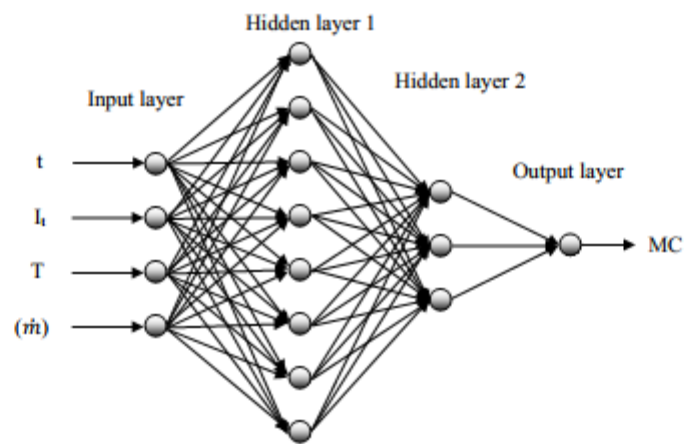


Figure 3 The structure of the artificial neural network of the greenhouse solar dryer model for drying litchi: t is time (hour), I_s is solar radiation (W/m^2), T is drying air temperature at the middle of the dryer ($^{\circ}\text{C}$), (\dot{m}) is air flow rate (m^3/h) and MC is moisture content (% wb).

The use of a number of hidden layers in the ANN depends on the degree of the complexity of the problem [31, 42-44] and on the application of the network [25]. There are no fixed rules for determining the number of hidden layers and nodes [35]. In general, one hidden layer has been found to be adequate, but in some cases a slight advantage may be achieved using two hidden layers [45]. Therefore, the number of hidden layers used was two. Larger number of neurons can represent the system more precisely, but complication arises to attain proper training [46]. After evaluating a large number of ANN, the number of neurons in hidden layers 1 and 2 of the model were found to be 8 and 3, respectively. All inputs were normalized between the values of 0.00 to 1.00. In this study the learning rate was initially set at 0.1 but finally reduced to (0.01) and momentum was chosen to be 0.7 in order to prevent over training. The networks were trained for a fixed number of 1000 cycles and the minimum value of root mean square error was always achieved. The performances of the ANN models were compared using the root mean square error (RMSE), the square of correlation coefficient or coefficient of determination, r^2 . All the trials were conducted using a computer program written in C++. The program used values of moisture content, solar radiation and flow rate obtained from measurements as its input data and these varied with time.

2.2.2 Training of the ANN model

ANN can modify their behavior in response to their environment. This factor, more than any other, is responsible for the interest they have received. Unlike a mathematical model, the structure of an ANN model itself cannot represent the system behavior, unless it is properly trained. The objective of training the network is to adjust the weights of the interconnecting neurons of the network so that application of a set of inputs produces the desired set of outputs. Initially, random values were used as weights and it was set to be 1.0. For brevity, one input–output set can be referred to as a vector. Training assumes that each input vector is paired with a target vector representing the desired output; together these are called a training pair. Usually, a network is trained over a number of training pairs.

A wide variety of training algorithms has been developed, each with its own strength and weakness. The ANN dryer models are trained by the back propagation algorithm so that the application of a set of inputs would produce the desired set of outputs [27]. The steps of the training procedure are summarized as follows: (1) an input vector is applied; (2) the output of the network is calculated and compared to the corresponding target vector; (3) the difference (error) is fed back through the network; and (4) weights are changed according to an algorithm called the delta rule [47] that tends to minimize the error. The vectors of the training set are sequentially applied. This procedure is repeated over the entire training set for as many times as necessary until the error is within some acceptable criteria, or until the outputs did not significantly change anymore. After the end of training, simulations are done with the trained model to check the accuracy of the training achieved. In this work, this procedure and the experimental input values were used in the simulation.

3. Results and Discussion

3.1 Experimental performance of the parabolic greenhouse dryer

Ten tests of the dryer for the drying of litchi flesh were performed during three harvest seasons of litchi, namely 2008, 2009 and 2015. Typical results for the drying of litchi flesh are shown in Figs 4-8. Fig. 4 shows the variations of solar radiation during a typical experiment of solar drying of litchi flesh in the parabolic greenhouse dryer. Maximum solar radiation is 1,222 W/m² during the drying.

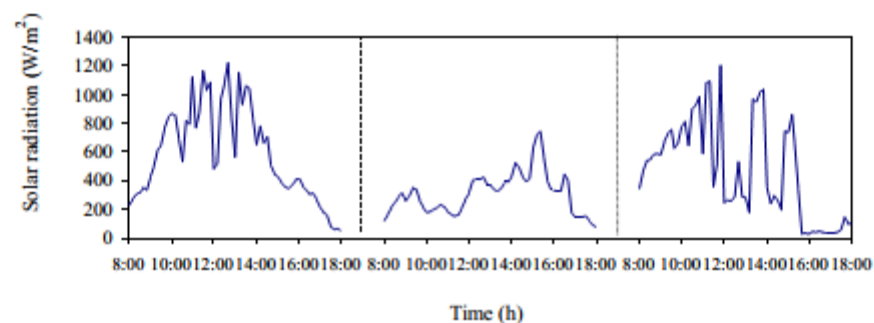


Figure 4 Variations of the solar radiation during the drying of litchi flesh

Fig. 5 shows the comparison of air temperatures at three different locations inside the dryer, namely front, middle and back, for a typical experiment of solar drying litchi flesh. Temperatures at different positions in these three locations varied within a narrow band. In addition, temperature at each of the locations significantly differed from the ambient air temperature.

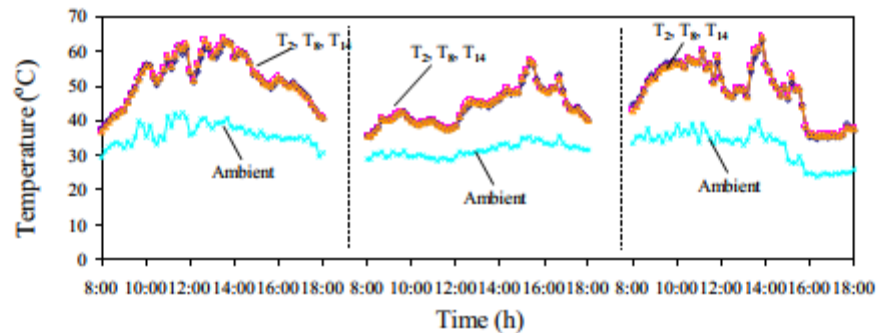


Figure 5 The variations of the temperatures at different positions inside the dryer

Fig. 6 shows air flow rates of a typical experiment during the drying of litchi flesh. The airflow rate increases sharply in the early part of the day, then becomes fairly constant and then drops sharply in the afternoon. The pattern of changes in airflow rate follows the pattern of the changes of solar radiation (Fig. 4), since the airflow is regulated by three fans powered by a solar cell module. The maximum air flow rate is $950 \text{ m}^3/\text{h}$.

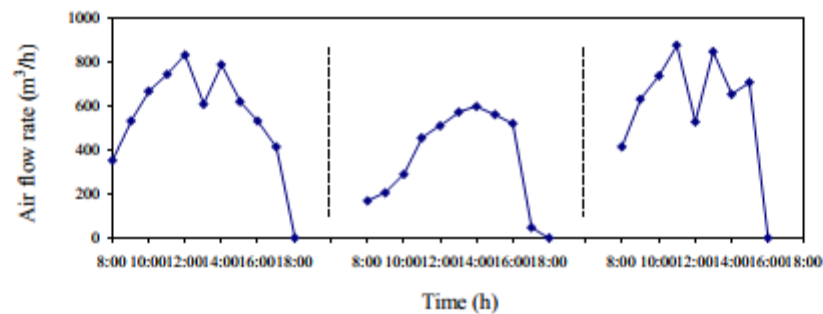


Figure 6 Variations of air flow rate inside the dryer during drying of litchi flesh

Fig. 7 shows the variations of moisture content of litchi flesh samples in the dryer for a typical experiment compared to the control sample dried by open-air natural sun drying. The moisture content of the litchi flesh in the solar dryer was reduced from an initial value of 84% (wb) to a final value of 13% (wb) within 3 days whereas the moisture content of the natural sun-dried samples was reduced to only 25% (wb) within the same period. The drying time of litchi flesh in the dryer was significantly reduced to 3 days as compared to 5-6 days in natural sun drying. Thus, the drying rate of litchi flesh dried in the dryer is higher than that dried by natural sun drying. This is because the litchi flesh in the dryer received energy both from direct exposure to solar radiation and heated air in the dryer, however the litchi flesh dried with natural sun received only incident solar radiation and part of the received energy was lost, especially by wind.

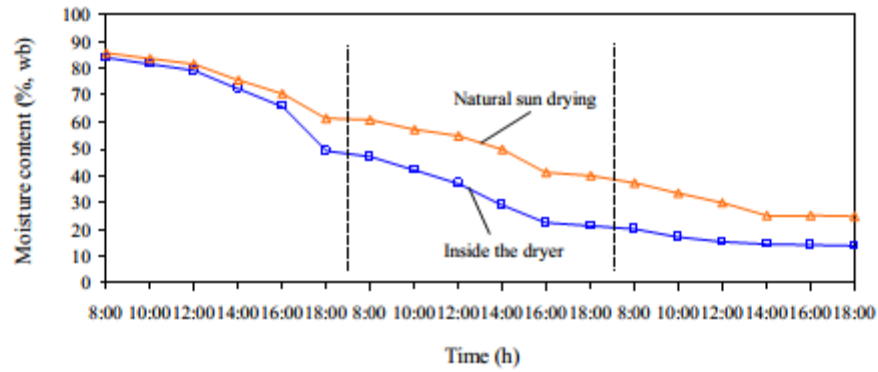


Figure 7 Variations of the moisture contents (M) during the drying of litchi flesh

It is interesting to investigate the heat losses from the dryer to surrounding environments, based on the typical experimental results. The analysis of heat losses was undertaken as follows.

The heat losses from the dryer consist mainly of four parts. The first part is the heat loss from the polycarbonate cover to ambient air due to convection ($Q_{conv,c-a}$), the second part is the heat loss from the cover to the sky due to radiation ($Q_{rad,c-sky}$), the third part is the heat loss from the floor of the dryer to the ground due to conduction ($Q_{cond,f-g}$) and the last part is the heat loss due to the out-flow of drying air from the dryer to the surroundings (Q_{flow}). The total heat losses (Q_{total}) can be written as:

$$Q_{total} = Q_{conv,c-a} + Q_{rad,c-sky} + Q_{cond,f-g} + Q_{flow} \quad (3)$$

Heat losses from medium i to medium j (Q_{i-j}) by convection, radiation and conduction for each day, was calculated from:

$$Q_{i-j} = \int_{8am}^{6pm} \mathcal{Q}_{i-j} dt \quad (4)$$

where \mathcal{Q}_{i-j} is the rate of heat transfer between medium i and j .

The values of \mathcal{Q}_{i-j} by convection and conduction were estimated by:

$$\mathcal{Q}_{i-j} = A_{ij} h (T_i - T_j) \quad (5)$$

where A_{ij} is the area of the medium where the heat transfer takes place, h is the heat transfer coefficient and T_i and T_j are temperatures of medium i and j , respectively. The heat transfer coefficients by convection and conduction and the rate of heat loss by radiation was calculated using the method described in Duffie and Beckman [48]. The heat loss Q_{flow} was estimated from the rate of the out-flow of the enthalpy of the drying air from the dryer [49]. Afterward, the heat losses for each day were summed up over the entire drying period to obtain the total heat loss.

Based on the typical experimental results, Q_{total} , $Q_{conv,c-a}$, $Q_{rad,c-sky}$, $Q_{cond,f-g}$ and Q_{flow} were estimated to be 1962.0, 513.4, 597.5, 582.3 and 268.8 MJ, respectively. The total solar radiation incident on the dryer during the entire period of the drying is 3868.5 MJ. Considering the total heat losses and the total solar radiation incident on the dryer, the dryer performed fairly well.

3.2 Colour of dried litchi

The quality of dried litchi flesh was evaluated. The colour of the dried litchi flesh was measured using a chromometer (Hunter Lab, Miniscan XE Plus) and the results are shown in Table 1. The values of the colour indices indicate that the colour of dried litchi is bright yellow reddish. Although the colour intensity was moderate, the colour combination was high. The colour of dried litchi flesh is comparable with high quality dried litchi flesh in markets.

Table 1 Colour of solar dried litchi flesh

Status	Colour Value				
	L*	a*	b*	C*	h
Solar dried litchi flesh	37.90	6.83	11.38	13.46	58.69

3.3 Performance prediction by ANN model

The artificial neural networks trained with experimental data representing the characteristics of drying litchi flesh should achieve a higher generalization ability. Thus, the experimental data of 7 sets were used for training to construct the models and the data of another 3 sets were reserved for testing the predictive capability of the models. The ANN model of the parabolic greenhouse dryer developed for drying litchi flesh was trained with field-level experimental data. After 1000 cycles of training, the square sum of difference (error) between the observed and the predicted output reached a significantly low level (0.05). Using the trained model, simulations were conducted to check the performance of the model. All the input variables, except moisture content (MC) of the training pairs, were used in the simulation so that the comparison can be done between the observed and the simulated output. The MC value in the simulation was similar to that of the observed one. For every step of the calculation, the output value (FMC) was used as the input value (IMC) in the next step. The comparison between the observed and simulated drying performances of the litchi flesh for the test data is shown in Fig. 8 and Fig. 9. From these figures, it was found that the agreement between the predicted and the observed moisture contents for the litchi flesh is very good. For the selected ANN model, root mean square difference (RMSD) and coefficient of determination (r^2) were 8.7-10.8% and 0.98-0.99, respectively. Judging from the method and equipment involved in the determination of moisture content, the moisture content from the experiment is not more than 5%. The agreement between the moisture content from the experiments and that from the ANN was within the acceptable limits [50]. Thus, if the model is adequately trained, it can appropriately represent the performance of the parabolic greenhouse dryer for drying litchi flesh, and can predict very well the moisture content at any time during drying. Several studies [51-53] reported the use of the ANN models for process control and predictive optimal control and the ANN model developed in this study can be used for process control and predictive optimal control of the greenhouse solar dryers for efficient production of quality dried products.

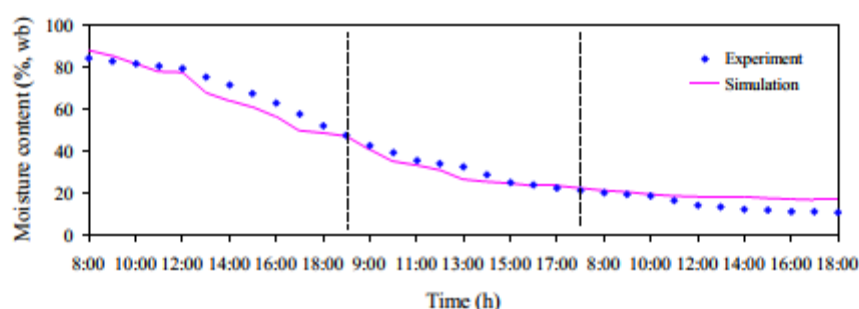


Figure 8 Comparison of the simulated and observed moisture content during the drying of litchi flesh between 29-31 May 2009 (RMSD = 10.8%)

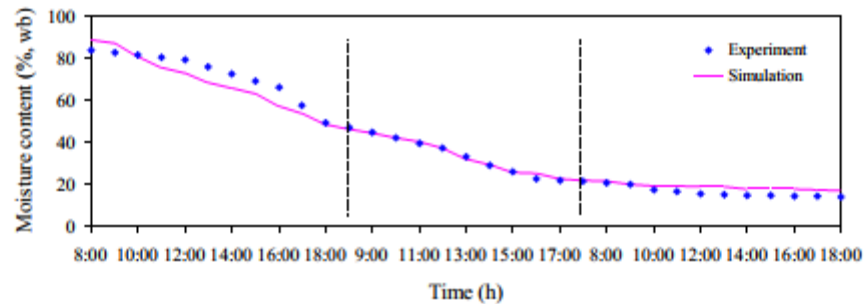


Figure 9 Comparison of the simulated and observed moisture content during the drying of litchi flesh between 10-12 June 2009 (RMSD = 8.7%)

4. Conclusion

Solar drying of litchi flesh was conducted in the parabolic greenhouse solar dryer. Solar radiation followed similar patterns for all days during drying. Moisture content of the litchi flesh was reduced from an initial value of 84 % (wb) to the final value of 13 % (wb) within 3 days. The dryer can be used to dry up to 100 kg of litchi flesh. In all the cases, the use of this dryer led to considerable reduction in drying time in comparison to that of natural sun drying, and the products dried in the dryer were of good quality. Considering the heat losses and the solar radiation input, the dryer performed fairly well. An ANN approach is used to predict the performance of the dryer, and the model was trained using the solar drying data of litchi flesh. An ANN with four inputs, one output and two hidden layers was found to be able to predict the operation of the dryer after it was adequately trained. The prediction of the model is very good.

Acknowledgement

The authors would like to thank Dr. Sarawut Nabnean for his assistance in conducting the experiments. We are grateful to Dr. Busarakorn Mahayothee for the valuable advice on the quality of dried product.

References

- [1] El-Shiatry MA, Muller J, Muhlbauer W, (1991). Drying fruits and vegetables with solar energy in Egypt. *Agricultural Mechanization in Asia Africa and Latin America* 22(2), 61–64.
- [2] Sharma VK, Colangelo A, Spanga G, (1995). Experimental investigation of different solar driers suitable for fruits and vegetable drying. *Renewable Energy* 6, 413–424.
- [3] Schirmer P, Janjai S, Esper A, Smitabhindu R, Muhlbauer W, (1996). Experimental investigation of the performance of the solar tunnel dryer for drying bananas. *Renewable Energy* 7(2), 119–129.
- [4] Karathanos VT, Belessiotis VG, (1997). Sun and artificial air drying kinetics of some agricultural products. *Journal of Food Engineering* 31, 35–46.
- [5] Bala BK, Mondol MRA, (2001). Experimental investigation on solar drying of fish using solar tunnel drier. *Drying Technology* 19(2), 1–10.
- [6] Bala BK, Mondol MRA, Das Choudhury BL, (2002). Solar drying of mango using solar tunnel drier. *Journal of Agricultural Engineering* 38(14), 43–50.
- [7] Bala BK, Mondol MRA, Biswas BK, Das Choudhury BL, Janjai S, (2003). Solar drying of pineapple using solar tunnel drier. *Renewable Energy* 28, 183–190.
- [8] Janjai S, Lambert N, Intawee P, Mahayothee B, Haewsungcharern M, Bala BK, Müller J, (2008a). Finite element simulation of drying of mango. *Biosystems Engineering* 99, 523–531.

- [9] Janjai S, Lambert N, Intawee P, Mahayothee B, Haewsungcharern M, Bala BK, Nagle M, Leis H, Müller J, (2008b). Finite element simulation of drying of longan fruit. *Drying Technology* 26, 666–674.
- [10] Janjai S, Mahayothee B, Lambert N, Bala BK, Precoppe M, Nagle M, Müller J, (2010). Diffusivity, shrinkage and simulated drying of litchi fruit (*Litchi Chinensis* Sonn.). *Journal of Food Engineering* 96, 214–221.
- [11] Janjai S, Precoppe M, Lamler N, Mahayothee B, Bala BK, Nagle M, Müller J, (2011). Thin-layer drying of litchi (*Litchi chinensis* Sonn.). *Food and Bioproducts Processing* 89, 194-201.
- [12] Amer BMA, Hossain MA, Gottschalk K, (2010). Design and performance evaluation of a new hybrid solar dryer for banana. *Energy Conversion and Management* 51, 813-820.
- [13] Nilnont W, Thepa S, Janjai S, Kasayapanand N, Thamrongmas C, Bala BK, (2012). Finite element simulation of coffee (*Coffea Arabica*) drying. *Food and Bioproducts Processing* 90, 341-350.
- [14] Reyes A, Mahn A, Cubillos F, Huenlaf P, (2013). Mushroom dehydration in a hybrid-solar dryer. *Energy Conversion and Management* 70, 31-39.
- [15] Mohajer A, Nematollahi O, Joybari MM, Hashemi SA, Assari MR, (2013). Experimental investigation of a hybrid solar drier and water heater system. *Energy Conversion and Management* 76, 935-944.
- [16] Mohanraj M, (2014). Performance of a solar-ambient hybrid source heat pump drier for copra drying under hot-humid weather conditions. *Energy for Sustainable Development* 23, 165-169.
- [17] Shalaby SM, Bek MA, (2014). Experimental investigation of a novel indirect solar dryer implementing PCM as energy storage medium. *Energy Conversion and Management* 83, 1-8.
- [18] Fudholi A, Sopian K, Yazdi MH, Ruslan MH, Gabbasa M, Kazem HA, (2014). Performance analysis of solar drying system for red chili. *Solar Energy* 99, 47-54.
- [19] Reyes A, Mahn A, Vasquez F, (2014). Mushrooms dehydration in a hybrid-solar dryer, using a phase change material. *Energy Conversion and Management* 83, 241-248.
- [20] Fudholi A, Sopian K, Bakhtyar B, Gabbasa M, Othman MY, Ruslan MH, (2015). Review of solar drying systems with air based solar collectors in Malaysia. *Renewable and Sustainable Energy Reviews* 51, 1191-1204.
- [21] Hussadin M, Pongtornkulpanich, (2015). Solar-biomass drying system for para rubber sheet. *International Journal of Renewable Energy* 10, 37-46.
- [22] Nabnean S, Janjai S, Thepa S, Sudaprasert K, Songprokorp R, Bala BK, (2016). Experimental performance of a new design of solar dryer for drying osmotically dehydrated cherry tomatoes. *Renewable Energy* 94, 147 – 156.
- [23] Ju H, El-Mashad HM, Fang X, Pan Z, Xiao H, Lui Y, Gao Z, (2016). Drying characteristics and modeling of yam sliced under different relative humidity conditions. *Drying Technology* 34, 296-306.
- [24] Kaminski W, Tomczak E, Strumill P, (1998). Neurocomputing approaches to modeling of drying process dynamics. *Drying Technology* 16, 967–992.
- [25] Huang B, Mujumdar AS, (1993). Use of neural network to predict industrial dryer performance. *Drying Technology* 11, 525–541.
- [26] Trelea IC, Courtois F, Trystram G, (1997). Dynamic models for drying and wet milling quality degradation of corn using neural networks. *Drying Technology* 15, 1095–1102.
- [27] Farkas I, Remenyi P, Biro A, (2000). Modelling aspects of grain drying with a neural network. *Computers and Electronics in Agriculture* 29, 99–113.
- [28] Hernandez-Perez JA, Garcia-Alvarado MA, Trystram G, Heyd B, (2004). Neural networks for the heat and mass transfer prediction during drying of cassava and mango. *Innovative Food Science and Emerging Technologies* 5, 57–64.
- [29] Bala BK, Ashraf MA, Uddin MA, Janjai S, (2005). Experimental and neural network prediction of the performance of a solar tunnel drier for drying jackfruit bulbs and leather. *Journal of Food Process Engineering* 28, 552–566.
- [30] Erenturk S, Erenturk K, (2007). Comparison of genetic algorithm and neural network approaches for the drying process of carrot. *Journal of Food Engineering* 78, 905–912.
- [31] Movagharnjad K, Nikzad M, (2007). Modeling of tomato drying using artificial neural network. *Computers and Electronics in Agriculture* 59, 78–85.

- [32] Chegini GR, Khazaei J, Ghobadian B, Goudarzi AM, (2008). Prediction of process and product parameters in an orange juice spray dryer using artificial neural networks. *Journal of Food Engineering* 84, 534–543.
- [33] Cakmak G, Yildiz C, (2001). The prediction of seedy grape drying rate using a neural network method. *Computers and Electronics in Agriculture* 75, 132–138.
- [34] Aghbashloa M, Mobli H, Rafice S, Madadlou A, (2012). The use of artificial neural network to predict exergetic performance of spray drying process: A preliminary study. *Computers and Electronics in Agriculture* 88, 32–43.
- [35] Khazaei NB, Tavakoli T, Ghassemian H, Khoshtaghazaa MH, Banakar A, (2013). Applied machine vision and artificial neural network for modeling and controlling of the grape drying process. *Computers and Electronics in Agriculture* 98, 205–213.
- [36] Janjai S, Lambert N, Intawee P, Mahayothee B, Bala BK, Nagle M, Müller J, (2009). Experimental and simulated performance of a PV-ventilated solar greenhouse dryer for drying of peeled longan and banana. *Solar Energy* 83, 1550–1565.
- [37] Janjai S, Khamvongsa V, Bala BK, (2007). Development, design, and performance of a PV-ventilated greenhouse dryer. *International Energy Journal* 8, 249–258.
- [38] Krokida MK, Tsami E, Maroulis ZB, (1998). Kinetics on color changes during drying of some fruits and vegetables. *Drying Technology* 16(3–5), 667–685.
- [39] Maskan M, (2001). Kinetics of colour change of kiwifruits during hot air and microwave drying. *Journal of Food Engineering* 48(2), 169–175.
- [40] Zhang M, De Baerdemaeker J, Schrevens E, (2003). Effects of different varieties and shelf storage conditions of chicory on deteriorative color changes using digital image processing and analysis. *Food Research International* 36(7), 669–676.
- [41] Janjai S, Precoppe M, Lamlert N, Mahayothee B, Bala BK, Nagel M, Muller J, (2011). Thin-layer drying of litchi (*Litchi Chinensis* Sonn.), *Food and Bioproducts Processing* 89, 194–201.
- [42] Chen CR, Ramaswamy HS, (2002). Modeling and optimization of variable retort temperature (VRT) thermal processing using coupled neural networks and genetic algorithms. *Journal of Food Engineering* 28, 552–566.
- [43] Izadifar M, Jahromi MZ, (2007). Application of genetic algorithm for optimization of vegetable oil hydrogenation process. *Journal of Food Engineering* 78, 1–8.
- [44] Erzin Y, Rao HB, Singh DN, (2008). Artificial neural network models for predicting soil thermal resistivity. *International Journal of Thermal Sciences* 47, 1347–1358.
- [45] Hecht-Nielsen R, (1989). Theory of backpropagation neural network. In *Proceedings of International Joint Conference on Neural Networks*. Washington DC, 593–605.
- [46] Zhang Q, Yang SX, Mittal GS, Yi S, (2002). Prediction performance indices and optimal parameters of rough rice drying using neural networks. *Biosystems Engineering* 83(3), 281–290.
- [47] Wasserman PD, (1989). *Neural Computation: Theory and Practice*. Van Nostrand Reinhold, New York, NY.
- [48] Duffie JA, Beckman WA, (2013). *Solar Engineering of Thermal Process*, Fourth edition, John Wiley & Sons. New Jersey.
- [49] Janjai S, Intawee P, Kaewkiew J, Sritus C, Khamvongsa V, (2011). A large-scale solar greenhouse dryer using polycarbonate cover: Modeling and testing in a tropical environment of Lao People's Democratic Republic. *Renewable Energy* 36, 1053–1062.
- [50] O'Callaghan JR, Menzies DJ, Bailey PH, (1971). Digital simulation of agricultural drier performance. *Journal of Agricultural Engineering Research* 16, 223–244.
- [51] Lee M, Park S, (2000). Process control using a neural network combined with convention PID controllers. *ICASE: The Institute of Control, Automation and Systems engineers* 2(3), 196–200.
- [52] Draeger A, Engell S, Ranke H, (1995). Model predictive control using neural network. *IEEE, Control Systems*, October 1995, 61–66.
- [53] Pandhi R, Balakrishnan SN, (2003). Optimal process control using neural networks. *Asian Journal of Control* 5(2), 217–229.

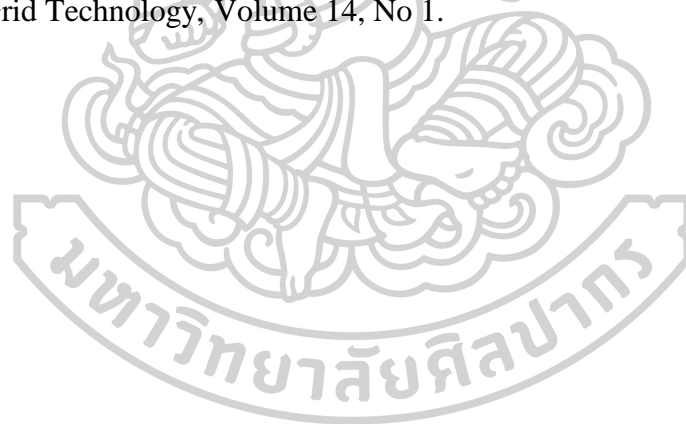
- [32] Chegini GR, Khazaei J, Ghobadian B, Goudarzi AM, (2008). Prediction of process and product parameters in an orange juice spray dryer using artificial neural networks. *Journal of Food Engineering* 84, 534–543.
- [33] Cakmak G, Yildiz C, (2001). The prediction of seedy grape drying rate using a neural network method. *Computers and Electronics in Agriculture* 75, 132–138.
- [34] Aghbashloa M, Mobli H, Rafice S, Madadlou A, (2012). The use of artificial neural network to predict exergetic performance of spray drying process: A preliminary study. *Computers and Electronics in Agriculture* 88, 32–43.
- [35] Khazaei NB, Tavakoli T, Ghassemian H, Khoshtaghazaa MH, Banakar A, (2013). Applied machine vision and artificial neural network for modeling and controlling of the grape drying process. *Computers and Electronics in Agriculture* 98, 205–213.
- [36] Janjai S, Lambert N, Intawee P, Mahayothee B, Bala BK, Nagle M, Müller J, (2009). Experimental and simulated performance of a PV-ventilated solar greenhouse dryer for drying of peeled longan and banana. *Solar Energy* 83, 1550–1565.
- [37] Janjai S, Khamvongsa V, Bala BK, (2007). Development, design, and performance of a PV-ventilated greenhouse dryer. *International Energy Journal* 8, 249–258.
- [38] Krokida MK, Tsami E, Maroulis ZB, (1998). Kinetics on color changes during drying of some fruits and vegetables. *Drying Technology* 16(3–5), 667–685.
- [39] Maskan M, (2001). Kinetics of colour change of kiwifruits during hot air and microwave drying. *Journal of Food Engineering* 48(2), 169–175.
- [40] Zhang M, De Baerdemaeker J, Schrevens E, (2003). Effects of different varieties and shelf storage conditions of chicory on deteriorative color changes using digital image processing and analysis. *Food Research International* 36(7), 669–676.
- [41] Janjai S, Precoppe M, Lamlert N, Mahayothee B, Bala BK, Nagel M, Muller J, (2011). Thin-layer drying of litchi (*Litchi Chinensis* Sonn.), *Food and Bioproducts Processing* 89, 194–201.
- [42] Chen CR, Ramaswamy HS, (2002). Modeling and optimization of variable retort temperature (VRT) thermal processing using coupled neural networks and genetic algorithms. *Journal of Food Engineering* 28, 552–566.
- [43] Izadifar M, Jahromi MZ, (2007). Application of genetic algorithm for optimization of vegetable oil hydrogenation process. *Journal of Food Engineering* 78, 1–8.
- [44] Erzin Y, Rao HB, Singh DN, (2008). Artificial neural network models for predicting soil thermal resistivity. *International Journal of Thermal Sciences* 47, 1347–1358.
- [45] Hecht-Nielsen R, (1989). Theory of backpropagation neural network. In *Proceedings of International Joint Conference on Neural Networks*. Washington DC, 593–605.
- [46] Zhang Q, Yang SX, Mittal GS, Yi S, (2002). Prediction performance indices and optimal parameters of rough rice drying using neural networks. *Biosystems Engineering* 83(3), 281–290.
- [47] Wasserman PD, (1989). *Neural Computation: Theory and Practice*. Van Nostrand Reinhold, New York, NY.
- [48] Duffie JA, Beckman WA, (2013). *Solar Engineering of Thermal Process*, Fourth edition, John Wiley & Sons. New Jersey.
- [49] Janjai S, Intawee P, Kaewkiew J, Sritus C, Khamvongsa V, (2011). A large-scale solar greenhouse dryer using polycarbonate cover: Modeling and testing in a tropical environment of Lao People's Democratic Republic. *Renewable Energy* 36, 1053–1062.
- [50] O'Callaghan JR, Menzies DJ, Bailey PH, (1971). Digital simulation of agricultural drier performance. *Journal of Agricultural Engineering Research* 16, 223–244.
- [51] Lee M, Park S, (2000). Process control using a neural network combined with convention PID controllers. *ICASE: The Institute of Control, Automation and Systems engineers* 2(3), 196–200.
- [52] Draeger A, Engell S, Ranke H, (1995). Model predictive control using neural network. *IEEE, Control Systems*, October 1995, 61–66.
- [53] Pandhi R, Balakrishnan SN, (2003). Optimal process control using neural networks. *Asian Journal of Control* 5(2), 217–229.

Appendix 2

Publications

Parts of this thesis have been published or accepted to published in international journal or conference proceedings as follows:

1. S. Janjai, K. Tohsing, S. Pattarapanitchai, S. Buntoung, B. Mahayothee, **T. Mundpookhier**, Y. Boonrod, S. Koch, (2017). Experimental performance and artificial neural network modeling of parabolic greenhouse type solar dryers. Proceeding of the 2nd Nordic Baltic Drying Conference, Hamburg, Germany.
2. K. Tohsing, S. Janjai, N. Lamlert, **T. Mundpookhier**, W. Chanalert, B.K. Bala, (2018). Experimental performance and artificial neural network modeling of solar drying of litchi in the parabolic greenhouse dryer. Journal of Renewable Energy, Volume 13, No 1.
3. **T. Mundpookhier**, S. Pattarapanitchai, P. Pankaew, O. Aumporn, S. Janjai. (2018). Performance investigation of the parabola dome solar dryer equipped with phase-change-thermal energy storages. Proceeding of the 14th Conference on Energy Network of Thailand.
4. P. Pankaew, O. Aumporn, S. Janjai, **T. Mundpookhier**, B.K. Bala, (2019). Performance of parabolic greenhouse solar dryer equipped with rice husk burning system for banana drying. Journal of Renewable Energy and Smart Grid Technology, Volume 14, No 1.



Appendix 3

Nomenclature

[A]	intermediate parameter matrix
a_w	water activity (decimal)
A_{dryer}	dryer area, (m ²)
a_m	proportion of molten mass compared to the total mass of phase change (-)
[C]	global capacitance matrix
[c]	element capacitance matrix
C_{annual}	annual cost, (Baht)
C_{burner}	cost of rice husk burning system, (Baht)
C_{dryer}	cost of the parabolic greenhouse dryer, (Baht)
$C_{electricity}$	electricity consumption cost, (Baht)
C_{husk}	rice husk consumption cost, (Baht)
C_i	cash flow at year i
C_{labor}	labor cost, (Baht)
C_{lp}	the heat capacity of PCM in solid state (J/kg. °C)
C_{main}	maintenance cost, (Baht)
C_{op}	operating cost, (Baht)
C_{pa}	specific heat of air, (J·kg ⁻¹ °C ⁻¹)
C_{sp}	the heat capacity of PCM in liquid state (J/kg. °C)
C_T	capital cost of the dryer equipped the burning system, (Baht)
$C_{unit\ electricity}$	unit cost of electricity, (Baht·kWh ⁻¹)
D	moisture diffusivity (m ² /s)
D_{air}	diffusivity of air (m ² /s)
d	equivalent diameter (m)
E_{dryer}	dryer output, (J)
E_{PV}	energy output from solar cell panel, (J)
$E_{rice\ husk}$	energy output from rice husk burner, (J)
E_{solar}	solar energy input to the dryer, (J)
{F}	global load force vector
{F*}	intermediate parameter vector
{f}	element load force vector
h_m	mass transfer coefficient (m/s)
h_f	heating value of rice husk, (J·kg ⁻¹)
i_f	inflation rate, (%)
i_{in}	interest rate, (%)

IRR	internal rate of return, (%)
$[K]$	global stiffness matrix
$[k]$	element stiffness matrix
L_g	latent heat of vaporization of moisture, ($J \cdot kg^{-1}$)
M	moisture content of product on dry basis (% , db.)
MR	moisture ratio
M_o	initial moisture content of product (% , db.)
M_e	equilibrium moisture contents of banana on dry basis (% , db.)
M_s	surface moisture content on dry basis (% , db.)
m_a	mass flow rate of air, ($kg \cdot s^{-1}$)
m_f	mass flow rate of rice husk, ($kg \cdot s^{-1}$)
M_f	Quantity of fresh banana, (kg)
M_d	Quantity of dried banana, (kg)
m_r	moisture removed, (kg)
N	life span of the dryer, (years)
$[N]$	matrix of interpolating function
n	magnitude of the outward normal vector to the surface
$[P]$	intermediate parameter matrix
P_f	price of fresh banana, ($Baht \cdot kg^{-1}$)
P_d	price of dried banana, ($Baht \cdot kg^{-1}$)
PB	payback period, (year)
R	correlation coefficient
RH	relative humidity (%)
Re	Reynolds number
Sc	Schmidt number
$S_r(t)$	solar radiation at time t, ($W \cdot m^{-2}$)
T_a	air temperature ($^{\circ}C$)
T_{ab}	absolute temperature (K)
T_{out}	temperature of hot air input from the heat exchanger, ($^{\circ}C$)
T_{in}	ambient air temperature, ($^{\circ}C$)
T_m	melting temperature ($^{\circ}C$)
t	time, (s)
u	air velocity (m/s)
x	spatial coordinate in x direction
y	spatial coordinate in y direction
Δh_m	latent heat (J/kg)
Δt	time step (s)

x_i	actual value
x_{mean}	measure value (mean value of the measurement)
Z	drying cost, (Baht·kg ⁻¹)
δx_i	uncertainly in a measurement
ε	overall effectiveness
ε_{eff}	efficiency of the dryer equipped with the burning system, (%)
ω	economic parameter defined
ρ_{air}	density of air (kg/ m ³)
μ	viscosity of air (m ² /m)
Ω	banana domain
∇	operator $\frac{\partial}{\partial x} + \frac{\partial}{\partial y} + \frac{\partial}{\partial z}$



REFERENCES

- Abdullah, K., Wulandani, D., Nelwan, L., & Manalu, L. (2001). Recent development of GHE solar drying in Indonesia. *Drying Technology*, 19(2), 245-256.
- Audsley, E., & Wheeler, J. (1978). The annual cost of machinery calculated using actual cash flows. *Journal of Agricultural Engineering Research*, 23(2), 189-201.
- Bala, B. (2017). *Drying and storage of cereal grains*: Wiley Online Library.
- Bala, B. K. (1998). *Solar drying systems: simulations and optimization*: Agrotech Publishing Academy.
- Bena, B., & Fuller, R. J. (2002). Natural convection solar dryer with biomass back-up heater. *Solar Energy*, 72(1), 75-83.
- Boonlong, P., Hirun, A., Siratanapanta, T., Siriplapla, P., Sitthipong, N., Sucharitakul, P., Rerkkringrai, P. (1984). *Solar-assisted tobacco curing*. Paper presented at the Regional Seminar on Solar Drying, Yogyakarta, Indonesia.
- Bowrey, R., Buckle, K., Hamey, I., & Pavenayotin, P. (1980). Use of solar energy for banana drying. *Food technology in Australia*.
- Cengel, Y. A., Turner, R.H., Cimbala, J.M. and Kanoglu, M. . (2008). *Fundamentals of thermal-fluid sciences*: McGraw-Hill New York.
- Champion, W., & Halsey Jr, G. (1953). Physical adsorption on uniform surfaces. *The Journal of Physical Chemistry*, 57(7), 646-648.
- Chung, D. S., & Pfost, H. B. (1967). Adsorption and desorption of water vapor by cereal grains and their products Part II: Development of the general isotherm equation. *Transactions of the ASAE*, 10(4), 552-0555.
- Day, D., & Nelson, G. (1965). Desorption isotherms for wheat. *Transactions of the ASAE*, 8(2), 293-0297.
- De Neufville, R. (1990). *Applied systems analysis*: McGraw-Hill New York.
- Dhanushkodi, S., Wilson, V. H., & Sudhakar, K. (2015). Life cycle cost of solar biomass hybrid dryer systems for cashew drying of nuts in India. *Environmental and Climate Technologies*, 15(1), 22-33.
- Diamante, L. (1993). Mathematical modelling of the thin layer solar drying of sweet potato slices. *Solar Energy*, 51.
- Doiebelin, E. (1976). Measurement systems. In: McGraw Hill, New York.
- Eissen, W., Mühlbauer, W., & Kutzbach, H. (1985). Solar drying of grapes. *Drying Technology*, 3(1), 63-74.
- El-Sebaili, A., Aboul-Enein, S., Ramadan, M., & El-Gohary, H. (2002). Experimental investigation of an indirect type natural convection solar dryer. *Energy conversion and management*, 43(16), 2251-2266.
- Exell, R., & Kornsakoo, S. (1976). A low-cost solar rice dryer. *Appropriate Technology (UK)*, 5, 23-25.
- Fudholi, A., Mat, S., Basri, D. F., Ruslan, M. H., & Sopian, K. (2016). Performances analysis of greenhouse solar dryer with heat exchanger. *Contemporary Engineering Sciences*, 9(3), 135-144.
- Fudholi, A., Sopian, K., Alghoul, M., Ruslan, M. H., & Othman, M. Y. (2015). Performances and improvement potential of solar drying system for palm oil fronds. *Renewable Energy*, 78, 561-565.
- Fudholi, A., Sopian, K., Ruslan, M. H., Alghoul, M., & Sulaiman, M. (2010). Review of solar dryers for agricultural and marine products. *Renewable and Sustainable*

- Energy Reviews*, 14(1), 1-30.
- Haghighi, K. (1988). Modeling simultaneous heat and mass transfer in an isotropic sphere—a finite element approach. *Transactions of the ASAE*, 31, 629-637.
- Henderson, S. (1974). Progress in developing the thin layer drying equation. *Transactions of the ASAE*, 17(6), 1167-1168.
- Holman, J. P. (1978). *Experimental Methods for Engineers* “McGraw-Hill Book Company. New York.
- Iqbal, M. (1983). *An Introduction to Solar Radiation*. New York: Academic Press.
- Janjai, Bala, B., Tohsing, K., Mahayothee, B., Haewsungcharern, M., Mühlbauer, W., & Müller, J. (2006). Equilibrium moisture content and heat of sorption of longan (*Dimocarpus longan* Lour.). *Drying Technology*, 24(12), 1691-1696.
- Janjai, Chaichoet, C., & Intawee, P. (2005b). Performance of a PV-ventilated Greenhouse Dryer for Drying Banana. *Asian journal on energy and environment*, 6(02), 133-138.
- Janjai, Khamvongsa, V., & Bala, B. (2007). Development, design, and performance of a PV-ventilated greenhouse dryer. *International Energy Journal*, 8(4).
- Janjai, Laksanaboonsong, J., Nunez, M., & Thongsathitya, A. (2005a). Development of a method for generating operational solar radiation maps from satellite data for a tropical environment. *Solar Energy*, 78(6), 739-751.
- Janjai, Lamler, N., Intawee, P., Mahayothee, B., Bala, B., Nagle, M., & Müller, J. (2009). Experimental and simulated performance of a PV-ventilated solar greenhouse dryer for drying of peeled longan and banana. *Solar Energy*, 83(9), 1550-1565.
- Janjai, Lamler, N., Intawee, P., Mahayothee, B., Haewsungcharern, M., Bala, B., & Müller, J. (2008). Finite element simulation of drying of mango. *Biosystems Engineering*, 99(4), 523-531.
- Janjai, Masiri, I., & Laksanaboonsong, J. (2013). Satellite-derived solar resource maps for Myanmar. *Renewable Energy*, 53, 132-140.
- Janjai, Pankaew, P., Laksanaboonsong, J., & Kitichantaropas, P. (2011). Estimation of solar radiation over Cambodia from long-term satellite data. *Renewable Energy*, 36(4), 1214-1220.
- Janjai, S., Intawee, P., Kaewkiew, J., Sritus, C., & Khamvongsa, V. (2011). A large-scale solar greenhouse dryer using polycarbonate cover: Modeling and testing in a tropical environment of Lao People’s Democratic Republic. *Renewable Energy*, 36(3), 1053-1062.
- JP., H. (1978). *Experimental Method for Engineering*. 3 ed.: New York: McGraw-Hill Book Company.
- Kaleemullah, S., & Kailappan, R. (2004). Moisture sorption isotherms of red chillies. *Biosystems Engineering*, 88(1), 95-104.
- Karathanos, V. T., & Belessiotis, V. G. (1999). Application of a thin-layer equation to drying data of fresh and semi-dried fruits. *Journal of Agricultural Engineering Research*, 74(4), 355-361.
- Nguyen, M.-H., & Price, W. E. (2007). Air-drying of banana: influence of experimental parameters, slab thickness, banana maturity and harvesting season. *Journal of Food Engineering*, 79(1), 200-207.
- Oswin, C. (1946). The kinetics of package life. III. The isotherm. *Journal of the Society of Chemical Industry*, 65(12), 419-421.

- Pankaew. (2016). Moisture desorption isotherm, diffusivity and finite element simulation of drying of macadamia nut (*Macadamia integrifolia*). *Food and Bioproducts Processing*, 100, 16-24.
- Pratoto, A., Daguinet, M., & Zeghmami, B. (1998). A simplified technique for sizing solar-assisted fixed-bed batch dryers: application to granulated natural rubber. *Energy conversion and management*, 39(9), 963-971.
- Ranjan, R., Irudayaraj, J., Reddy, J., & Mujumdar, A. (2004). Finite-element simulation and validation of stepwise drying of bananas. *Numerical Heat Transfer, Part A*, 45(10), 997-1012.
- Seeger, L. J. (1984). *Applied finite element analysis*: Wiley New York.
- Smitabhindu, R., Janjai, S., & Chankong, V. (2008). Optimization of a solar-assisted drying system for drying bananas. *Renewable Energy*, 33(7), 1523-1531.
- Sonthikun, S., Chairat, P., Fardsin, K., Kirirat, P., Kumar, A., & Tekasakul, P. (2016). Computational fluid dynamic analysis of innovative design of solar-biomass hybrid dryer: An experimental validation. *Renewable Energy*, 92, 185-191.
- Soponronnarit, S., Assayo, M., & Rakwichian, W. (1991). Performance of a solar banana dryer. *RERIC Int Energy J*, 13, 71-79.
- Souraki, B. A., & Mowla, D. (2008). Experimental and theoretical investigation of drying behaviour of garlic in an inert medium fluidized bed assisted by microwave. *Journal of Food Engineering*, 88(4), 438-449.
- van Nydeck Schenck, H., & Hawks, R. (1979). *Theories of engineering experimentation*: McGraw-Hill Companies.
- Whith, G., Bridges, T., Loewer, O., & Ross, I. (1978). Seed coat damage in thin layer drying of soybeans as affected by drying conditions. *American Society of Agricultural Engineers paper*(78-3052).
- Wibulsawas, P., & Thaina, S. (1980). *Comparative performance of a solar cabinet dryer*. Paper presented at the Proceedings of a workshop on fuel and power.
- Zhang, Q., & Litchfield, J. (1991). An optimization of intermittent corn drying in a laboratory scale thin layer dryer. *Drying Technology*, 9(2), 383-395.

VITA

NAME Tawedach Munepookher

DATE OF BIRTH 13 March 1990

PLACE OF BIRTH Khon Kaen

INSTITUTIONS ATTENDED 2009 Bachelor of Science (Physics) Loei Rajabhat University, Loei, Thailand

HOME ADDRESS 2013 Master of Science (Physics), Silpakorn University, Graduate School, Nakhon Pathom, Thailand
30 M. 12 T. Nachan A. Si Chomphu, Khon Kaen, 40220

PUBLICATION S. Janjai, K. Tohsing, S. Pattarapanitchai, S. Buntoung, B. Mahayothee, T. Mundpookhier, Y. Boonrod, S. Koch, (2017). Experimental performance and artificial neural network modeling of parabolic greenhouse type solar dryers. Proceeding of the 2nd Nordic Baltic Drying Conference, Hamburg, Germany.

K. Tohsing, S. Janjai, N. Lamlert, T. Mundpookhier, W. Chanalert, B.K. Bala, (2018). Experimental performance and artificial neural network modeling of solar drying of litchi in the parabolic greenhouse dryer. Journal of Renewable Energy and Smart Grid Technology, Volume 13, No 1.

T. Mundpookhier, S. Pattarapanitchai, P. Pankaew, O. Aumporn, S. Janjai. (2018). Performance investigation of the parabola dome solar dryer equipped with phase-change-thermal energy storages. Proceeding of the 14th Conference on Energy Network of Thailand.

P. Pankaew, O. Aumporn, S. Janjai, T. Mundpookhier, B.K. Bala, (2019). Performance of parabolic greenhouse solar dryer equipped with rice husk burning system for banana drying. Journal of Renewable Energy and Smart Grid Technology, Volume 14, No 1.